



Universidade do Porto

Faculdade de Engenharia

FEUP

VitalLogger: An Adaptable Wearable Physiology and Ambiance Data Logger for Mobile Applications

Duarte Filipe Dias

Master Thesis elaborated on the
Integrated Master in Bioengineering
Branch of Biomedical Engineering

Supervisor: Prof. Ph.D. João Paulo Cunha

Collaborator: Nuno Ferreira

September 2015

© Duarte Filipe Dias, 2015

VitalLogger: An Adaptable Wearable Physiology and Ambiance Data Logger for Mobile Applications



BRAIN-Biomedical Research And INnovation



Author: Duarte Filipe Dias¹

Supervisor: Prof. Ph.D. João Paulo Cunha²

Collaborator: Nuno Ferreira³

¹ Faculty of Engineering of University of Porto - Master Student in Bioengineering, bio10040@fe.up.pt

² Faculty of Engineering of University of Porto – DEEC / INESC TEC, jpcunha@fe.up.pt

³ Biodevices, S.A., nuno.ferreira@biodevices.pt

“Why do we fall? So we can learn how to pick ourselves up.”

Alfred

Resumo

A revolução dos dispositivos móveis está a originar um aumento de dispositivos de saúde vestíveis, levando a um crescimento na área da monitorização ambulatória. Estes dispositivos podem ser utilizados no tratamento ambulatório de doenças e seu diagnóstico, área onde já possuem uma posição de relevo, na monitorização pessoal e na melhoria do desempenho desportivo, fornecendo informações fisiológicas e ambientais ao longo das diferentes situações diárias. Actualmente, existem vários dispositivos de saúde vestíveis no mercado, sendo um deles produto da Biodevices, S.A., denominado de Vital Jacket®. Este é capaz de monitorizar, continuamente, o sinal de electrocardiograma, ritmo cardíaco e dados de acelerómetro, utilizando uma *smart* t-shirt, isto é, uma t-shirt com electrónica incorporada no tecido.

Esta Tese de Mestrado tem como objetivo propor, desenhar e implementar o primeiro protótipo de um novo dispositivo de saúde vestível, denominado VitalLogger. Este dispositivo estende a tecnologia da Biodevices, S.A., viabilizando uma possível expansão do Vital Jacket® para outros mercados.

VitalLogger é um novo dispositivo capaz de adquirir vários sinais fisiológicos e ambientais, de acordo com as preferências do utilizador, que estende o número de variáveis adquiridas pela tecnologia da Biodevices, S.A.. Antes do desenvolvimento desta extensão, foi necessário realizar uma pesquisa aprofundada sobre dispositivos de saúde vestíveis e quais os sensores/cenários com maior necessidade de monitorização ambulatória, de forma a realizar uma extensão com viabilidade económica e procura no mercado. Esta pesquisa abordou as seguintes áreas: arquiteturas dos dispositivos de saúde vestíveis e quais os sensores onde se está a fazer um maior esforço de implementação na monitorização ambulatória; sinais fisiológicos e ambientais mais necessitados, tanto na área médica como na monitorização pessoal; quais as tendências de mercado para os próximos anos, para perceber se os avanços tecnológicos e as necessidades são, economicamente, interessantes e viáveis para investir num futuro próximo. Após reunir esta informação, a Biodevices, S.A. decidiu estender a sua tecnologia de forma a adquirir valores de saturação de oxigénio, temperatura ambiental, humidade relativa ambiental e dados de giroscópio, não sendo este último implementado, por falta de tempo.

O desenvolvimento do VitalLogger consistiu na criação e implementação de uma placa electrónica que estende a tecnologia da Biodevices, S.A, sendo este processo dividido em três fases: desenho, produção e montagem da placa electrónica, recorrendo a um *software* de desenho de circuitos impressos; desenvolvimento em C do *firmware* necessário para incorporar os sensores implementados no microcontrolador, utilizando o *software* de IDE da Microchip; por fim, calibração e validação dos sensores, utilizando dispositivos comerciais.

No final, o primeiro protótipo do VitalLogger foi contruído com sucesso, obtendo-se um novo dispositivo de saúde vestível, capaz de adquirir, continuamente, valores de electrocardiograma, ritmo cardíaco, acelerómetro, saturação de oxigénio e temperatura e humidade relativa ambiente.

O VitalLogger está totalmente adaptado à tecnologia da Biodevices, S.A. e é desenvolvido a pensar nas tendências de mercado e necessidades dos próximos anos, capaz de contribuir para uma possível expansão desta empresa para outras áreas de monitorização ambulatória.

Abstract

Current mobile revolution is leading to an increase of wearable health device development and consequently a growth in ambulatory monitoring area. These systems can be applied in ambulatory diseases management and it's diagnose, a very relevant use, in personal health monitoring or in sports performance enhancement, providing physiological and ambiance data during daily normal activities. Nowadays there are several devices in the market with this type of technology, being one of them the main product of Biodevices, S.A., named Vital Jacket®. It can continuously monitoring electrocardiogram, heart rate and accelerometer data using a smart t-shirt, a t-shirt with textile embedded electronic.

This Master Thesis objective is to propose, design and implement the first prototype of a new wearable health device denominated VitalLogger. This device extends Biodevices, S.A. technology allowing a possible market expansion of Vital Jacket®.

VitalLogger is a new device capable of acquire physiological and ambiance variables according to the user preferences, extending the amount of signals acquired by Biodevices, S.A. technology. After the extension development, a deep research was made regarding wearable health devices and their sensors/scenarios with a higher ambulatory monitoring need, enabling to design an extension with economic viability and market desire. This research addressed the following areas: wearable health devices architecture and technological improvements, including in which sensors is being made a higher effort to implement them in ambulatory monitoring; the main required physiological signs to be monitored, both in medical and health areas; market trends for the next few years, understanding the economic viability of the technological advances and costumers needs. After gather all this information, it was presented to Biodevices, S.A., who decided to extend its technology to acquire oxygen saturation values, ambiance temperature, ambiance relative humidity and gyroscope data. This last one was not implemented due to lack of time.

The development of VitalLogger consisted in the design and implementation of an electronic that extends Biodevices, S.A. technology. This process was divided in three main phases: design, production and assembling of the electronic board using printed circuit board design software; development in C of the firmware needed to incorporate the implemented sensors in the microcontroller with *Microchip IDE* software; for last, calibration and validation of the sensors using commercial devices.

In the end, the first VitalLogger was successfully built, obtaining a new wearable health device capable to continuously acquire electrocardiogram, heart rate, accelerometer data, oxygen saturation values and ambiance temperature and relative humidity.

VitalLogger is totally adapted to Biodevices S.A. technology and developed according to market trends and necessities for the following years, with the possibility to contribute in a potential expansion of this company in other ambulatory monitoring areas.

Agradecimentos

Em primeiro lugar quero agradecer à minha família, principalmente ao meu Pai, à minha Mãe e à minha Irmã por me terem acompanhado durante estes cinco anos de vida universitária, pois sem a ajuda deles, todo este caminho não seria possível nem tão bem aproveitado a nível académico e pessoal como foi. Um especial obrigado aos meus Padrinhos e aos meus Avós, que estavam sempre disponíveis para me ajudar. Quero também agradecer aos meus Tios e Primos pelo acompanhamento ao longo do curso.

Durante estes cinco anos longe de casa, novas amizades foram feitas, algumas delas para o resto da vida. Agradeço a todos os que me acompanharam e viveram comigo a experiência desta vida académica, pois sem eles não seria possível viver os momentos inesquecíveis que foram passados na Invicta Cidade do Porto. Obrigado a todos e espero que daqui a uns anos possamos relembrar estes tempos com alegria e orgulho, mas principalmente para partilhar novas aventuras. Grande parte da vida académica foi também devido a Metal&Bio, um grupo académico cheio de alma e coração no qual vivi momentos únicos como estudante. Um especial obrigado a ti que estiveste sempre lá quando precisei.

Relativamente a esta Tese de Mestrado, quero agradecer ao Professor Doutor João Paulo Cunha pela oportunidade única de realizar este trabalho, que graças ao seu esforço, tem a contribuição da Biodevices, S.A.. Queria ainda agradecer a sua disponibilização para discutir todos os assuntos e problemas relacionados com este trabalho, assim como na utilização de recursos pertencentes tanto à Faculdade de Engenharia da Universidade do Porto, como ao INEST TEC Porto. A todos os membros do BRAIN-LAB um grande obrigado por toda a ajuda, assim como pelos momentos que partilhámos todos juntos. Obrigado também ao Professor Doutor Miguel Velhote por ter arguido esta Tese de Mestrado e ter referido alguns melhoramentos que contribuíram para um maior rigor científico da mesma.

A contribuição da Biodevices, S.A. neste projeto foi muito importante, pois sem eles todo o processo de aprendizagem e integração nas tecnologias utilizadas teria sido muito mais demorado. Agradeço à Catarina Ricca e muito especialmente ao Nuno Ferreira e ao Vítor Castro por todo o apoio e disponibilidade durante toda a fase de desenvolvimeto, partilhando conhecimentos e recursos necessários durante o trabalho. A experiência ganha nesta parceria foi muito gratificante para meu futuro profissional.

Por fim, quero agradecer ao Laboratório de Metrologia do Hospital de São João, nomeadamente ao Nelson Santos e ao Filipe Moreira por disponibilizarem os equipamentos necessários para realização da calibração e validação do sensor de saturação de oxigénio desenvolvido neste trabalho.

Contents

List of figures.....	xv
List of Tables	xxi
List of Acronyms	xxiii
Chapter 1	1
Introduction	1
1.1. Background and Context	1
1.2. Motivation	3
1.3. Objectives	3
1.4. Contributions	4
1.5. Work Structure	5
Chapter 2	7
Wearable Health Devices -State of the Art and Market Trends Analysis-.....	7
2.1. Generic Device Architecture	8
2.1.1. Patient or Normal Subject	9
2.1.2. Body Area Network	10
2.1.3. Portable Unit.....	13
2.1.4. Real-time Monitoring.....	14
2.1.5. Offline Monitoring	15
2.2. Wearable Health Devices Developed	16
2.2.1. Biodevices, S.A.	17
2.2.1.1. Vital Jacket® Wearable Health Device	17
2.2.2. Commercial Wearable Health Devices Available	18
2.2.3. Recent Prototypes	19
2.3. Wearable Sensing of Physiological and Ambiance Parameters	21
2.3.1. Electrocardiogram.....	22
2.3.2. Heart Rate	23
2.3.3. Blood Pressure	24
2.3.4. Respiration Rate.....	25
2.3.5. Blood Oxygen Saturation	26
2.3.6. Blood Glucose	28
2.3.7. Skin Perspiration	29
2.3.8. Capnography.....	30
2.3.9. Body Temperature	31
2.3.10. Other physiological parameters.....	32
2.3.10.1. Motion Evaluation	32
2.3.10.2. Cardiac Devices.....	32
2.3.10.3. Stroke Volume	33
2.3.10.4. Pain, Level of consciousness and Urine Output	33

2.3.11. Ambiance Parameters Measurement	33
2.4. Market and Trends Analysis	35
2.5. Challenges and Future Perspectives	39
Chapter 3.....	41
VitalLogger: An adaptable Wearable Health Device	41
3.1. System Architecture	42
3.2. Monitoring Scenarios	43
3.2.1. Description	44
3.2.2. Associated Costs	45
3.2.3. Biodevices, S.A. Development Decision	46
3.3. Hardware Development	47
3.3.1. Electronic Circuits Schematics	48
3.3.1.1. Blood Oxygen Saturation Module	49
3.3.1.2. Power Management Module	51
3.3.1.3. Ambiance Temperature and Relative Humidity Module	52
3.3.1.4. Gyroscope Module	53
3.3.1.5. External Connections Modules	54
3.3.2. Printed Circuit Board Design	54
3.3.3. Board Assembly	56
3.4. Firmware Development	59
3.4.1. Blood Oxygen Saturation Module	61
3.4.2. Theoretical fundamentals for SpO2 Calculation	65
3.4.3. Evaluation of the Best Method to Calculate the R Value	67
3.4.4. Ambiance Temperature and Relative Humidity Module	72
3.4.5. Gyroscope Module	74
3.5. Sensors Calibration and Validation	75
3.5.1. Blood Oxygen Saturation	75
3.5.1.1. Sensor Calibration	75
3.5.1.2. Sensor Validation	80
3.5.2. Ambiance Temperature and Relative Humidity Validation	84
3.6. Prototype Specifications Analysis	89
3.7. Prototype Improvements	92
Chapter 4.....	97
Conclusions and Future Work.....	97
References	99
Appendix	105
Appendix A – Second Version of VitalLogger Extension Board	105
Appendix B - VitalLogger Modular Extension Power Supply Verification	106

List of figures

Figure 1.1.1- Component Architecture of the Project where VitalLogger is inserted.	2
Figure 2.1.1 – Generic architecture of a wearable health device. Adapted from [6, 8-11]	9
Figure 2.1.2- Schematic overview of the main three data mining processes (prediction, anomaly detection and diagnose/decision making) in relation to different aspects of wearable sensing in wearable health devices. Adapted from [16].	12
Figure 2.1.3- Number of scientific papers published according to the most six used wearable sensors in WHD’s, with a distribution of the presented data mining task for each one. Adapted from [16].	13
Figure 2.2.1- Examples of wearable medical devices and prototypes. From the top in clockwise: a new ear prototype to measure several physiological parameters; smartwatch Basis PEAK™ [21]; a finger ring prototype for plethysmography; an ECG BioModule (BioPatch™) attached to normal electrodes in the chest [22]; a prototype jacket with several sensors; a wrist-worn device (AMON); and a chest belt to measure respiration rate and ECG (Bmedical®). Adapted from [4, 23, 24]	16
Figure 2.2.2- Vital Jacket® product. Beside T-shirt and portable unit, it comes with a software to analyze ECG, a portable unit charger and gel electrodes. Adapted from [25]	18
Figure 2.2.3- Smart shirts for ambulatory monitoring with CE approval. a) nECG TEXTILE from Nuubo® (MDD 93/42/EEC, ISO13485, ISO9001) [27]; b) Smartex Wearable Wellness System from Vivonoetics® [28]; c) hWear™ from HealthWatch (FDA approval) [29].	19
Figure 2.3.1- Illustration of an ECG heart cycle, with the characteristic oscillations due to the cardiac electrical activity. It is constituted by: a baseline-starting point of the electrical activity; P wave-auricular depolarization (0.11 s; 0.15 mV); P-R segment- Delay time between auricular-ventricular nodule (heart pacemaker) and ventricles (0.12 a 0.20 s); QRS complex-Ventricular depolarization, where ventricular contraction starts and auricles repolarize (0.09 s; 1.1 mV); S-T segment-temporal region where ventricles are uniformly depolarized (0.05 a 0.15 s); T wave-ventricular repolarization (0.2 s; 0.2 mV). Adapted from [40].	22
Figure 2.3.2- Respiratory waveform obtained from both chest movement (RC wave) and abdominal movement (AB wave). It is possible to observe a normal respiration waveform at the beginning and end of the image, and at the middle is it represent a stimulation of an airway obstruction where a subject closes his mouth and attempt to take in air by moving his abdomen in and out, a common test in the respiratory evaluation. Adapted from [47].	25
Figure 2.3.3- The figure represent the variation in light attenuation by tissue on colored part, and the PPG signal waveform conventionally representation. The PPG signal obtained depends of the absorption process and is composed by a Direct Current (DC) and Alternating Current (AC) components as shown in this figure. The DC component represents the transmitted or reflected signal from the tissue and depends of tissue structure and average blood volume of both arterial and venous blood. The AC component shows the blood volume variations that occurs between systolic and diastolic phases, being it fundamental frequency dependent of the heart rate. Adapted from [42].	27

Figure 2.3.4- Capnography waveform illustration, composed by a periodic sign that reflects the CO₂ partial pressure during a respiratory cycle. A – during a normal respiratory cycle CO₂ partial pressure varies according to the illustration and is divided in four phases: I, II, III and 0 that correspond to the inspiration. Just before this action, a maximum pressure of CO₂ is verified, nominated as end-tidal PCO₂ (PETCO₂). Arterial PCO₂ is always higher than the higher level of PCO₂ measure due to the alveolar dead space. B – Capnography volume different components which are correlated to the expired volume of air. C – An example of a recorded time capnogram during cesarean delivery general anesthesia (phase IV corresponds to PETCO₂). Adapted from [68]..... 30

Figure 2.4.1- Shipments of wearable computing devices worldwide by category from 2013 to 2015 (in millions). Adapted from [79]..... 35

Figure 2.4.2- Shipments of smart clothing/fabrics worldwide from 2013 to 2015 (in millions). Adapted from [80]..... 36

Figure 2.4.3- mHealth Wellness/Sports & Fitness Device Market (in millions). The orange color is referred to connected weighing scales. Adapted from [81]..... 36

Figure 2.4.4- Connected home medical monitoring devices (in million). Adapted from [82]. 37

Figure 2.4.5- Growth rate of China wearable mobile medical equipment market from 2012 to 2017. Adapted from [83]. 37

Figure 2.4.6- The World Market for Telehealth – Patient by Conditions. This is a patient distribution made for 2014 with a total number of patients of 725 thousand. Adapted from [84]. 38

Figure 2.4.7- Ambulatory/Home Portable Sleep Testing Devices (Left axis: Unit Shipments; Right axis: Growth percentage). Adapted from [84]..... 38

Figure 3.1.1 – Component Architecture where VitalLogger is inserted. VitalX is the Android platform where all the sensors data are collected, including VitalLogger device. 42

Figure 3.2.1 - Wearable health devices ambulatory monitoring scenarios, with the respective wearable sensors setup, according to each scenario needs..... 44

Figure 3.3.1-Component diagram of VitalLogger prototype..... 47

Figure 3.3.2- Schematic representation of the developed prototype hardware architecture, representing each developed module and their SPI communication interaction..... 48

Figure 3.3.3- Sampling cycles of AFE4400. This images shows two complete cycles of acquisition and ADC conversion [86]. 50

Figure 3.3.4- AFE4400 adapted schematic implemented in VitalLogger prototype [86]..... 51

Figure 3.3.5- AFE4400 power management adapted schematic implemented in VitalLogger prototype [87]..... 52

Figure 3.3.6- HIH6130 adapted schematic implemented in VitalLogger prototype [88]. 53

Figure 3.3.7- LSM330DLC adapted schematic implemented in VitalLogger prototype [89]..... 54

Figure 3.3.8- PCB design of VitalLogger extension board first prototype. The left image shows the top layer and the right image the bottom layer..... 55

Figure 3.3.9- 3D model of the VitalLogger extension board first prototype. The left image shows the top view of the prototype and the right image the bottom view..... 56

Figure 3.3.10- Produced PCB of the first VitalLogger prototype. 57

Figure 3.3.11- The first version of VitalLogger prototype assembled with each module and connector label..... 57

Figure 3.3.12-VitalLogger first prototype connected to a main board through a flat connection. 58

Figure 3.3.13- VitalLogger first prototype connected to the main board and with the Oxygen Saturation sensor plugged in. 58

Figure 3.4.1- Workflow diagram representing the main file of the developed firmware..... 59

Figure 3.4.2- SPI digital acquisition of the initialization process. First the pins are initialized such as the SPI microcontroller module. The HIH6130 initialization occurs when its slave select (“SS_T&H”) goes down, which is a very quick process. Just after that the AFE4400 slave select (“SS_AFE4400”) goes active to start AFE4400 initialization process that will be discuss in the following topic. 60

Figure 3.4.3- SPI digital acquisition of the first cycle including the initialization. First it is visible a higher density of SPI communication which represents the initialization referred above. Then a reading until 100 samples it’s made. The following space without communication corresponds to the time where the oxygen saturation value is computed and then an ambiance temperature and relative humidity reading is performed. It is still possible to view the start of a new reading, without the initialization process. 61

Figure 3.4.4- Workflow diagram representing the AFE4400 initialization process. 62

Figure 3.4.5- SPI digital acquisition showing the process to get a reading from AFE4400. First, AFE4400 slave select (“ENABLE”) is activated (value zero) and then the first 8 bits send the register address that the microcontroller wants to get the information. The next 24 bits are received by the microcontroller and represent the value of the requested register. 63

Figure 3.4.6- SPI digital acquisition of the process to acquire both needed readings to obtain oxygen saturation signal from the Red and the Infrared LEDs. The readings have some space after them due to a debug process that is not implemented in the final firmware version. The ADC_RDY is represented in the last channel and is constantly being actualized. After some tests, it was possible to verify its independence with the reading process, being disconnected from the microcontroller..... 63

Figure 3.4.7- Sampling acquisition procedure to acquire the oxygen saturation curve..... 64

Figure 3.4.8- Oxygen saturation sensor acquisition with the VitalLogger prototype, showing the PPG waveform. The left image represents the acquired signal and the right image represents an inversion of this signal..... 64

Figure 3.4.9- Absorbance spectrum of oxyhemoglobin (HbO₂) and deoxyhemoglobin (Hb) from 600nm to approximately 1000nm. The wavelengths used in pulse oximetry are represented in a red stripe for the Red source (660nm) and in a blue stripe the Infrared source (910nm). Adapted from [92]. 65

Figure 3.4.10- Example of an oxygen saturation curve that correlates the R value with the oxygen saturation level with a polynomial second degree equation. Adapted from [91]..... 66

Figure 3.4.11- Workflow diagram representing the signal processing made until the R value calculation..... 68

Figure 3.4.12- Example of the signal processing steps made before R value calculation using a signal acquired on a human finger with the developed prototype. To obtain this signal the number of samples restriction was increased to 150 and the finger was moved during the acquisition. The first image (top left) represents the signal acquired by the prototype. The second image (top right) shows the signal after the first mean filter (N=3). The third image (bottom left) shows the normalization result of both waves. The last image (bottom right) represents the final signal after the baseline construction..... 69

Figure 3.4.13- Photoplethysmograph signal obtained using the developed prototype and acquired from the oxygen saturation simulator at 80 BPMs. In this case, the signal processing and R value calculation (“MaxMin Method”) were both made using the developed *MATLAB* script. The abscissa values correspond to the number of the sample and the ordinate values to integer values acquired from the sensor, but these do not represent the acquired voltage..... 71

Figure 3.4.14- Workflow diagram representing the HIH6130 reading cycle. 72

Figure 3.4.15- SPI digital acquisition of the HIH6130 reading cycle, where the slave select channel is represented by the “ENABLE” channel. The time distance between the measurement request command and the reading is approximately 50ms as it can be seen in the “width” measurement represented in the right corner of the figure..... 72

Figure 3.4.16- SPI digital acquisition of the HIH6130 data request made by the microcontroller. 72

Figure 3.4.17- SPI digital acquisition of the HIH6130 reading process. First 32-bit represents the temperature reading and the remaining 32-bit represents the relative humidity reading..... 73

Figure 3.4.18- Workflow diagram representing the working cycle of LSM330DLC gyroscope sensor. First it is represented the initialization process and then the reading process..... 74

Figure 3.5.1- This image shows the *FLUKE* simulator device and the prototype during the calibration process. The prototype was connected with a laptop through a Bluetooth connection, sending the calculated R values. 76

Figure 3.5.2- Graphical representation of the correlation between the R value obtained from 60 to 180 BPM (differences represented by the standard deviation) and the oxygen saturation level. The respective trendline and square error from the acquired samples are below the graphic legend..... 77

Figure 3.5.3- Two different calibration curves obtained due to a different position in the simulator probe. For these tests it was used only the oxygen saturation levels at 80 BPMs..... 78

Figure 3.5.4- Workflow diagram of the automatic adjustment of the sensor LEDs supply current. This is performed after verifying that the finger is inserted in the sensor. After the acquisition of HIH6130 the “Adjustment made” is equaled to “no”. The samples acquired in this procedure are not use in the oxygen saturation calculation, for which 100 samples are needed. 79

Figure 3.5.5- Calibration curve obtained with the new calibration made using the new voltage regulator. The respective trendline and square error from the acquired samples are below the graphic legend..... 80

Figure 3.5.6- Apparatus used in the validation procedure of the oxygen saturation values. In this image it is possible to see the *Philips* device with its SpO₂ sensor and the VitalLogger Prototype also with its SpO₂ sensor. The external laptop Bluetooth is also present to acquire VitalLogger transmitted data..... 81

Figure 3.5.7- First test experimental results obtained during the acquisition of oxygen saturation percentage values to validate the prototype values. This image presents the values from VitalLogger prototype and *Philips* device during the acquisition of one hundred samples. 81

Figure 3.5.8- On the right side is represented the Bland Altman plot (blue line-mean difference; red lines- limits of agreement; red dotted line- mean difference CI; blue dotted line- limits of agreement CI). On the left side a distribution plot of the differences is presented. Although normality is not accepted according to D’Agostino-Pearson test (P=0.0465), due to its very small difference from normality acceptance the Bland Altman plot was done considering that the differences are normally distributed..... 82

Figure 3.5.9- Experimental results obtained during the second test made in the validation procedure. This image presents the values from VitalLogger prototype and *Philips* device during the acquisition of twenty samples. 83

Figure 3.5.10- On the right side is represented the Bland Altman plot (blue line-mean difference; red lines- limits of agreement; red dotted line- mean difference CI; blue dotted line- limits of agreement CI). On the left side a distribution plot of the differences is presented. Normality of the differences is accepted according to D’Agostino-Pearson test (P=0.9693)..... 83

Figure 3.5.11- In this image it is possible to observe the *Velleman* device and the developed prototype inside the container to simulate a different atmosphere from the one in the outside. 84

Figure 3.5.12- This image shows both devices sensors, visualizing their high proximity. In the red circle is the prototype HIH6130 sensor and in the blue circle is the *Velleman* device air entry. 85

Figure 3.5.13- Graphical representation of the samples acquired from the *Velleman* device and the developed prototype during the procedure above described..... 85

Figure 3.5.14- Calibration curves obtained from the experimental results presented in Figure 3.5.5. The left image represent a graphical representation of the samples from *Velleman* device versus the developed prototype and the respective regression line. The right image shows the same relation but for the relative humidity samples..... 86

Figure 3.5.15- Graphical representation of the obtained values after the adaptation of the regression lines. The calculation was made in the computer applying the regression lines to the already obtained samples values. 86

Figure 3.5.16- On the right side is represented the Bland Altman plot (blue line-mean difference; red lines- limits of agreement; red dotted line- mean difference CI; blue dotted line-limits of agreement CI). On the left side a distribution plot is presented. Although normality of the differences is not accepted according to D’Agostino-Pearson test ($P=0.0473$), due to its very small difference from normality acceptation and shape, the Bland Altman plot was done considering that the differences are normally distributed. 87

Figure 3.5.17- On the right side is represented the Bland Altman plot (blue line-mean difference; red lines- limits of agreement; red dotted line- mean difference CI; blue dotted line-limits of agreement CI). On the left side a distribution plot of the differences is presented. Normality of the differences is accepted according to D’Agostino-Pearson test ($P=0.5561$)..... 87

Figure 3.6.1- Final developed VitalLogger prototype system with the following sensors: electrocardiogram (ECG) and heart rate and tri-axis accelerometer from the main board and oxygen saturation percentage and ambiance temperature and relative humidity from the developed extension board. 90

Figure 3.6.2- Windows SDK application from Biodevices, S.A. during a normal acquisition from VitalLogger prototype. It is possible to see the new variables above the ECG waveform..... 91

Figure 3.6.3- Windows SDK application from Biodevices, S.A. during a normal acquisition from VitalLogger prototype, but without a finger inserted in the oxygen saturation sensor..... 91

Figure 3.7.1- Programming connector used to program the microcontroller in the module. This connector has six connections with spring connector and three metal guides to help in the connector positioning in the board. It is developed by Tag-Connect and the other side of the cable is an internet connector (RJ12 connector) that plugs directly to ICD-3, which is the programmer used in this work. [97]..... 92

Figure 3.7.2- New VitalLogger components architecture with the new suggested module implemented in the main board. 93

Figure 3.7.3- Microcontroller schematic (PIC18F26K20_Spo2) designed for this module application. In the left bottom of the image is represented the schematic of the programming connector (TC1) and below is the pull-up resistor used in the 3.3V supply voltage. [97, 98]..... 93

Figure 3.7.4- Adapted schematic of the AFE4400 module from the developed module prototype to be included in this new module unit. 94

Figure 3.7.5- Adapted schematic of HIH6130 module from the developed prototype to be included in this new module unit..... 94

Figure 3.7.6- Printed circuit board layers of the new module unit (top layer-left image; bottom layer-right image)..... 95

Figure 3.7.7- 3D model of the new developed module unit. The label in the figure indicates the main components and the AFE4400 module..... 95

Figure A. 1- PCB design of VitalLogger extension board second prototype that was not produced. The left image shows the top layer and the right image the bottom layer..... 105

Figure A. 2- 3D model of the VitalLogger extension board second prototype that was not produced. The left image shows the top view of the prototype and the right image the bottom view. 106

Figure A. 3- Prototype extension board adaptation to test the direct power supply of 3.3V and 5V..... 106

Figure A. 4- TXP (yellow signal) and TXN (green signal) signals obtained, when the sensor is disconnected, from the developed prototype extension (left image) and from the board with a new configuration (right image). 107

Figure A. 5- TXP (yellow signal) and TXN (green signal) signals obtained, when the sensor is connected, from the developed prototype extension (left image) and from the board with a new configuration (right image). 107

List of Tables

Table I- The most used vital signs in WHDs, its source and some of the sensors technologies used to measure each one. Adapted from [4, 9, 11-15]	11
Table II- List off all the Physiological/ Ambiance Variables needed to be implemented to complete all the setups of sensor from each scenario. For each sensor it is made a public cost estimation based on the referred approaches made for each sensor, regarding its technology and way to wear or use.	45
Table III- Public cost estimation for each setup of sensor of the presented scenarios. This estimation is based on the values presented in the individual sensor cost estimation.	46
Table IV- Values of Oxygen Saturation levels and heart rate (BPM) levels simulated by the simulator device. For each value of these two variables the other variable can assume all the referred values. For example, for a 70% of oxygen saturation, it is possible to simulate this level in all the heart rate levels presented in the table.	67
Table V- This table shows the mean values and respective standards deviation of the R value result for each oxygen saturation level when the heart rate frequency goes from 30 to 240 BPMs according to the simulator scale. The R value is calculated using two methods, “MaxMin” and “By Parts” in order to analyze the best method to calculate the R value.	70
Table VI- This table shows the mean values and respective standards deviation of the R value result for each oxygen saturation level when the heart rate frequency goes only from 60 to 180 BPMs according to the simulator scale. The R value is calculated using two methods, “MaxMin” and “By Parts” in order to analyze the best method to calculate the R value.	70
Table VII- This table shows the R values obtained for each oxygen saturation level at 80 BPMs in the oxygen saturation simulator. The R values presented in the “ <i>MATLAB</i> ” column are the ones calculated using the <i>MATLAB</i> script and the values obtained directly from the microcontroller on the developed prototype are represented in the “Prototype” column. The last column shows the error percentage of Prototype obtained values in relation to the values obtained using the <i>MATLAB</i> script.	71
Table VIII- This table shows the associated costs of the VitalLogger second version prototype regarding the electrical components and PCB costs per each unit produced according to the number of units produced. In the last column of the table a total cost per unit is presented.	89
Table IX- This table shows the associated costs of the designed module regarding the electrical components and PCB costs per each unit produced according to the number of units produced In the last column of the table a total cost per unit is presented.	96

List of Acronyms

WHD	Wearable health device
BAN	Body Area Networks
CVD	Cardiovascular Diseases
ECG	Electrocardiogram
HR	Heart Rate
BP	Blood Pressure
SpO ₂	Blood oxygen saturation
DC	Direct Current
AC	Alternating Current
LED	Light-Emitting Diode
RR	Respiration Rate
BG	Blood Glucose
PU	Portable Unit
MDD	Medical Device Directive
FDA	Food and Drug Administration
PPG	Photoplethysmography
CHF	Congestive Heart Failures
RIP	Respiratory Inductive Plethysmography
ANS	Autonomic Nervous System
GSR	Galvanic Skin Response
CO ₂	Carbon Dioxide
ICU	Intensive Care Unit
SV	Stroke Volume
SPI	Serial Peripheral Interface
PCB	Printed Circuit Boards
AFE	Analog Front End
SS	Slave Select
SCLK	Serial Clock
MOSI	Master Output/Slave Input
MISO	Master Input/Slave Output
TX	Transmit Route
RX	Receive Route
ADC	Analog-to-Digital Converter
ADC_RDY	ADC Ready
HbO ₂	Oxyhemoglobin
Hb	Deoxyhemoglobin
FFT	Fast-Fourier Transform
BPM	Beats Per Minute
SD	Standard Deviation
CI	Confidence Interval

Chapter 1

Introduction

Wearable Health Devices are becoming one of the next generations gadgets, regarding medical and personal use. Besides their medical applications, these monitoring devices are increasing their reputation in personal monitoring, leading to a self-monitoring between athletes and common people to get information about their physiologic status anytime and anywhere. Wearable health devices are expanding their application to be included in daily activities, so there is a need for improving their technology to get higher viability, portability and autonomy.

This Master Thesis was developed in the Faculty of Engineering of the University of Porto and in INESC TEC Porto with the collaboration of Biodevices, S.A. The aim of this work directly related to wearable health devices, presenting the development of a wearable health device prototype that can be implemented as a possible future product. This work was included in the Biomedical Research And INnovation LABoratory (BRAIN-LAB), one of the I&D groups hosted in INESC TEC Porto, and supervised by Professor Ph.D. João Paulo Cunha.

1.1. Background and Context

Wearable health devices are able to continuously monitoring physiological parameters for several purposes, from a simple fitness activity, evaluating human body response during physical efforts to a medical situation where patients' monitoring, inside and outside clinical environments, is indispensable. The use of wearable health devices in fitness and wellness as also in healthcare and medical applications is increasing and a higher viability of these devices is

leading to a revolution in this area, which is expected to grow about 30% only this year comparing to the last one, according to IHS Inc. [1]

Nowadays, people have a higher desire to monitoring their human body with new gadgets. Wearable health devices meets this recent trend, being able to monitor one or more vital signs using one or more small wearable devices, registering vital data and/or sending it in real-time using wireless protocols or mobile communications. These characteristics allow medical specialists to receive patient's physiological data anywhere, improving healthcare conditions, lowering clinical costs and enabling the acquisition of vital parameters during daily activities. [2, 3] There are already commercial devices with all these requirements and with multiple physiological signs acquisition, but normally only for personal use because most of them are not certified as medical devices to be used in clinical environment, providing viable medical information. Vital Jacket®, from Biodevices, S.A., is one of the few exceptions to the previous statement. It is the first worldwide certified smart t-shirt medical device, able to acquire and record ambulatory electrocardiogram (ECG) signal, with a Bluetooth connection to transmit real-time ECG data to a mobile device, if required.

Although Vital Jacket® is on the top edge of technology, it is always good to think in possible new market expansions to this product. This Master Thesis is inserted in this theme, presenting a new device, named VitalLogger, containing an implementation for a possible expansion of Vital Jacket® device. This possible expansion can contribute to help medical specialist in disease prevention, prediction and management of disorders. This possible expansion will also result in a more reliable and useful device, when compared to a single physiological parameter monitoring device [2]. More monitored parameters can also increase the commercial desire outside clinical areas, providing a more complete monitoring of human body, during daily activities and wellness or sport activities. This is an important aspect which is considered to have a direct influence in personal health monitoring, leading to a healthier worldwide population [4].

VitalLogger development is part of a bigger project that includes another student's Master Thesis projects. This big project has the aim to aggregate and synchronize as many vital and ambiance data as possible according to the user desire as it is explained in the beginning of Chapter 3. Figure 1.1.1 shows a resume of this bigger project, where VitalX, an Android application developed in another student Master Thesis, has an aggregate module that is able to gather, synchronously, all the data from external devices and smartphone sensors. The communication between VitalLogger and smartphones was also developed by another student during his Master Thesis project. This Master Thesis focus on the implementation of new sensors in VitalLogger and in the development of the low level firmware needed.

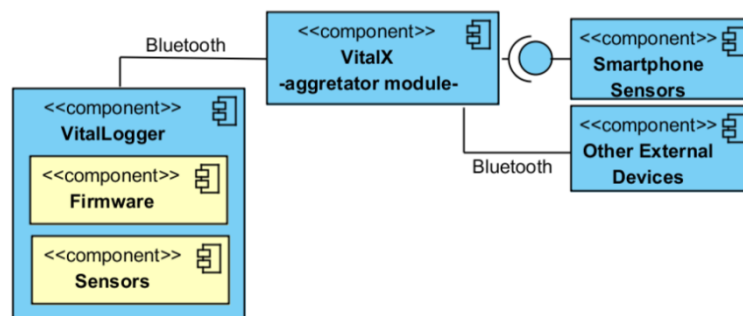


Figure 1.1.1- Component Architecture of the Project where VitalLogger is inserted.

1.2. Motivation

Wearable health devices are evolving fast nowadays, attracting all kind of persons to use them on the daily activities, including medical specialist to get continuous physiological data from their patients to perform a reliable diagnostic or disease monitoring.

The application of new electronic technology to capture physiological signs is one of the Biomedical Engineering areas, joining the human physiology with the electronic development. The physiological knowledge allows understanding human signals origin and its meaning in the human health; the electronic skills are important to be able to design a device capable to acquire these signals, using nowadays technologies or developing new ones. The relation between these two areas is increasing and leading to new technological advances in human body monitoring.

To endorse my knowledge about this emerging area, nothing better than make a Master Thesis related to it, mainly when the work is made with the contribution of one of the pioneering companies on this area, Biodevices, S.A.

This Master Thesis objective to create a proposal of a possible extension implementation for a wearable health device, that is already a product, is one of a kind opportunity. In this experience it was possible to apply knowledge acquired during this Master Degree and learned how to transform it in a commercial product with a promising place in the market.

1.3. Objectives

This Master Thesis covers different areas related to wearable health devices, regarding their technology, how do they work, market trends and health and medical approaches. The development phase of this work is based on the creation of a prototype to extend an existing wearable health device, creating, for the first time, the VitalLogger device.

This work main objective is to propose a possible market expansion to Biodevices, S.A. with a VitalLogger prototype containing more sensors, being capable to acquire more physiological data from the user. To perform such proposal, this work presents what is close to a complete process to decide and implement a new wearable health device prototype. After the prototype development itself, a research was made based on health and medical ambulatory necessities and their market viability, choosing and understanding what will be the best technological bet in this area. To perform all this process this work is divided in four main objectives.

First one is to better understand how wearable health devices works, their generic architecture and the most recent technological advances worldwide in this area to comprehend in which branches of these devices is being made a higher effort in technological advances.

The second objective is to research and analyze which are the most wanted and needed physiological parameters to be measured in an ambulatory monitoring, regarding a medical

approach and also a health approach, including self-monitoring, an area with a high growing nowadays.

The third objective is related to the market and its future trends. An analysis of this area has a major importance when a product is proposed to a company, supporting its market viability and future sales profit. An overall market research was performed and then each wearable health device segment was deeper analyzed to obtain a feasible information about the future of this emerging area.

Last, but not least objective is the prototype development. To get a decision from Biodevices, S.A., it was presented a proposal with the most promising monitoring scenarios and respective set of sensors based on the research made. Joined to this proposal, a market and trends analysis such as associated costs estimation were also presented to better support the company decision. The company verdict and forth objective of this Master Thesis is to develop a possible implementation of a prototype capable to extend their technology to acquire four new variables including oxygen saturation level, ambiance temperature and relative humidity and gyroscope data, taking the first step in the VitalLogger prototype.

1.4. Contributions

This Master Thesis had two main contributions, one that is related to personal skills improvement, and other related to Biodevices, S.A. and their possible future expansion.

Regarding the personal experience, this work was challenging, mainly in the prototype development phase where firmware and production hardware were made for the first time. The direct connection with Biodevices, S.A. personnel is one of the main enrichments of this work, leading to a faster learning process and easier adaptation to their technology. In the end, with the acquired skills during this Master Thesis concerning all the process from wearable health devices research passing for market analysis and ending in a product conception is going to be part of my personal education. This is one of the main contributions of this work because it will allow expanding my knowledge by learning new engineering areas that were not covered during this Master graduation and are directly related to future personal career interests.

The collaboration of Biodevices, S.A. in this Master Thesis was an added value, enabling to contribute in a possible market expansion of this company regarding the implementation of new sensors. The final proposed prototype is totally adaptable to the most recent technology of Biodevices S.A. being totally able to be incorporated in their device and, who knows, be part of a possible future product. Moreover, this new prototype as the aim to contribute for the growing of wearable health devices worldwide, proposing a new device with real-life application that can contribute for a better health monitoring and human well-being.

The collaboration of Biodevices, S.A. would never be possible without the non-disclosure agreement with INEST TEC. This Master Thesis was developed under this association, contributing to a higher proximity of these two identities, which directly led to a higher share of knowledge, technology and resources.

1.5. Work Structure

This Master Thesis is divided in 4 chapters. After first Chapter of introduction, three more chapters are presented: the second one is related to the wearable health devices research made; the third Chapter with the prototype development process; and the fourth Chapter makes some final remarks and conclusions, as also a discussion about what can be made as future work.

Chapter 2 presents wearable health devices according to the literature in this area. The components architecture of these devices consists in the interconnection between several modules, so, an analysis of each one is made, discussing possible functionalities variations. Then, Biodevices, S.A. is presented, including their own wearable health device named Vital Jacket®. After this, some similar commercial devices and recent prototypes are shown to a make technological and market comparison. The following topic is focused on physiological signs in ambulatory monitoring, regarding two main aspects: medical specialists need to get the most complete monitoring from their patients to obtain reliable physiological information in ambulatory cases; nowadays society needs in their life care improvement and self-monitoring activities. The devices used to acquire each physiological sign are covered, regarding their technologies, implementations and also some recent prototypes in wearable health devices area. Still in Chapter 2, after this discussion regarding wearable health devices and wearable sensors, it is shown and analyzed a market and trends analysis of wearable health devices with the aim to understand which areas of these devices will have a higher economical viability to invest in a near future. In the end of this Chapter, future perspectives and challenges in wearable health devices are covered, understanding their main barriers to overcome in the following years.

The development phase of this Master Thesis is presented in Chapter 3. First, the proposal made to Biodevices, S.A. is discussed regarding the chosen scenarios and their set of sensors according to the previous research. Then, an estimation of the cost associated to each scenario is done and the decision of Biodevices, S.A. presented. The following topics of this Chapter are related to all the prototype development process. The next step presented is the calibration and validation of the sensors implemented in the developed prototype. To finalize this development Chapter, a new prototype is designed with some improvements and with a higher ability to easily integrated in Biodevices, S.A. technology, granting also a higher viability in a possible implementation for a possible future market expansion.

In the final chapter of this Master Thesis, Chapter 4, some conclusions are presented such as suggestions for future improvements and future work, in order to achieve a prototype even more close to be incorporated in Biodevices, S.A. technology.

Chapter 2

Wearable Health Devices

-State of the Art and Market Trends Analysis-

Wearable Health Devices (WHDs) consists in the interconnection of several modules that are capable to monitoring human vital signs during a person normal day during work, at home, during sport activities or in a clinical environment, without interfering with the normal human activity and comfort [5].

WHDs are a specific category of personal health systems, a concept introduced in the late 90s, with the purpose to place the individual citizen or patients in the center of the healthcare delivery process, managing its own health and interacting with care providers. This has the aim to raise people interest about their health status, improving the quality of care and making use of the new technology capabilities. These devices create a synergy between multiple science domains such as biomedical technologies, micro and nanotechnologies, materials and electronic engineering and information and communication technologies. [3, 6]

In a common situation, when a patient needs to be monitored, it is necessary for him to be hospitalized with expensive equipment and medical personnel on hand. Using wearable health devices it is possible to obtain a ubiquitous ambulatory monitoring of vital signs over extensive periods and outside clinical environment. This feature allows to obtain vital data during different daily activities than a traditional clinical acquisition, ensuring a better support in medical diagnosis and/or helping in a better and faster recovering from a medical intervention or body injury. [2]

Wearable health devices can be used in many medical situations according to patient disease or rehabilitation program, but are also very useful in sport activities to monitor athlete performance or even in fire fighters and combatants to evaluate and monitor their body

response in different situations. Independently of the WHD purpose there are four main constraints on its design: low power requirements, reliability and security, comfort and an adapted design for the human body. [2, 7]

According to IHS Inc. WHDs only in fitness and wellness applications will increase 23.2% this year, and then will have a rate of growing of about 9% per year until 2019. The application of WHDs in healthcare and medical environments will growth 6% this year, but in 2019 it is expected to grow 10%, corresponding almost to \$15 billion only in 2019. [1]

This chapter will start with a description of WHDs generic architecture, making a division in several modules, discussing each one and the main variations between developed devices. Then, the main types of WHDs already developed are going to be introduced, including some commercial WHDs and recent prototypes. In this section Biodevices, S.A. and their WHD, named Vital Jacket®, are going to be presented and this smart t-shirt is going to be compared with other similar commercial products. After this, a discussion will be presented about the most needed physiological and ambiance parameters to be monitored in ambulatory situations concerning medical, personal healthcare, fitness/wellness and sport activities areas. To understand how WHDs market will evolve, a market and trends analysis will be presented according to the areas referred. In the end, a future perspective and challenges regarding the introduction of these devices in the community will also be discussed.

2.1. Generic Device Architecture

Since the last decade, due to a higher elderly population and to the emergence of chronic diseases, the research interest in wearable physiological measurements devices has been growing, resulting in the development of many different devices. This effort is resulting in small wearable devices, with the benefits of a lower cost and higher mobility while the physiological data is being collected. [2]

A research was done with the purpose to create the most global possible device architecture with features from several wearable devices already developed, such as researched prototypes and commercial products. The generic architecture is presented in figure 2.1.1, and is mainly divided in four modules. The first one is the human body that can be from a patient with a disease that has the need to be monitored or from a normal person with the aim, for example, to monitor his personal vital sings during fitness activities. Then, the vital signs are captured by biosensors, being this the second stage of the workflow. These sensors can also measure ambiance variables, capturing, for example, temperature or relative humidity of the air around the person. This second module of the WHD is defined as the Body Area Networks (BAN), a very used terminology to describe the sensors around the human body. All these electrical analog signs goes to a portable unit (third module), where they are processed and stored or/and sent to other devices, allowing vital signs monitoring in real-time during long periods. The last module of WHDs architecture is divided in two, online and offline monitoring. This allows the visualization and analysis of the captured signals in real-time or In the end of a certain period. The following topics will explain each of these modules from the architecture, to better

understand each one and its several variations according to some existing wearable health devices. [8, 9]

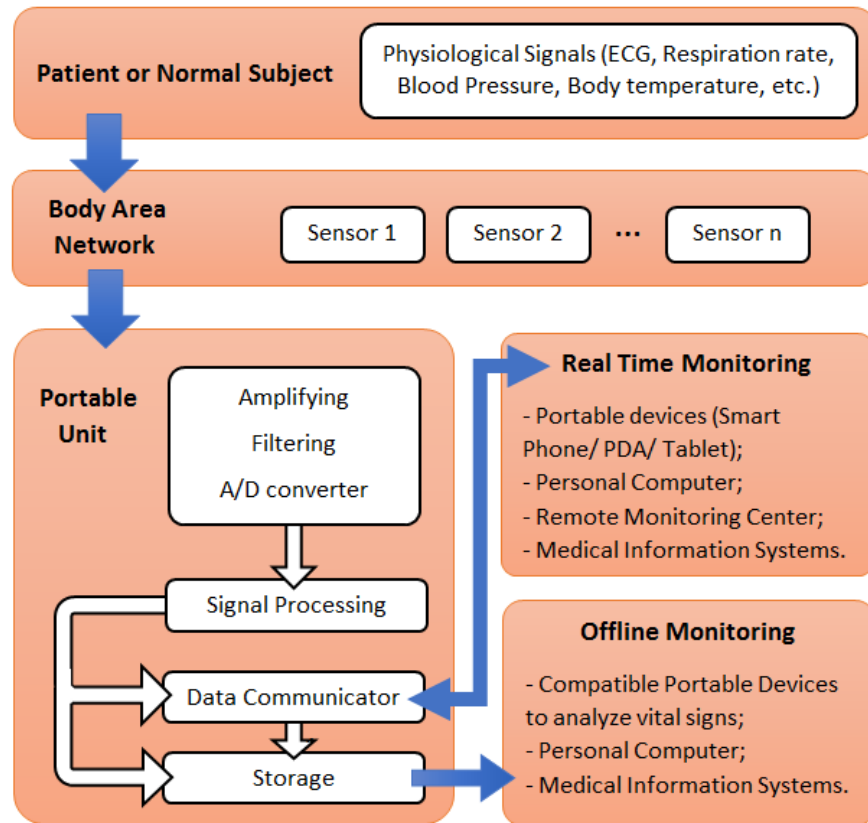


Figure 2.1.1 - Generic architecture of a wearable health device. Adapted from [6, 8-11]

2.1.1.1. Patient or Normal Subject

The use of a WHD is not only necessarily to be included in clinical cases monitoring, but also to be used in normal subjects, such as in fitness, wellness and sport activities, being perfectly adapted to all these situations. Monitoring patient’s health out of the hospital environment is growing due to the increase of healthcare costs and the ageing of the world population. In this way, WHDs can provide real-time information about health’s condition, transmitting it to a medical center or to a supervising professional. This enables to alert patients from a possible imminent health threatening independently of the place where he is. [11]

There are several physiological signs that can be measured, gathering information with the aim to obtain an overall estimation of the subject health condition at any time. In order to understand the applicability of WHDs in patients with different diseases and in normal subjects, a resume approach of clinical cases where WHD can be used is going to be presented in section 3 of this Chapter.

According to The World Health Organization, it is expected that, in 2015, 20 million deaths will happen due to cardiovascular diseases (CVD), and an effort is being made to reduce this

number, implementing WHDs in the clinic. As European guidelines on CVD refer, the best prevention in cardiovascular disease is to frequently monitor blood pressure, a problem that WHDs can solve, using several methods as it will be discussed in section 3. Electrocardiogram (ECG) and blood oxygen levels measurements can be used to diagnose early signals or cardiac abnormalities leading to better outcomes in cardiac patients. As an example, atrial fibrillation, a common cardiac disorder and sometimes asymptomatic, in most patients is not diagnosed until worse heart conditions, like heart attack or stroke. A recent study proved that *AliveCor's*, a WHD, has a higher sensitivity and specificity than a standard 12-Lead ECG normal device, providing accurate and reliable data for an earlier detection of atrial fibrillation. Respiration rate can also be measured to monitor coughing events and other respiratory variables. [12]

Glucose monitoring using a WHD is a great benefit for patients who suffer from diabetes allowing a continuous self-monitoring, resulting in a higher patient autonomy. It also provides a more effective process to manage the disease, indicating the right quantity of insulin to prevent hypoglycemia complications. [4, 12]

Another area where WHDs can be used is in neurological function monitoring, mainly in the post-operative management, outpatient care and rehabilitation areas. Here, the devices are used to analyze gait, limb paralyse and cerebral palsy, and have the capability of early detect Parkinson's and Alzheimer disease in apparent normal patients. [12]

In physical therapy and rehabilitation WHDs are also used to monitor patient mobility, but with the aim of provide objective criteria of the patient progression through therapeutic exercises analysis. This feature helps in the improvement of exercises techniques, minimizing therapeutic recovery time. With a real-time analysis device it is possible to generate alerts providing guidance and feedback to the patient according to the activity level and ambient conditions. [4, 12]

Beside patients, WHDs are used also in sports, mainly in highly competitive teams. The tracking of physiological signals and body kinematics during exercise provides information that helps in a better understanding of the athlete and possible improvements on his performance. An example is the study of how a race driver responds during simulated conditions, analyzing sweat and heart rate for instance. [4]

2.1.2. Body Area Network

Body Area Network (BAN) is defined as the amount of sensors that acquire vital signs from the human body and are connected to a main unit through wires or wireless communication protocols. These sensors can be placed in different parts of the body and nowadays are being combined with textiles resulting in the so-called smart fabrics, providing a more comfortable and user-friendly way to monitor human body physiological parameters. [9]

For each physiological sign referred in the previous topics, there can be one or more ways to measure it requiring different technologies and sensors. The following table (Table I) resumes some of the sensors used to measure health parameters with WHDs. The selection of these vital parameters was based on the most referred vital signs parameters used in developed WHDs present in the researched literature of this study.

Table I- The most used vital signs in WHDs, its source and some of the sensors technologies used to measure each one. Adapted from [4, 9, 11-15]

Type of Bio-signal	Signal Source	Type of sensor
Electrocardiogram (ECG)	Electrical activity of the heart	-Skin/chest electrodes
Heart Rate (HR)	Frequency of the heart cycle	-Pulse oximeter -Skin electrodes -Optical -Radio-frequency identification -Phonocardiograph
Blood pressure (systolic and diastolic) (BP)	Force exerted by circulating blood on the walls of blood vessels, especially in arteries.	-Ultrasound -Arm cuff-based monitor
Blood oxygen saturation (SpO₂)	Oxy-hemoglobin that is being transported in blood vessels.	-Pulse oximeter
Respiration Rate (RR)	Chest movement giving inspiration and expiration per unit time	-Elastomeric, impedance and respiratory inductive plethysmography -Extracted from ECG
Blood Glucose (BG)	Amount of glucose (main type/source of sugar/energy) in blood	-Strip-based glucose meters -Ocular glucose meter -Tissue glucose meter
Perspiration or skin conductivity	Sweat glands activity which is associated with skin electrical conductivity	-Woven metal electrodes -Electrochemical electrodes
Body and/or Skin temperature	Body and/or skin temperature	-Temperature probe -Skin patch -Radio-frequency identification -Optical Infrared thermometer

The vital signs presented in the previous table, except perspiration and body and/or skin temperature are the main used sensors to perform three predominant data mining task in medical environment using WHDs: prediction, anomaly detection and diagnosis. To better analyze these three data mining tasks, figure 2.1.2 shows a schematic overview of these three processes in relation to three dimensions. On the bottom of this figure are two main places where patients are monitored (Home or Clinical), where clinical settings are typically focused on diagnosis making. On the top of the image it is made a distinction of subjects, between healthy subjects or patients. On the left of the figure are presented two possible data processing methods, an online or an offline method. The figure also present a subtask named Alarm, mainly used in patients, facilitating independent living in home environments and increasing the sense of security. [16]

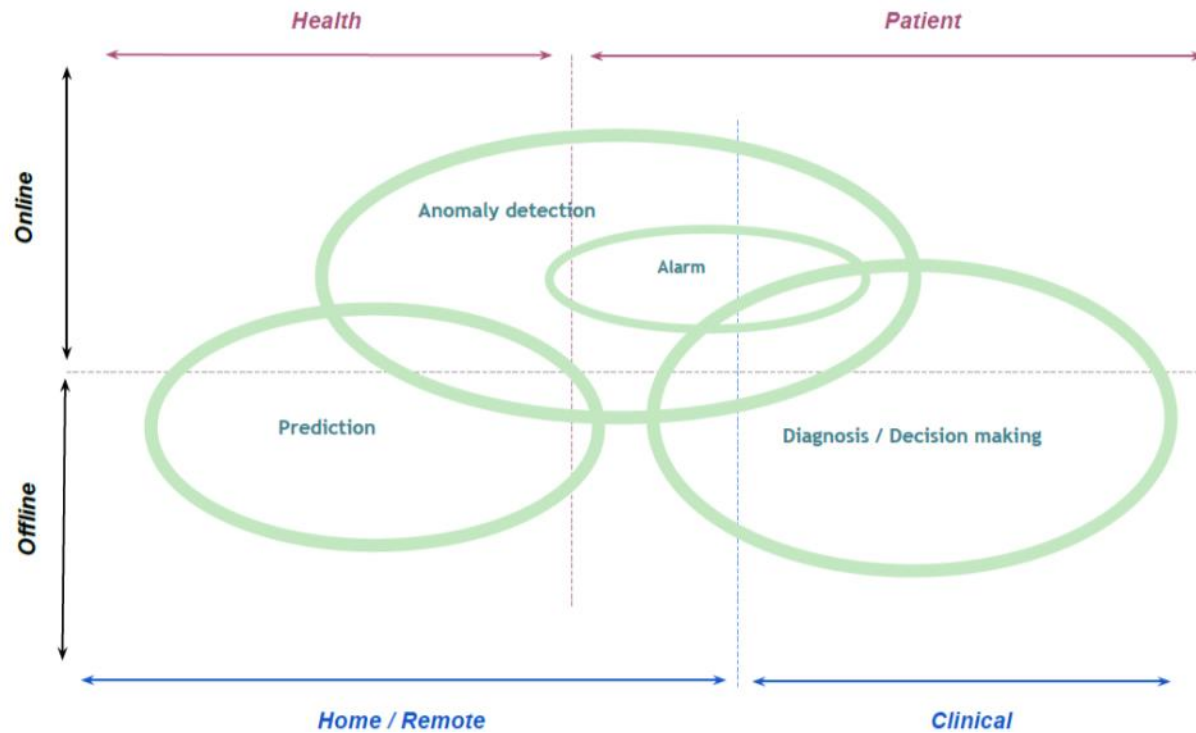


Figure 2.1.2- Schematic overview of the main three data mining processes (prediction, anomaly detection and diagnose/decision making) in relation to different aspects of wearable sensing in wearable health devices. Adapted from [16].

Prediction area consists in the identification of events which haven't occurred yet, providing medical information to help in the prevention of further chronic problems, leading sometimes to a decision about the diagnosis. Anomaly detection is responsible for the identification of unusual patterns that are not conformed to the expected behavior, being based on classification methods to distinguish normal data from outlier data, such as irregular patterns in ECG waveform or in SpO₂ signal for example. The alarm subtask is mainly used in anomalies detection, raising an alarm as soon as an anomaly is detected. Diagnose is one of the most important tasks of clinical monitoring, resulting in a clinical decision according to retrieved knowledge of vital sings, health records and anomaly detection data. [16]

To analyze the research that is actually being made with WHDs in each of these data mining tasks it is presented in the figure 2.1.3 the number of papers publish related to wearable sensors, based on those three data mining task and according to the considerations made in the literature [16]. In this figure (Figure 2.1.3) it is possible to evaluate in which wearable sensors has been made a higher study and a higher effort to obtain reliable sensors for medical applications, predicting that exist a higher effort in ECG, heart rate and respiration rate sensors development. The fact that ECG and heart rate are the main used wearable sensor is important because they emphasizes the huge importance of Vital Jacket® in medical applications, since it measures ECG signal from where it is also possible to obtain heart rate measurements.

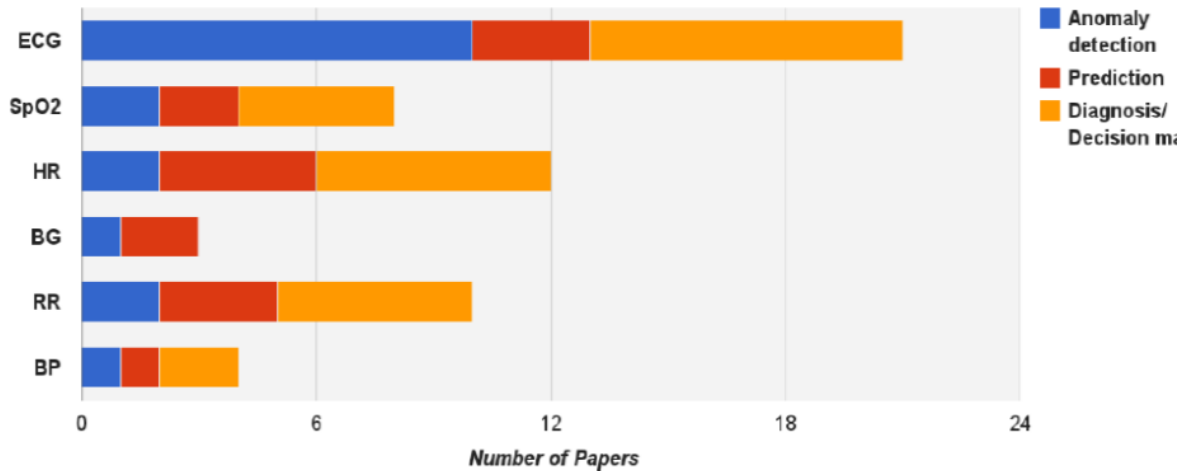


Figure 2.1.3- Number of scientific papers published according to the most six used wearable sensors in WHD's, with a distribution of the presented data mining task for each one. Adapted from [16].

These vital signs parameters are based on the most used vital sign monitored in WHDs according to the literature. In section 3 of this Chapter it will be made a deeper discussion about vital parameters, but with a selection based on the needs in ambulatory monitoring of patients from a medical point of view and also based on society needs to improve their life healthcare.

2.1.3. Portable Unit

The Portable Unit (PU), also denominated as user interface box or datalogger, is where all the information is gathered, containing the outputs and inputs of the WHDs. The main inputs are the vital signs from sensors, but it can also receive data from connected portable devices.

The communication between sensors and the PU is normally made through wires, resulting in a simpler and cheaper WHD. Some variations in this communication technique have been emerged, such as in smart clothes, where the interconnections (wires) are embedded and woven into the fabrics. This is a much more favorable approach in WHDs, avoiding loose wires around the body leading to a higher comfort and movement liberty. There is an innovative approach where the communication is made through biological channels, where the human body is used as a transmitter using electrostatic fields. [2]

The PU receives the analogic vital signs where the signal can be amplified and/or filtered, converting then it to a digital signal. This process can also be made outside PU, consisting in an optical sensor array with integrated analog-to-digital convertors.

Signal processing can be made in the PU or in other device after data transmission to it. This processing extracts features to evaluate the subject health, allowing the detection of an anomaly, a disease prediction or helping in diagnoses.

Then, data in the PU can be transmitted or storage, for example by wireless protocol or in a SD memory card, respectively. As it can be seen in figure 2.1.1, PU can also receive data from online monitoring devices storing it. This receiving process from other devices allows the storage of possible sensor data from external connected devices, reducing the number of

wearable sensors needed in the WHD. This communication is normally performed by one of the three wireless communication protocols: Bluetooth, Wi-Fi or ZigBee. [2, 8, 11]

Bluetooth is a short-range radiofrequency based connectivity between portables and also fixed devices requiring low-power and with a low-cost consumption. It is ideal for WHDs and widely implemented in commercial devices like smartphones or laptops. Wi-Fi protocol lower layers were adopted, allowing higher data throughput for low power requirements applications, being also a good connection protocol to use in WHDs. ZigBee is another technology used for low power and low data rate communication protected by the use of the Advanced Encryption Standard. This feature makes ZigBee ideal to medical applications with the advantage of consume much less energy than Bluetooth, but with a lower data transferring rate. Mobile telecommunications technologies can also be used to transmit real-time data using GPRS, a standard mobile data service in the global mobile communication. [2, 8, 11]

In offline cases the data transferring can be perform by reading the SD memory card or, if possible, through a USB connection between the WHD and another device, where data from the SD card is transferred.

In the next two topics it will be presented two possible types of ambulatory monitoring, online/real-time and offline, referring the main different situations where they can be used.

2.1.4. Real-time Monitoring

A higher need of monitor patients during long periods in the hospital led to a real-time monitoring, providing health condition feedback at any time. With WHDs it is possible to have this monitoring outside a medical environment, alerting the patient in case of any physiological problem or just to monitor himself and be updated of his vital signs during daily activities. [11]

In a medical environment WHDs allows the patients monitoring inside the boundaries of a specific area, normally a Hospital, where the patients can move while their vital information is being wirelessly transmitted to a remote monitoring center. Some devices also send the patient location. All these features allow the patient to move without any machines with him instead of being laid in the Hospital bed. In these live systems it can also be configured a set of alarms for each patient helping in the detection of some required anomaly. This type of monitoring systems are defined by the literature as “Controlled Area” and “Wide Area” systems and always has a medical specialist to provide information to the patients if needed. The vital signs can also be recorded in Medical Information Systems to be later analyzed by a doctor. [8, 17]

The biggest advantage of WHDs is the real-time monitoring in the patient’s home and outdoors, according to preventive medicine protocols, normally using regular Internet communications at home and mobile technologies in the outdoor. This feature allows the patient to have a normal life while is being monitored, being his vital signs continuously or intermittently transmitted to a remote monitoring center, with health support and, if needed, inform the patient of his medical status. The ambiance data is also important to know the conditions which people are exposed. For example, if an elderly person is subjected to an excessive cold or hot weather that can cause lung infection, dehydration or other diseases, a therapy can be immediately initiated, preventing a dangerous situation. [4, 8]

For last, vital signs can also be transmitted via Bluetooth to portable devices or personal computers to visualize and analyze the health status of an individual. This type of real-time monitoring can be used in sport activities to analyze the athlete vital signs during exercise, or in a simple daily run. This type of system is referred in the literature as “Wide Areas” and “Self-Monitoring” due to the non-involvement of medical specialists. Another example is the use of these devices in the health status monitoring of firefighters and combatants in field using mobile technologies, such as GPRS. [8, 10]

2.1.5. Offline Monitoring

All the data from vital signs can be stored in the storage of the portable unit (SD memory card for example), being then used for medical analysis or just for personal record. The data can be stored at the same time that a real-time monitoring is occurring, saving the data for a later analysis of vital signs. The main aim of these monitoring is to record vital data for clinic diagnosis and prediction by a medical specialists. For example, sleep issues such as apnea, can be analyzed through saved data from the patient, allowing him to sleep at home, a familiar environment, acquiring a higher reliable data. [10, 16]

2.2. Wearable Health Devices Developed

Wearable health devices are becoming important ambulatory monitoring systems helping in medical prediction, anomaly detection and diagnose (Figure 2.2.1). One of the problems is the limited number of measured physiological parameters. Many WHDs are developed with the aim to measure only one physiological sign, adapting its design and use to that only parameter. This fact results in several WHDs able to monitor a certain amount of vital parameters, but with monitoring limitations.

Wristwatches, also known as smartwatches, are under development for a few years. One of the first's devices of this type was AMON, first presented in 2002 and capable of monitoring heart rate, blood oxygen saturation and skin temperature, already with a wireless data communication module [18]. More recently, a new smartwatches generation is emerging with wireless and mobile communication, able to provide more than 24 hours of vital monitoring [19]. Their comfortable design, similar to a normal watch, allows to worn it constantly. These are being developed as activity and fitness trackers, monitoring physical activity like burned calories and distance traveled, heart rate, and, more recently, sleep monitoring, like PEAK™ which is the first smartwatch able to track sleeping cycles [20, 21].



Figure 2.2.1- Examples of wearable medical devices and prototypes. From the top in clockwise: a new ear prototype to measure several physiological parameters; smartwatch Basis PEAK™ [21]; a finger ring prototype for plethysmography; an ECG BioModule (BioPatch™) attached to normal electrodes in the chest [22]; a prototype jacket with several sensors; a wrist-worn device (AMON); and a chest belt to measure respiration rate and ECG (Bmedical®). Adapted from [4, 23, 24]

Finger sensors, as rings, have also been developed, but with the only propose to use photoplethysmography (PPG) technology to measure blood oxygen saturation, not being a viable human body place to monitor other vital signs. Armbands and chest belts are more capable to acquire several vital signs, but they are not so comfortable and easy to wear as a simple part of clothing, being denominated as accessories [4, 23]. Another accessory device was recently developed with a “special form optical PPG sensor” to be used in the human ear, being able to measure and estimate several physiological parameters, like oxygen saturation level and heart rate [24].

Sensors embedded in the user outfit as parts of clothing, more known as smart clothes, are the best bet to acquire a higher amount of physiological signals. Vital Jacket® is one of these cases; it is a t-shirt with embedded electronics, capable to monitor ECG signal and heart rate. With the aim to analyze developed WHDs similar with Vital Jacket® technology, the following discussion will present Biodevices, S.A. and their WHD, such as similar WHDs commercially available and recent prototypes of smart clothes that are being developed.

2.2.1. Biodevices, S.A.

Biodevices, S.A. was born as a spin-off in Aveiro University at IEETA (Instituto de Engenharia Electronica e telemática de Aveiro). Their mission is to “develop, commercialize and export biomedical engineering solutions for medical diagnose”. All started with the Vital Jacket® project in 2002, when it was only a prototype capable of measuring several vital signs. To turn this prototype into a commercial high tech textile medical device Biodevices, S.A. was created and, along with Petrutex S.A. for the textile development, Vital Jacket® as a product was developed and launched in the market. Vital Jacket® is the first certified medical device of its kind and nowadays is considered an added value in clinical daily work. It is certified according the MDD 93/42/EEC, holding the CE mark and is also certified under standards ISO 9001 and ISO 13485 as a medical “Ambulatory ECG device”. It has also Brazil Certification according to ANATEL and ANVISA regulations. [10, 25]

In the following section, a Vital Jacket® device description will be made, regarding its characteristics, sensors and applications.

2.2.1.1. Vital Jacket® Wearable Health Device

Vital Jacket® (Figure 2.2.2) is a smart cloth with a wearable vital sign monitoring device, designed and developed with the aim to have a practical approach for several clinical scenarios, such as in hospitals, at home or during movement, where a continuous or frequent cardiologic monitoring is required. This t-shirt with embedded electronics can acquire 1, 3 or 5 ECG leads using gel electrodes up to 7 days and it is totally washable. The data is collected in a small and lightweight portable unit (66x38x16 mm) that fits easily in the t-shirt pocket, being used for adult and pediatric ambulatory ECG acquisition in cardiac rehabilitation, sport medicine and occupational medicine. It is equipped with a Bluetooth transmitter which enables the

visualization of ECG signal in real-time, saving the data, at the same time, in a SD memory card for a possible offline monitoring if necessary. This characteristic also allows to send the signal remotely to another location using either a computer, personal digital assistant, smartphone or tablet with internet connection. With this option, Vital Jacket® can be used in telemetry systems and remote monitoring, enabling physicians to follow their patients. Vital Jacket® portable unit is equipped with a 3-axis accelerometer allowing to evaluate patient or normal subjects' movement intensity. [10, 26]



Figure 2.2.2- Vital Jacket® product. Beside T-shirt and portable unit, it comes with a software to analyze ECG, a portable unit charger and gel electrodes. Adapted from [25]

In order to perform real-time monitoring and signal analysis, Biodevices, S.A. has also several developed software, such as *VJ Holter Pro* that automatically analysis, identify and separate ECG signals by class and morphology and *Vital Jacket® Cardiac Rehabilitation System* to receive ECG signals through internet connection and analysis it in real-time or In the end of the training. [10, 26]

Vital Jacket® device architecture shows a comfortable and reliable ambulatory ECG device to monitor adult patients, children or athletes during their daily life activities. Beside the characteristics already referred, this device can be adapted to acquire other different vital signs (temperature, respiration, movement/fall, posture, blood oxygen saturation) and psycho-social variables (panic button, medication delivery, activity habits, location) as cited by developers. These new signals can be embedded in the t-shirt or acquired from other devices through Bluetooth connection, saving all the data in the SD memory card. [10, 26]

To better understand what is already developed worldwide in this area of smart t-shirts, the following sections will present WHDs similar to Vital Jacket® device and also some of the most recent prototypes developed.

2.2.2. Commercial Wearable Health Devices Available

There are not many commercial WHDs based on smart clothes for ambulatory monitoring. Beyond Vital Jacket®, nowadays there are about four commercial products that are able to provide ECG signal, where only three have CE mark certificate, and just one is certified with the

Medical Device Directive (MDD) 93/42/EEC and under standards ISO 13485 and ISO 9001, like Vital Jacket®. These three CE mark certified WHDs are nECG TEXTILE, the only certified as medical device, from Nuubo® [27], Smartex Wearable Wellness System from Vivonoetics® [28] and hWear™ from HealthWatch [29], the only one with Food and Drug Administration (FDA) approval (Figure 2.2.2). Hexoskin® [30] is a WHD smart T-shirt capable of acquire ECG signal, but without CE mark and medical device certification. Vivonoetics® WHD and Hexoskin® also can monitor respiratory signals. All these WHDs communicate with mobile devices using Bluetooth communication protocol and have applications to provide real-time vital parameters measurements to the user.



Figure 2.2.3- Smart shirts for ambulatory monitoring with CE approval. a) nECG TEXTILE from Nuubo® (MDD 93/42/EEC, ISO13485, ISO9001) [27]; b) Smartex Wearable Wellness System from Vivonoetics® [28]; c) hWear™ from HealthWatch (FDA approval) [29].

Several more wearable smart clothes are commercialized, but do not acquire ECG, only heart rate and some other physiological parameters like respiration rate, being mainly used in sports physical evaluation and also sleep monitoring. For example, there are BioMan™ from AiQ Smart Clothing Inc. [31], OMsignal Biometric Smartwear from OMsignal Inc. [32] and BioHarness™ 3 from Zephyr™ [22], all capable to communicating with mobile devices via Bluetooth and also with their own application, to give human body vital information to the user.

2.2.3. Recent Prototypes

In this topic it will be only presented the most recent WHDs prototypes (since 2010, including) which are similar to Vital Jacket®.

In 2010 it was presented the LOBIN device, a physiological monitor of ECG, heart rate, angle of inclination, activity index and body temperature monitoring, tracking the location of the patients within the hospital. This device can store and transmit wirelessly vital data, supporting the configuration of alarms by setting different triggers for each patient. With LOBIN it was possible to monitor patient health status in real-time easily using a graphical user interface, which allowed the monitoring of several patients at the same time in the same screen, independently of the patient location. [8]

The Sensing Shirt was prototype proposed in 2011 by Zheng-Bo Zhang *et al.* [33], a device capable to acquire basic cardiopulmonary parameters such as ECG, abdominal and chest respiration, and blood oxygen saturation using PPG. All sensors, except PPG, are integrated in the shirt fabric and connected to a data acquisition unit by wires also integrated in the fabric. PPG sensor can be placed at the index finger/ear lobe and is plugged to the data acquisition unit through a cable and secure connector. This device has a 3-axis accelerometer to record body posture and activity, storing all the collected data in a micro SD memory card. In 2011 it was also presented a multi-parameter wireless shirt to monitor ECG, heart rate and respiratory rate by Emilio Sardini *et al.* [34], with a communication channel for remote assistance. This device has contactless ECG electrodes to avoid gels and skin irritations and all the data is transmitted by Bluetooth to a PC, being visualized or sent via internet for remote assistance. The authors defend the use of this device to home telemonitoring, evaluating vital parameters of the patient and his activity using a 3-axis accelerometer.

More recently, in 2013, a different sensorized shirt was presented by Amer Farjadian *et al.* [35], named SQUID. This prototype was developed with the aim of home rehabilitation to monitor and evaluate physical therapy exercise with an online database for therapist's remote supervision from Hospital. Although it does not monitor ECG, it can monitor muscle activity using electromyography and heart rate, being capable to create an objective biofeedback so as to guide the user to follow the correct procedure as prescribed by the physical therapist.

One of the most recent prototypes was developed by Carmela Cafagna *et al.* [36] in 2014, and it is called MyWear. This smart T-shirt device as the disadvantage to measures only the heart rate, concerning heart monitoring, but it has an innovative respiration rate measuring technology. This is based on PolyPower, a recent polymer that changes its conductivity when stretch. It also has a fall detection system and a plantar pressure distribution system in a shoe. These systems can connect to a smartphone for real-time monitoring functionalities and features visualization. Future research has the aim to validate the developed technology and platform.

2.3. Wearable Sensing of Physiological and Ambiance Parameters

In this section, physiological parameters measured nowadays using WHDs are going to be presented. In order to understand why those vital parameters are the most common used in WHDs, it is important to analyze the medical perspective concerning vital signs used to ambulatory monitoring. This section will focus on the physiological parameters that are medically considered as vital signs and has a relevant importance in health monitoring. This will allow us to conclude if the already referred physiological signals are relevant and why, and if there are more physiological parameters that can also be important to obtain a more complete health monitoring. Some ambiance parameters are also discussed evaluating their contribution in health monitoring. The information needed for this section was collected from a research based on medical protocols and medical journals, as also in ambulatory healthcare needs, diseases and human activities.

To evaluate each physiological parameter, it is important to define first the most important vital signs measured in medical healthcare. This is a relevant problem because there are several opinions of which vital signs should be measured to identify clinical deterioration. There are five traditional vital signs that have a major importance to be measured: heart rate, blood pressure, respiratory rate, blood oxygen saturation and body temperature. These five signals are essential to evaluate human health and a continuous monitoring should be made, mainly in patients. Thomas Ahrens in [37] presented two more vital signs that he consider important to be immediately measured if the patient is in any danger, which are capnography and stroke volume. More recently, Malcolm Elliott and Alysia Coventry in [38] described another three important vital signs that should also be considered as part of routine patient assessment, such as pain, level of consciousness and urine output. According to these authors, the union of these five signals with the five essential ones referred allows to obtain an accurate recognition of changes in patient's physiology.

Although it is not referred, ECG will also be referred due to its major importance in heart electrical analysis, fact very important to predict and diagnose cardiovascular diseases. [39]

Diabetes mellitus is a disorder that must be carefully discussed in order to understand the huge effort in research that has being made to develop non-invasive methods to monitoring glucose levels. [4, 12]

Beside these medical parameters there are other parameters that are also important to monitoring in order to evaluate neurological function, rehabilitation procedures, posture, motion control and sports performance, such as skin perspiration. [4, 12]

In this chapter, nine physiological parameters were chosen to be independently discussed with the aim to understand their medical and health importance in ambulatory monitoring. Some of the main diseases which require continuous monitoring are going to be presented, as also some of the main technologies to acquire these parameters. The physiological parameters are going to be the five essential ones and four more: ECG ambulatory monitoring; Glucose level monitoring due to its relevance in society needs; Capnography, a method to evaluate physiologic ventilation; and skin perspiration, a physiological parameter involved in several human activities and behavior, such as in sport, emotions and stress. [4, 12] The remaining

physiologicparameters referred will also be discussed in a single topic, named “Other physiological parameters”.

After the discussion of physiological parameters, ambiance parameters will be briefly discussed, to analyze their importance in human health monitoring.

2.3.1. Electrocardiogram

Electrocardiogram (ECG) is one of the most widely used biosignals, as a diagnostic tool in healthcare environment, providing information of the cardiac cycle. It is used to analyze the cardiac rhythm, ischemic changes and early prediction and treatment of acute myocardial infraction and coronary events. ECG signal is the most common technique to measure heart electrical activity.

Its patterns changing analysis are used in the diagnose of cardiovascular diseases (CVD), such as angina, atherosclerosis, cardiac dysrhythmia, congestive heart failures (CHF), coronary artery disease, heart attack and tachycardia. ECG signal is basically a spectrum of the heart bioelectricity, where it can measure the depolarization (contraction) and repolarization (relaxation) of the cardiac muscle cells (Figure 2.3.1). [39]

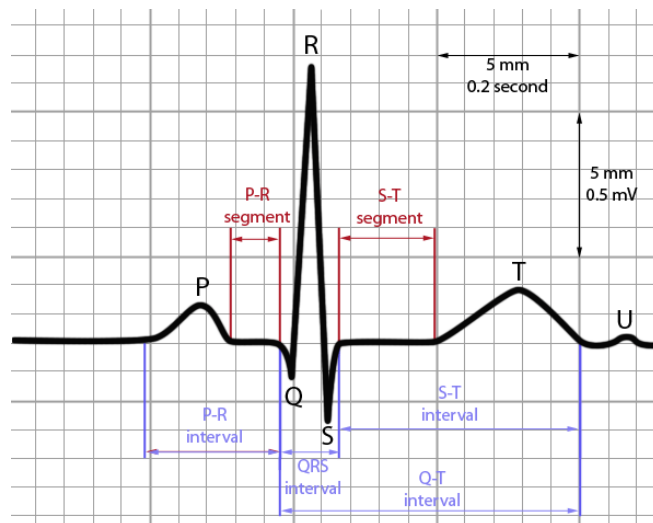


Figure 2.3.1- Illustration of an ECG heart cycle, with the characteristic oscillations due to the cardiac electrical activity. It is constituted by: a baseline-starting point of the electrical activity; P wave-auricular depolarization (0.11 s; 0.15 mV); P-R segment-Delay time between auricular-ventricular nodule (heart pacemaker) and ventricles (0.12 a 0.20 s); QRS complex-Ventricular depolarization, where ventricular contraction starts and auricles repolarize (0.09 s; 1.1 mV); S-T segment-temporal region where ventricles are uniformly depolarized (0.05 a 0.15 s); T wave-ventricular repolarization (0.2 s; 0.2 mV). Adapted from [40].

To measure these bioelectric changes in heart muscle cells are used electrodes. These sensors transduce ionic current skin into electron current in metallic wires, and their characteristics have in consideration cells low electrical potential difference (from -40 to -80 mV) and also skin impedance. The commonly-used electrodes in clinical are wet electrodes, based on Ag/AgCl, which contacts with the skin using a gel to improve skin contact. These electrodes are very reliable, compact and low cost, but causes skin irritation due to adhesives properties. During

long acquisitions the gel dries, reducing the contact with skin. To obtain longer acquisitions, hollers are normally used, but with the main disadvantage of interrupt daily routine, not being feasible for unobtrusive continuous monitoring. To overcome this problem, dry electrodes and embedded wires in the fabrics are being developed using several materials. This type of electrodes has the main advantage of causing no skin irritation, but, as they are not adhesive, artifacts appear due to body movement. [2, 39]

In order to reduce the artifacts produced by body movement and skin irritation, Ningqi Luo *et al.* [41] developed a new technology of dry sensors that are flexible and stretchable, but with the disadvantage of being attached to the human skin, making it not very viable to use out-side the medical diagnose monitoring.

A possibility to overcome the adhesive properties is to have a dry electrode without adhesive properties resulting in proper electrodes for wearable applications. Yu Chin *et al.* developed a wearable, unobtrusive and patient friendly sensor that is able to acquire ECG signals through insulation such as fabric, being this technology firstly reported in 1969. Wearable electrodes are being embedded in textile fabrics where the fiber must be electrically conductive with low current and low impedance. These types of electrodes are normally a bundle of a normal fiber filament, like nylon, that is electrochemically plated with a metal. The fiber used in its fabrication must undergo several actions as stretching, bending and twisting, in order to adapt to the body movement, and to be washable. [39]

2.3.2. Heart Rate

Heart rate (HR) is a standard vital sign and has become a routine measurement practice in general healthcare units. The monitoring of this signal provides information about specific physiologic status indicating changes in the heart cycle. The heart rate indicates the frequency of a heart cycle and is conventionally presented in cycles/beats per minute. This vital sign can be easily calculated from ECG or PPG signal, or it can be measured with characteristic sensors with the aim to only measure heart rate. HR is also simple to measure directly from the human body with no need to be calculated, informing of some cardiovascular parameters. HR is also very important in sport and activity context to evaluate or inform heart response to exercise and recovery. Heart rate variability analysis is gaining attention as an indicator of the health status of the cardiovascular system. [4, 23, 37]

Medical specialists propose other measurement related to heart rate that can substitute it, an important vital sign named pulse. This parameter is defined as the palpable rhythmic expansion of an artery produced by the increase of volume of blood pushed into the vessel by the contraction and relation of the heart, providing further than HR, such as strength or amplitude of the pulse and its regularity. A problem referred in the literature regarding the use of this technology is the decrease of blood volume in case of an irregular pulse or hypovolemia. This is a real problem that has not been solved yet, even though it is easy to overtake. It should not be considered the same as heart rate and it can be determined using pulse oximeter, the same method used to measure blood oxygen saturation. [38]

2.3.3. Blood Pressure

Blood pressure (BP) vital sign is considered the most important cardiopulmonary parameter, indicating the pressure exerted by blood against the arterial wall. It provides information about the blood flow when the heart is contracting (systole) and relaxing (diastole) and can also indicate cellular oxygen delivery. It is influenced by cardiac output, peripheral vascular resistance, blood volume and viscosity as well as vessel wall elasticity. [38, 42]

Ambulatory BP monitoring allows to collect BP readings several times at any hour across a 24-hour period. This is ideal to monitoring high blood pressure (hypertension) which is one of the greatest threats to the global burden of diseases. Hypertension diagnose require BP measurements and it accuracy can increase with ambulatory monitoring, increasing also the prediction of cardiovascular risk. There are three main BP problems related to hypertension that can be resolved with ambulatory monitoring. First one is normally, during sleep, blood pressure decrease in such way that it average is lower than average awake blood pressure. When it decreases more than 10% the individuals are called non-dippers and this problem affects about 70% of the population. A nocturnal hypertension and a non-dipper pattern are associated with the increased of cardiovascular morbidity and mortality, problem that can be easily diagnosed with BP ambulatory monitoring. Another problem is the white-coat hypertension: individuals who are not taking antihypertensive medication show an elevated BP in a clinical setting, and a normal one when assessed by ambulatory BP monitoring, a problem that occurs in 15% to 30% of individuals with clinical high BP. This may lead to a misdiagnosis, leading to unnecessary medications with potentially seriously debilitation side effects. The third main problem is the masked hypertension, the opposite phenomenon of white-coat hypertension and also affects 15% to 30% of adults with non-elevated clinical BP. [38, 43]

Regarding BP measurement, traditionally it is made using inflatable pressure cuffs with stethoscope on the patient's arm. This method was adapted to be performed autonomous BP measurement, including a fully automated inflatable cuff that measure BP by relating external pressure with the magnitude of arterial volume pulsations. [2]

Continuous monitoring with a cuff can result in unwanted side effects, such as sleep disruption, skin irritations and an increase in stress levels. With the aim to solve this problem, new technologies to ambulatory BP monitoring have been developed [2]. A developed method uses a BP estimation based on pulse wave transit time between the pulse wave obtained by PPG and the ECG, both measured on the chest [44]. This method has already been used, but with a PPG signal acquired on the wrist [12]. Yu-Pin Hsu and Darrin J. Young in [45] developed a BP measurement new technique based also in pulse wave velocity, but using two microeletromechanical sensors placed in two adjacent points of the body: in wrist or neck. More recently, Sung Hun Woo *et al.* in [46] proposed an experimental watch-type prototype which uses a pressure sensor near the radial artery, giving an accurate blood pressure measurement on a personal smart phone, a real-time continuous monitoring BP wearable device.

2.3.4. Respiration Rate

Respiration rate (RR) is a fundamental physiologic parameter in patient's observation, being accurate and carrying important health information, such as in case of acidosis. In critical illnesses this is one of the most sensitive indicators, also being an important sign of distress and potential hypoxemia. Malcolm Elliot and Alysia Convetry refer the following important statement: "respiratory rate is often not recorded in clinical settings or is simply guessed". This is a major problem since RR is the best predictor of adverse events like cardiac arrest. In the medical environment, normally, blood oxygen saturation is assumed as a reflection of RR, and this is not measured, also due to the inexistence of an automated machine capable acquire RR sign. When measured, using traditional methods (observation of the patient respiration during 30s), a classification is made according to the pattern observed, and can be classified as eupnoea, tachypnoea, bradypnoea and hypopnoea. Respiratory rate ambulatory monitoring is also important in the detection of symptoms of respiratory diseases such as sleep apnea syndrome, chronic obstructive pulmonary disease and asthma, facilitating the administration of treatments if needed. This constant monitoring is particularly important in children with pulmonary diseases. [4, 38]

This vital parameter is normally calculated from an acquired function (respiratory waveform) that reflects the chest volume variation due to the inspiration and expiration (Figure 2.3.2). From this function it is also important to obtain the thoracic expansion and, with muscle signs, calculate the respirator effort, which can indicate different physiological states. Respiratory effort can also be obtained by measuring changes in chest and abdominal volume, also known as plethysmography. The analysis of this vital function can also help in sport, mainly in competitive athletes with the aim to achieve a better respiratory performance. [4, 23, 38]

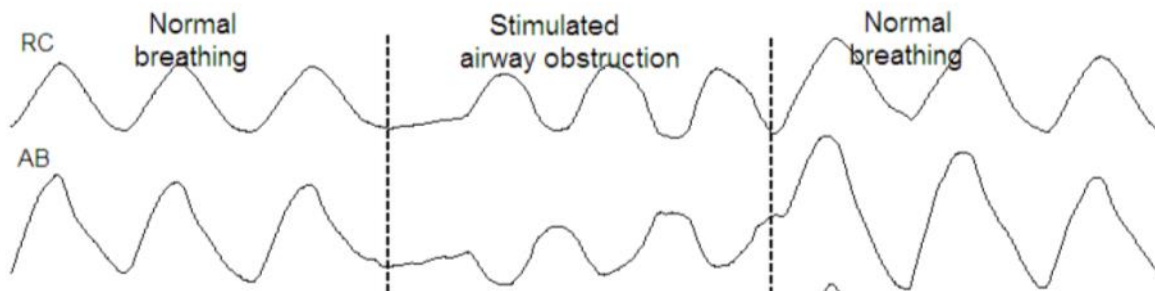


Figure 2.3.2- Respiratory waveform obtained from both chest movement (RC wave) and abdominal movement (AB wave). It is possible to observe a normal respiration waveform at the beginning and end of the image, and at the middle is it represent a stimulation of an airway obstruction where a subject closes his mouth and attempt to take in air by moving his abdomen in and out, a common test in the respiratory evaluation. Adapted from [47].

To obtain RR waveform, the variation of the chest volume, and if needed also abdominal volume, are measured as already referred. Nowadays, to obtain this function, there are three primary methods: Elastomeric plethysmography, impedance plethysmography and respiratory inductive plethysmography (RIP). Elastomeric technique converts current variation of piezoelectric sensors in an elastic belt to voltage. Li Guo *et al.* [48] developed a prototype garment based on this technology, capable to measure chest and abdominal volume changes with high accuracy, using a piezoresistive fabric sensor. The impedance plethysmography uses impedance changes of the body surface due to the expansion and contraction during breathing. Weak

alternating electrical current is applied to the body and measured with other sensor, allowing the body impedance to change measurement, obtaining a qualitative measurement of breath movement. This technology was used in the development of a uniform vest to be used in both soldiers and command [7]. RIP technology principle is based on the application of a current applied to a loop wire which generates a magnetic field normal to the loop orientation. Chest volume variations change the area enclosed by the loop, creating an opposing and directly proportional current [49]. Very recently, Ozgur Atalay *et al.* [50] presented a textile-based sensor with a conductive yarn embed in the fabric in a loop geometry. Using additional signal processing they were able to eliminate unwanted interferences from the breathing signal, such as body motion artefacts.

Beside these three primary methods, other technologies are also being used to obtain respiratory waveform: accelerometers [51]; extracted from ECG signal [15]; polymer-based transducers sensors [52]; optical fibers attenuation due to the chest movement [53]; most recently, using a polymer named Polypower. This dielectric active polymer (DEAP) is being commercially produced as Polypower and changes its electrical attenuation when stretch in one direction. Tognarelli *et al.* [54] are using this technology to obtain chest volume variations, demonstrating the potentiality of DEAP in this type of physiologic measurements.

2.3.5. Blood Oxygen Saturation

Blood oxygen saturation (SpO_2) is an extremely valuable vital parameter and easy to measure using PPG technology and pulse oximetry principles (Figure 2.3.3). It indicates the amount of oxygen that is being carried by blood cells and normally is between 95% and 100%. This measure may lead to a change detection in a patient condition that could otherwise be missed, resulting in a changed of patient management. For example, a lower percentage of oxygen (<95%) can indicate hypoxemia, causing an insufficient oxygen supply to the human body. One of the problems in blood oxygen saturation measurement in clinical environment is when the patient is anemic, a reduction of red blood cells or a lower ability of these cells in oxygen transportation. [38, 42]

Besides medical use, pulse oximetry ambulatory monitoring has a particular interest in the evaluation of aerobic efficiency of a person undertaking an exercise routine. A study about the oxygenation of capillary bed from muscles can lead to a maximization of the athlete performance. Limb and brain oxygenation information is also important in military and space applications, where gravity changes may affect the delivery of oxygen to these parts of the body, leading to blackouts. It has been discovered that exist a positive correlation between a individual's performance and oxygenation responses as a function of task load. [23]

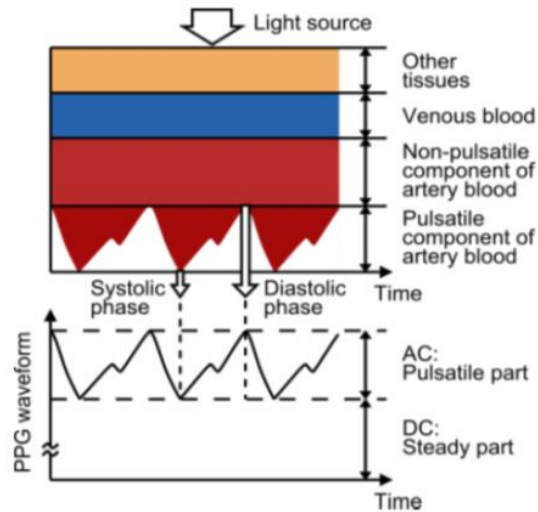


Figure 2.3.3- The figure represent the variation in light attenuation by tissue on colored part, and the PPG signal waveform conventionally representation. The PPG signal obtained depends of the absorption process and is composed by a Direct Current (DC) and Alternating Current (AC) components as shown in this figure. The DC component represents the transmitted or reflected signal from the tissue and depends of tissue structure and average blood volume of both arterial and venous blood. The AC component shows the blood volume variations that occurs between systolic and diastolic phases, being it fundamental frequency dependent of the heart rate. Adapted from [42].

There are several noninvasive technologies to measure blood oxygen saturation that can be applied to wearable devices, but PPG stands out, being very popular in medical environment [42]. This technology is based on the absorbance variation of blood cells at two wavelengths, normally using Light-Emitting Diodes (LEDs). There are two main modes, a reflectance mode and an emitting mode, and it can be applied to several body parts to evaluate blood oxygen saturation and is normally used in microvascular bed of the tissue. Since this sensor was one of the chosen one to be implemented in the developed prototype, a further research is presented in Chapter 3 to better understand the theoretical fundamentals behind this technology.

The finger is the most used place to acquire blood oxygen saturation levels and is the most used in clinic conditions. Ring PPG sensors are under development due to its more wearing-comfortability and easily adaptation. Mobile connections improve these sensors to a much more independent and wearable device [55]. Ear lobe can also be used and a recent research presented a very small chip ($3 \times 6 \text{mm}^2$) capable of measure blood oxygen saturation, with the aim to be used in future wearable devices. Forehead is also used to measure brain oxygenation and has already been developed as described in the literature [56]. A surface chest PPG reflectance prototype device was developed by Sawa Puke *et al.* [44] demonstrating the viability of oxygen continuous monitoring in this body location. Recent developments made by Chen *et al.* [57] allows adjust PPG sensor parameters to refine the depth of tissue measurement, enabling several body sensor location possibilities and improving its functionality for clinical applications.

Concerning textile technology, there is being a huge effort to implement PPG sensors in this area. Different approaches using textile fabrics have been intensively studied in recent years. One of these approaches is based on the integration of flexible plastic strips in weft direction: two LEDs strips and two photodiode strips, with cooper wires in the textile to conduct the signal in the textile fiber [58]. Another approach, and a very recent one, is the use of optical fibers

embroidered into textile. Marek Krehel *et al.* [59] developed this new textile technology, which is capable to analyze different depths of tissue using a ring design in the optical detection of the reflected light. This detection and the light-source are both made using optical fibers.

2.3.6. Blood Glucose

Blood glucose (BG) is a worldwide need measurement in diabetic's persons. Although this parameter is not measured in a normal procedure of a clinical environment, it is an important measurement in diabetic global population. According to World Health Organization, in 2014 it was estimated that 9% of the worldwide population among adults aged above 18 had diabetes and in 2012 it was estimated 1.5 million deaths directly caused by this disorder. Diabetes disease causes several physiological disorders such as cerebral vascular disturbance, retinopathy and nephropathy. To prevent these complications, diabetic individuals control their blood glucose concentration measuring BG levels and injecting insulin when needed to maintaining the standard values. The most used method to evaluate BG concentration is collecting a blood sample by pricking the finger with a lancet. This invasive technique is not the best way to continuous monitoring blood glucose and to resolve this problem non-invasive techniques were and are being developed to improve continuous self-monitoring, increasing subject efficacy in diabetes management during normal daily activities. [12, 60]

One of the first commercial wearable devices to continuous monitoring blood glucose was GlucoWatch® providing glucose readings every 20 min during 12 hours through the skin via reverse iontophoresis [61]. In 2007 it was discontinued due to skin burning effect. Besides the technology used in this device several more non-invasive techniques have been developed along these years: Bioimpedance spectroscopy, a non-viable technique to continuous monitoring, requiring 60 minutes of rest before BG measuring; Electromagnetic sensing, with the disadvantage of being strongly affected by the temperature [62]; Fluorescence technology that includes an implantable fluorescence-hydrogel sensor and a wearable photo detector to monitoring continuous BG [60]; Mid and near infrared spectroscopy are both possible technologies, but presents several barriers, like weak penetration and reading correlation respectively; Measurement of BG through the eye is also being developed through ocular glucose sensor, technology already used by Google to developed a prototype that has been recently taken to the FDA for early independent clinical trials [12]; Ultrasound can also be used, providing high sensitivity but with some interference due to biological compounds [62].

These technologies have been already used in the development of several non-invasive BG wearable monitoring devices, like EyeSense and SCOUT. In some of these devices there are also temperature sensors, skin perspiration sensors and actigraphy sensors to predict energy expenditure, helping in the insulin administration needed. There are still several challenges and barriers in this area, leading to a constant effort from many research groups to develop new technologies and methods to get a stable, reliable, conveniently and economic continuous monitoring wearable device. [61-63]

Very recently Dexcom, Inc has become the first company to obtain FDA pre-market approval for their mobile application to support continuous monitoring. This application can display data from their G4 Platinum CGM System, a system to measure blood glucose from a needle with a sensor inserted just under the skin. [64]

2.3.7. Skin Perspiration

Skin perspiration is not a clinical parameter but a physiological sign very used to analyze the human reaction to several situations. Depending of the subject, certain life situations will cause a reaction from the autonomic nervous system (ANS) that can stimulate an increase of skin sweating. This moisture will change the electrical conductance of the skin, allowing measuring the quantity of sweat produced by sweat glands, named as galvanic skin response (GSR). As ANS is responsible to control other physiological parameters like heart rate, respiration and blood pressure, GSR has been used alongside the acquisitions of some of these signals. For example, skin perspiration and heart rate variability can be used to classify mental states, helping in the distinction, as also in the detection of mental stress. [65, 66]

In sports, skin perspiration continuous monitoring is considered an important physiologic sign with enormous applications in this area and human behavior, opening a new field of research in the clinical settings, such as in dehydration area. A study presented in the literature showed that skin perspiration cannot be interpreted correctly without knowing the physical activity context. [4, 66]

From perspiration it is possible to obtained information about the physiological condition of the subject due to the several ions and molecules that constitutes it. For this reason it is considered an excellent biofluid for non-invasive chemical sense. This able the identification of pathological disorders through sweat through ions levels like: sodium, ammonium, calcium and lactate levels which are indicators of electrolyte imbalance but also of cystic fibrosis, osteoporosis, bone mineral loss and physical stress. As already referred, physical stress is an important factor, indicating in real-time a feedback about stress levels and is also used in the psycho-physiological evaluation of militaries undergoing intense training. Taking in account these possible molecules levels indication, skin perspiration would be a benefit in clinical environment. [4, 13]

Regarding the technology used to monitoring skin sweat, there are two main types of sensors: Epidermal-based sensors which have a conformal contact between the electrodes surface and the biofluid like elastomeric stamps to print electrodes directly on human epidermis for continuous monitoring; Fabric/flexible plastic-based sensors are the most used and have a main advantage of constant contact with a large surface area of the skin. These last sensors can be embedded in the fabric or screen-printed into it and their technology can be based on conductometry or potentiometry to obtain specifics measurements like pH, NH_4^+ , K^+ and Cl^- [13]. Jeehoon Kim *et al.* [65] have recently presented a new sensor to continuous measure GSR with high wearability and usability in a wide variety of fabrics. This feasible sensor is small, flexible and the surface is made of a dry polymer foam electrode with the aim to maintain a stable contact with the human body.

A new technology to continuous skin perspiration monitoring has been developed by Gengchen Liu *et al.* [67] based in microfluidic conductivity. Sweat passes through a microfluidic channel, where the application of a voltage results in the solution ionization. The resistance across this channel is measured obtaining the corresponding sodium concentration. There are still several problems related to the introduction of sweat in the channel, but according to the authors, this technology, with a microcontroller and a Bluetooth module, can have the ability to be used as a wearable continuous skin perspiration monitor.

2.3.8. Capnography

Blood oxygen saturation measurement by pulse oximetry is a widely used method to assess arterial oxygenation, but is not the best of the technologies. A better one is capnography, a non-invasive method and cost effective to avoid clinical complications that is becoming an important parameter in patient safety. [37, 68]

Capnography continuously measures the inhaled and exhaled concentration of carbon dioxide (CO_2) in the respiratory gases, calculating the CO_2 partial pressure in the arterial blood. This measurement is made through air capturing just below the nose, where then it goes to capnography device to perform a CO_2 quantification. Capnography sign has a characteristic waveform from which is possible to obtain the respiration rate (Figure 2.3.4). It is possible to visualize changes in CO_2 concentration and its maximum, as also the speed of expiration. The technology to CO_2 measurement is based on infrared, and an effort has been made to decrease response time and increase this technology accuracy. [69]

For more than 25 years, capnography has a widely use in clinical practice as integral part of anesthesia care in operating rooms. This allows the anesthesiologists to evaluate the consciousness level of the patient during the sedation process. When the patients are transported to the intensive care unit (ICU), they are not continuously monitored with capnography due to its absence, a problem that the American Heart Association has already reported, recommending the use of capnography also outside the operating rooms. Recent studies referred in the literature showed a high correlation of morbidity and mortality with the underuse of capnography in ICUs. [68]

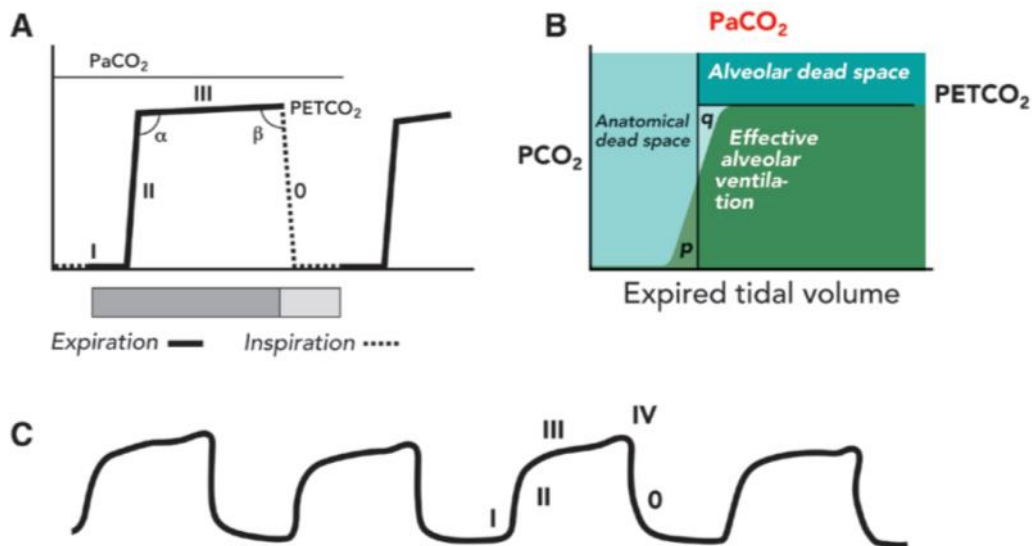


Figure 2.3.4- Capnography waveform illustration, composed by a periodic sign that reflects the CO_2 partial pressure during a respiratory cycle. A - during a normal respiratory cycle CO_2 partial pressure varies according to the illustration and is divided in four phases: I, II, III and 0 that correspond to the inspiration. Just before this action, a maximum pressure of CO_2 is verified, nominated as end-tidal PCO_2 (PETCO_2). Arterial PCO_2 is always higher than the higher level of PCO_2 measure due to the alveolar dead space. B - Capnography volume different components which are correlated to the expired volume of air. C - An example of a recorded time capnogram during cesarean delivery general anesthesia (phase IV corresponds to PETCO_2). Adapted from [68].

Several reasons have been enumerated by Bhavani Shankar [68] from Harvard Medical School, to explain why capnography should be considered a routine monitor, such as the fact that this method can be used as a guide to metabolic rate, or as an essential adjunct to monitor the integrity of airway, cardiac output and ventilation.

Capnography is becoming a prevalent vital sign on portable devices and is helping first responders make life-saving decisions, and also in sleep apnea diagnose and monitoring. Sleep apnea is where capnography is mainly used outside the clinical environment. Normally sleep apnea syndrome is diagnosed and monitored using polysomnography or cardio-respiratory polygraphy, both high costs methods and dependent on the access to a specialized sleep laboratory. An investigation published in 2005 by Rainer Dziewas *et al.* [70] showed that capnography by its own, can make an early diagnose of sleep apnea syndrome, facilitating patients in the diagnose obtainment. Nowadays, this technique is being used to monitor subject with sleep apnea. A continuous monitoring is possible due to portable and wearable devices like MediByte from Braebon Medical Company that can be used at home with only 10% of a sleep laboratory usage cost. [71]

In a near future it is expected that capnography become widely used outside clinical environments. To ensure this, manufactures should make an effort to produce reliable, cost effective and portable capnography units with quick calibration procedures. [68]

2.3.9. Body Temperature

Body temperature represents the balance between heat produced and heat lost, known as thermoregulation, and it can be affected by several factors, such as underlying pathophysiology, skin exposure and age. Body temperature deviations from normal are an indication of ill health, and an higher deviation represents a more severe health problem. Body temperature can be divided in two types: surface body temperature and core body temperature. In medical practice it is important to measure both of these values, in several body sites, as a recommendation of best practice. Skin temperature can be easily measured, using, for example, an optical infrared thermometer, and can be used in sport activities, joined with heart rate sensors, to monitor exercise intensity. On the other hand, core temperature is more important, indicating well-being and health condition of humans, but it is also more difficult to acquire. [14, 38, 72]

Several methods can be used to measure body core temperature in different places, such as through tympanic, oral and rectal measurements, but also in temporal and pulmonary artery. These places are not very feasible to be used in continuous monitoring, so new methods are in development. For example, Kumar Saurabh *et al.* [73] developed a body core temperature estimation method, using two heat flow channels with different thermal resistances. Using a simulation model they can estimate body core temperature, but further research is needed to enable an accurate result.

2.3.10. Other physiological parameters

2.3.10.1. Motion Evaluation

The evaluation of the human body movements has several applications in medical rehabilitation and posture evaluation. Beside these applications, motion evaluation is strongly used in actigraphy, a monitoring method to evaluate human rest and activity cycles, providing an insight of daily activities routine. [3, 12, 69]

In medical rehabilitation it is important to monitor mobility, in specific therapeutic exercises to evaluate movements and help in exercise techniques improvement, maximizing patient recover. A WHD, with the proper sensors, can provide guidance and feedback to the patient and, if needed, generate warnings based on the patient physiological conditions. Pulmonary rehabilitation can be also included in this type of monitoring, helping patient to complete a physical activity rehabilitation program. Muscle activity can be recorded and associated to motor functional tasks, as also muscle stimulation. Motion evaluation and muscle activity can be used in sport activities to assess physiological signals and body kinematics during exercise leading to athlete performance improvement. Posture is also an important factor that as a particular interest in patients submitted to hip surgery. [3, 12, 69]

To measure body movements, several sensors are embedded in textile WHD or in the portable units, like in the portable unit of Vital Jacket®. These sensors can be accelerometers, magnetometers, gyroscopes, electromyography electrodes and even stimulators. To obtain distance data, a GPS can be also added to the device. Complex body movement patterns can be measured, combining these sensors along with WHDs fabric, assessing to a higher amount of human body movements.

2.3.10.2. Cardiac Devices

The increase of implantable cardiac devices is leading to a development of long-terms surveillance, to improve patient safety and care. These devices are mainly implantable pacemakers, cardioverter defibrillators and cardiac resynchronization therapy systems. A remote monitoring of these devices will minimize the need of caregivers in several situations, allowing an early detection of adverse events and prompt corrective measure, also accessing to up-to-date information stored in the devices memory. The incorporation of new communication technologies will provide a daily, remote, wireless, patient independent ambulatory monitoring of medical and technical data. A study, in a large population sample with this type of system, was followed during four years, concluding that, if the system was intelligently used, it was capable to improve care and increase safety of these patients. [74]

2.3.10.3. Stroke Volume

According to Thomas Ahrens [37] stroke volume (SV) should be a vital sign to measure in patients monitoring. United Kingdom and United States encouraged clinicians to start to use technologies like flow Doppler to measure SV. This allows measuring the blood volume that is pumped from a ventricle of the heart during each beat, helping in a faster evaluation of the heart function. This is a clinical used technique which has not been implemented in wearable devices due to its specificity. [69]

2.3.10.4. Pain, Level of consciousness and Urine Output

These three parameters are proposed by Malcolm Elliot and Alysia Coventry, in the literature [38], as additional signals to identify patients who are clinically deteriorating. According to the authors, pain should be considered one of the most reliable indicators to ensure that management methods in the clinical environments are appropriate and effective. The level of consciousness is defended has a measure that can be assessed using a common neurological scale, named Glasgow Coma Scale, with no need of neurological sign assessment. Urine output evaluation is also recommended, but this monitoring is only made in a clinical environment to ill patients. Although these three signals are very important in patients' medical care, they do not require continuous monitoring that justifies the implementation of such parameters evaluation using a wearable device.

2.3.11. Ambiance Parameters Measurement

Ambiance parameters have a high relevance in several human body monitoring areas. The most used sensors are temperature, ambient light, humidity and sound level. The continuous monitoring of air pollutants is also important due to its association with cardiac diseases as it will be furthered discuss.

According to the measurements obtained in ambiance sensors it is possible to estimation the occupancy activity of subjects, easily estimating metabolic rate, mainly in indoors environments due to the non-contribution of external factors. According to a study made by Ming Jin *et al.* [75] it is possible to assume several daily indoor activities through light, temperature and humidity measurement patterns. They develop a wearable device with these three sensors and analyzed daily routines such as: climbing stairs due to a periodic pattern in the light level; the indoor location when their characteristics are known; and rest periods after walking or running due to a humidity increase. This study proved that is possible to analyze ambiance features with the aim to recognize indoor activities.

Outdoor daily activities should also be continuously monitored with ambiance sensors to analyze ambiance characteristics that the human body is subjected during sport activities or simply rehabilitation exercises. Temperature and humidity can be important to evaluate dehydration [12]. Air pollutants are also considerate an important variable to monitor due to the high correlation with cardiac diseases. Like is referred in the literature [76], although little is known about the possible mechanism for this correlation, it has been proved that air pollutants

have a strong association with a high risk of ventricular tachycardia in elderly subjects with coronary artery disease. High concentrations of these substances should be medically relevant since they can also increase arrhythmia occurrence rate.

Ambiance parameters such as ambient light, sound and temperature are also important in sleep quality and quantity evaluation. For example, a sound sensor joined with an actigraphy sensor is an important tool to study sleep disturbances suffered by people living near airports.[77]

2.4. Market and Trends Analysis

This section is going to analyze WHDs market and trends. Combined with the discussion of the previous section, it will allow to define the most usable and needed scenarios, both in medical and personal use monitoring.

To perform a complete market analysis of WHDs, it is necessary to understand in what part of the market these type of devices are included and then follow market lines, to analyze specific markets. This approach will allow us to understand market values and trends in near areas, which can also be possible target areas in a near future.

Wearable devices are estimated to grow at an high rate, with a market value of approximately \$12,500 million in 2018, which is much higher than the value of 2014 of \$5,000 million [78]. WHDs are included in this market segment and can be categorized according to classification shown in figure 2.4.1. In this figure it is possible to understand that, wearable devices, in general, are increasing with a high rate. From 2014 to 2015 it is expected that smart watches increase drastically (increase rate $\cong +250\%$). The use of wearable devices in healthcare (increase rate $\cong +55\%$) and sports/activity trackers (increase rate $\cong +36\%$) are also expected to increase considerably, which is a great prediction for Vital Jacket® since it can be applied in those areas. On the other hand, it is important to refer the smart clothing low increase prediction. This fact can mean two things: that there is a lack of this type of products in the market, which would be the more credible hypothesis, since this is a new area; or can represent a low market demand on smart clothes, which is less probable, due to the lower technology of smart clothes available in the market.

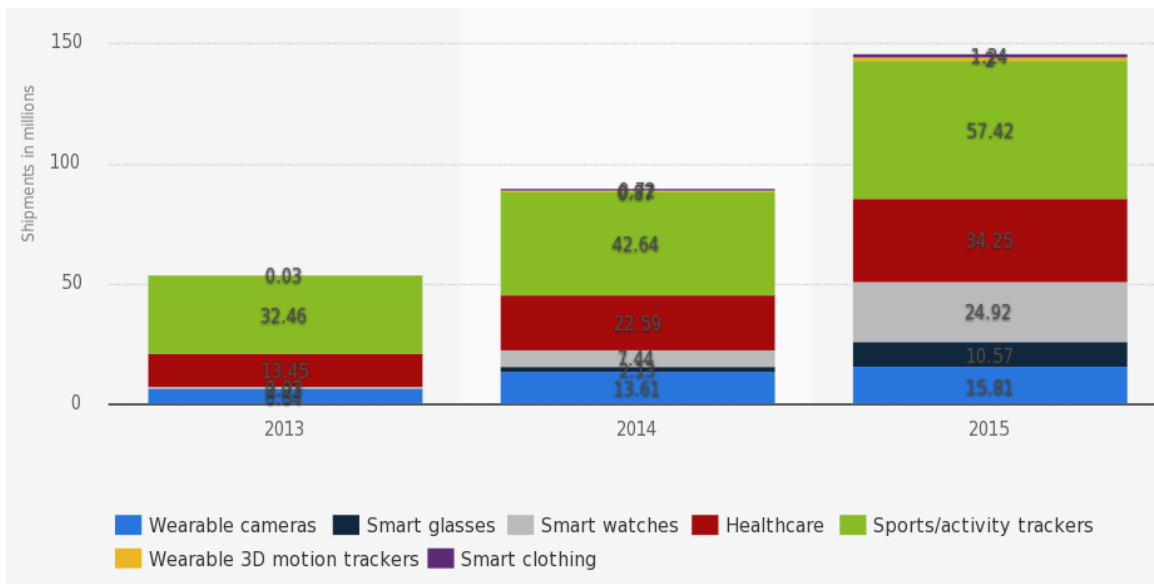


Figure 2.4.1- Shipments of wearable computing devices worldwide by category from 2013 to 2015 (in millions). Adapted from [79]

Independently of the smart clothes low increase, it is important to retain that main possible markets for Vital Jacket® (healthcare and sport/activity trackers) are expected to increase with a high rate as already referred. To evaluate these three segments, it is important to know their evolution independently and what are their trends in a near future.

To better evaluate the market sector of smart clothes, figure 2.4.2 shows a closer look of its evolution. In this figure it is possible to observe that, this year, a duplication of shipments is expected comparing to last year, 2014. Despite the low number of shipments in relation to the other segments, smart clothes market is increasing and fast, regarding that in 2013 this segment was almost inexistent.

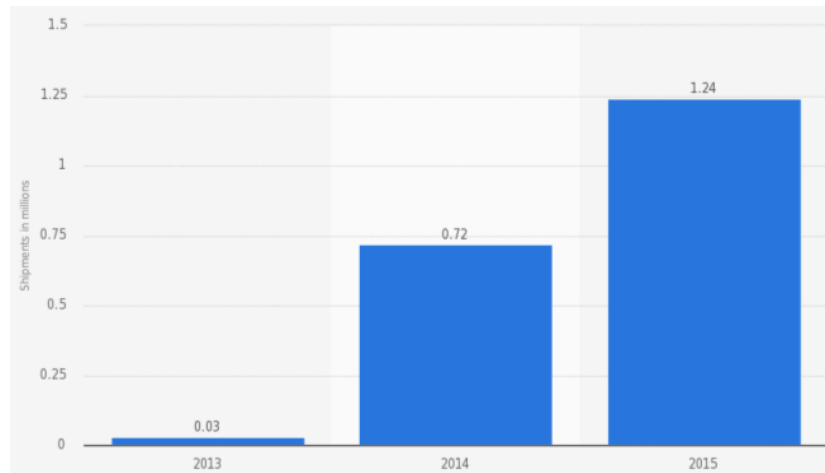


Figure 2.4.2- Shipments of smart clothing/fabrics worldwide from 2013 to 2015 (in millions). Adapted from [80].

Sport/activities trackers segment can be divided in several areas like it is shown in figure 2.4.3. The study made to get this data and trends included different types of devices, such as heart rate monitors, connected weighing scales, smart sports clothing, activity trackers and high end sports watches. The evaluation of the results obtained conclude that “mHealth Wellness/Sports & Fitness device market” is expected to grow to \$3.8 billion in 2020, mainly due to activities trackers and smart watches in general [81]. It is important to refer that smart sports clothing area is expected to increase, in fact, considerably in relation to present year. This trend information alerts us to a main increment for activity trackers in the near future, detail that should be taken in consideration for WHDs development in this segment.

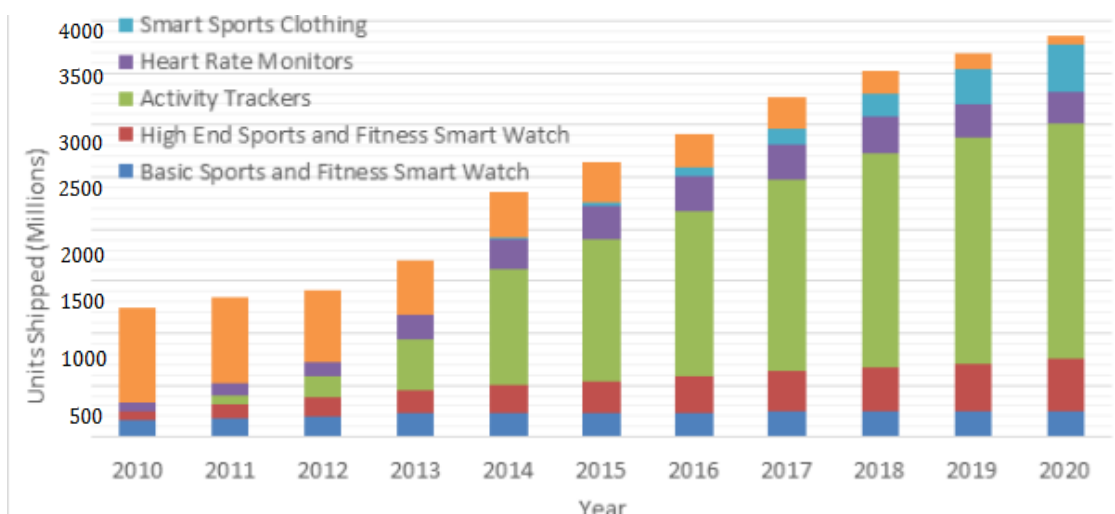


Figure 2.4.3- mHealth Wellness/Sports & Fitness Device Market (in millions). The orange color is referred to connected weighing scales. Adapted from [81].

To evaluate healthcare segment trends two approaches are made: one related to wearable medical equipment; and other concerning home healthcare monitoring devices. In this last one, market trends are presented in figure 2.4.4. This study was mainly based on the following home monitoring devices: diabetes care devices, blood pressure monitors, multi-parameter patient monitoring, apnea and sleep monitors, holter monitors and heart rate meters. From the market trends in figure 2.4.4, it is possible to conclude that in next three years, home monitoring devices will duplicate compared to 2014. The increase of home monitoring is a great contribution to predict a growth of WHDs in healthcare.

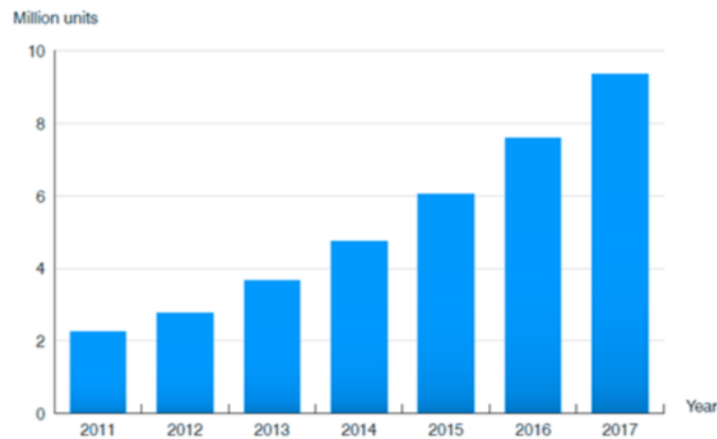


Figure 2.4.4- Connected home medical monitoring devices (in million). Adapted from [82].

Regarding wearable medical equipment, a study about China market is presented as an example to evaluate wearable medical equipment trends (Figure 2.4.5). In this approach, it is possible to see that the higher increase will not be from 2014 to 2015, but from 2015 to 2016, where a higher growth rate is observed. This trend is very favorable in Vital Jacket® sales estimation, but should also be taken in account to prepare this WHD for a possible increase of competitors, in its market, for the next years.

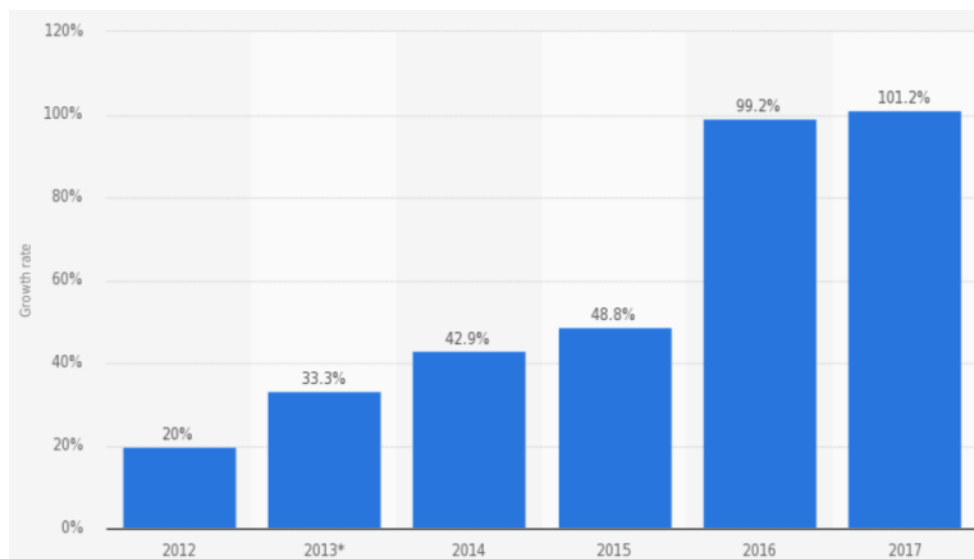


Figure 2.4.5- Growth rate of China wearable mobile medical equipment market from 2012 to 2017. Adapted from [83].

Healthcare ambulatory monitoring segment can be divided in several areas. A recent study by IHS Inc. [84], expects that mobile telehealth solutions are going to become the standard in remote patient monitoring. This study refers trends for 2014 according to a 2013 telehealth market and divides it in five main areas: congestive heart failures (CHF); chronic obstructive pulmonary disease (COPD); diabetes; hypertension; and mental Health. Figure 4.1.6 represents the distribution of each of these areas on the market.

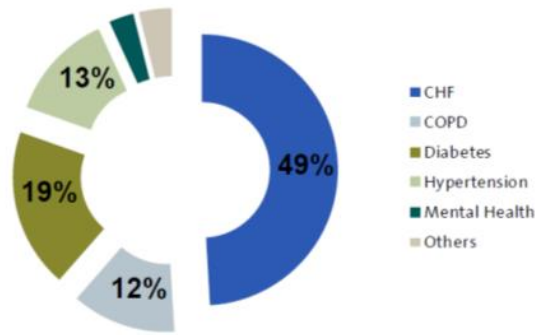


Figure 2.4.6- The World Market for Telehealth – Patient by Conditions. This is a patient distribution made for 2014 with a total number of patients of 725 thousand. Adapted from [84].

Sleep apnea, as already referred in the previous section, affects worldwide population, with an estimation of 40 million people only in the USA. To evaluate this market area trends, IHS Inc. made a research from where it can be concluded that ambulatory/home portable sleep devices presents the highest growth market in sleep diagnostic devices segment. It is also important to refer that it was projected that global home sleep market reach \$36.8 million this last year, with a growth percentage of 7.1% in relation to 2013.[84] This market trend is presented in figure 4.1.7, where it is possible to see a constant growth of ambulatory/home portable sleep testing devices.

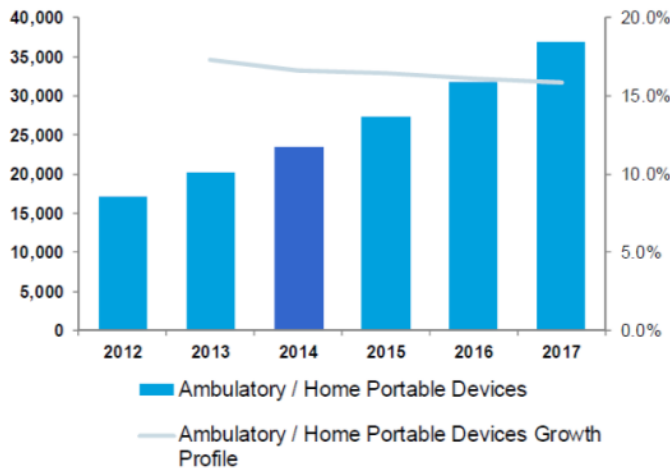


Figure 2.4.7- Ambulatory/Home Portable Sleep Testing Devices (Left axis: Unit Shipments; Right axis: Growth percentage). Adapted from [84].

To complete this market analysis it is important to mention a fact: mobile health technology worldwide market in 2011 was about \$1.2 billion and it is expected to reach an amazing \$11.8 billion value in 2018 [85]. This is a valuable estimation is also related to Vital Jacket® since it is prepared for mobile technology with Bluetooth technology.

2.5. Challenges and Future Perspectives

Wearable health devices are a recent area in healthcare and still under development with the aim to be integrate in the medical health system. There are some personal monitoring devices on the market capable to provide instantaneous single-parameter assessment and transmission. But, the main purpose of WHDs is to integrate several biosensors, intelligent processing and alerts, to support medical applications, while interacting with health providers, using some of the technology that is not yet available on the market, only in research. The existing devices are highly expensive and work wireless based, technology that is not available everywhere in many countries, such as France where many consumers do not have access to broadband internet as reported in the literature in 2012. This type of data communication leads to another problem: privacy. This is a problem that concern healthcare, in the prevention of information, leading people to have lower confidence in these devices, resulting in ethical problems. This is one of the main barriers and the suggested solution is to create clear guidelines to providing privacy, confidentiality and proper use of electronic medical information. All this effort will have an impact on societies, such as in China where WHDs may contribute to lower healthcare cost by introducing preventive healthcare strategies, cutting equipment and labor costs, eliminating unnecessary health services. [4]

The next few years present a set of new interesting challenges in WHDs and, to overtake them, an adaption of these technologies should be made, studying user requirements to develop an integrated approach in health and wellness services, instead of devices and applications for a single disease. To develop such devices and integrate them in an architecture of intelligent home services some main issues must have a special attention, such as: device efficiency, reliability and unobtrusiveness; privacy and ethical issues as already covered; legislation within and between states or countries; interoperability; end-user training to use WHDs; and social inclusion preventing users isolation, which can lead to a decrease of interaction with caregivers and physicians. [4, 16]

In the sensor technology area, there are three main aspects with particular attention: long-term stability; resiliency; and biocompatibility. In textile-based sensors, washes can cause mechanical, chemical and heat degradation, so an effort must be made to develop more resistant sensors to overcome stress caused by extended periods of use. Smaller sensors are also another important requirement, being associated to the electronics development, to increase functionality and portability of WHDs. The sensitivity of wearable sensors should be also analyzed, and a possible improvement includes the use of nanomaterial-based signal amplification. Biocompatibility must be highly considerate, covering sensors with antimicrobial or protective coating, preventing any potential toxicity of nanomaterials. [13]

Wearable health devices are able to monitor any vital sign of human body, from advance sensor supervision in the case of infant respiratory to soldiers on the battlefield or even in fitness applications. This particularity of WHDs creates a big excitement around this technology and many opportunities to continue its development. With new advances in new materials, electronics and telecommunication information technology, together with the entry of big multinational companies, such as Google and also smaller companies, like NovioSense, WHDs are expected to overcome their challenges and enter in the consumer market with a higher impact in the next few years. [4, 11, 13]

Chapter 3

VitalLogger: An adaptable Wearable Health Device

VitalLogger is a wearable health device that was developed for the first time in this Master Thesis. This device extends VitalJacket® main board, adapting it to be capable to acquire a higher amount of signals. VitalLogger device acquires and synchronizes signals mainly related to the human body but also with some ambiance conditions that can contribute to different physiological behaviors.

To analyze which are the most wanted sets of vital and ambiance variables to be monitored nowadays and the most needed ambulatory sensors, it was made a selection of the most important monitoring scenarios and the most needed sensors, based on the study performed in the previous Chapter. After Biodevices, S.A. analysis of these scenarios, a decision was made in order to develop a prototype that, joined with their technology, was able to offer a higher number of vital signs acquired, taking the first steps in VitalLogger design.

In this chapter the subjects referred above will be detailed and the development of the new prototype will be explained, such as all the steps, decisions and implementations made to get to the final prototype. A suggestion for the implementation of the developed prototype as a possible product will also be presented.

3.1. System Architecture

VitalLogger has the main objective to aggregate a specific set of sensors, according to the desired scenario, acquiring the maximum vital and ambiance data from the human body, leading to a better diagnostic in medical cases, or just to be used as a personal monitoring device. In the following picture (Figure 3.1.1) it is possible to see a components diagram where VitalLogger is inserted.

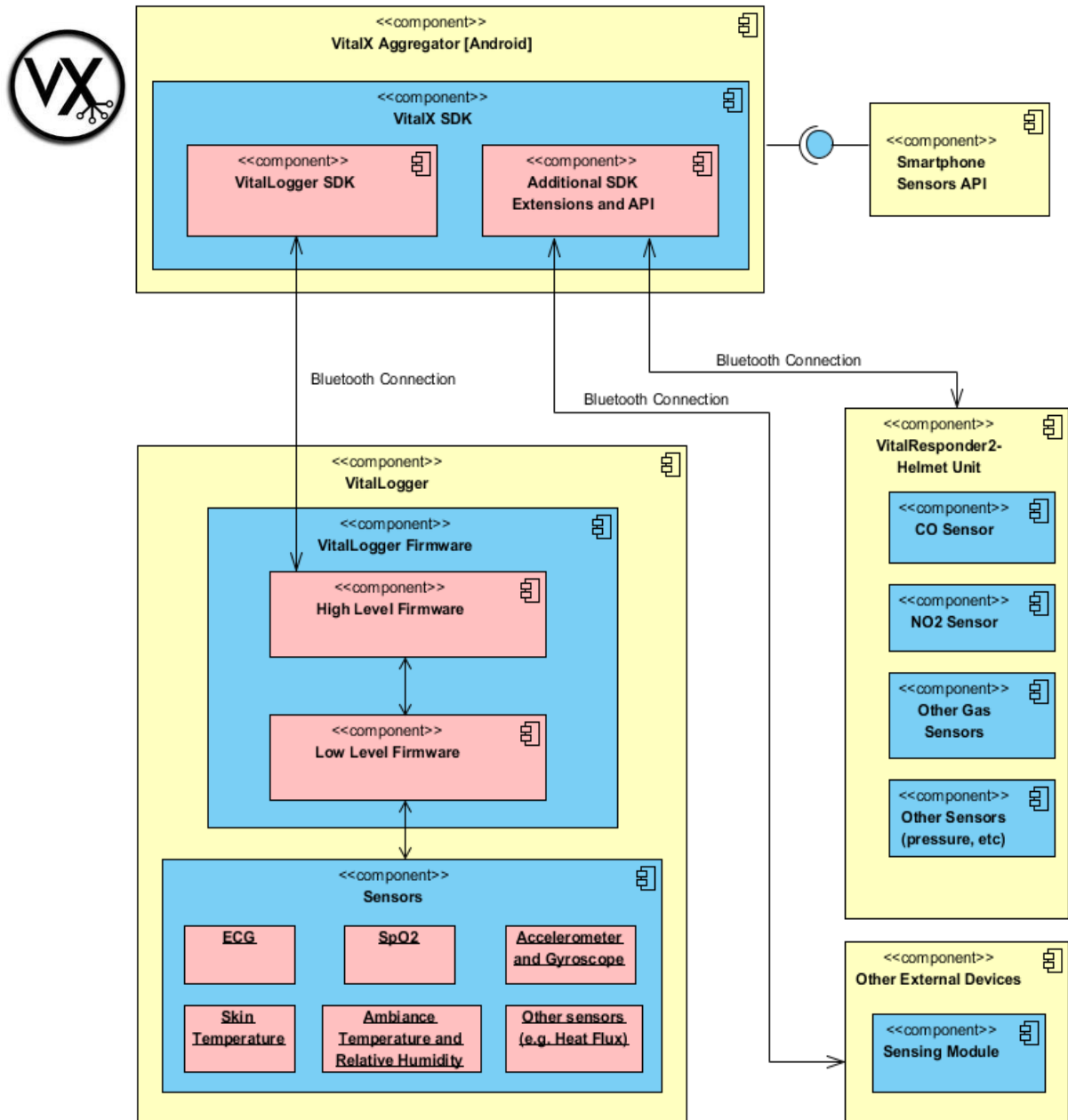


Figure 3.1.1 – Component Architecture where VitalLogger is inserted. VitalX is the Android platform where all the sensors data are collected, including VitalLogger device.

On the top of the image is the Android aggregator component which was named “VitalX” with the logotype presented in its left side. This is where all the information from several devices is gathered, stored and showed to the user. This Android application is being developed by another Msc. Student in his Master Thesis project and has the main goal to give the possibility to the user to choose which sensors he wants to acquire. These sensors can be from the Smartphone itself (e.g. gyroscope or light sensor), or can be from an external device that is connected. In this case it can be from VitalResponder2 (a monitoring unit to help first responder get access to ambience conditions to make important decisions), some external module wanted by the user and, the most important device in this Master Thesis, VitalLogger. As it can be seen in the component architecture image, VitalLogger device is mainly divided in two parts: its firmware and its sensors. In the first one, a division is made between the high level firmware and the low level firmware. The high level firmware consists in the communication implementation to transmit data between the VitalLogger and “VitalX” aggregator, allowing the user to select which sensors data he wants to acquire from VitalLogger. This last section is also being developed by another Msc. Student as his Master Thesis project. This Master Thesis is inserted in the low level firmware development, where all the integrated components (e.g. analog front-ends and microcontrollers) are programmed, and in the sensor module of VitalLogger.

This Master Thesis objective is to propose a possible extension of the number of sensors in Biodevices, S.A. technology, extending VitalJacket® device in order to design VitalLogger prototype. This work consists in the implementation of new sensors in Biodevices, S.A. technology such as the development of their low level firmware and calibration. With these three steps it is possible to obtain a viable prototype with a possible use as a wearable technology.

The contribution of this Master Thesis joint with the other two Msc. Students work, are the first steps in the creation of a user configurable and adaptable system, allowing to monitoring the desired signals, according to the devices connected to a smartphone.

In order to choose which set of sensors would be implemented, a deep analysis of wearable devices was presented in the second Chapter, giving information about the most used sensors in these devices, what are the most needed vital signs to be monitored in ambulatory cases and the future of wearable devices in the market, in both medical and health perspectives. Gathering all this information it was possible to create a set of sensors for the some important scenarios, such as cardiology scenario or sport scenario for example. The next topic will refer these scenarios and their set of sensors according to the information in the second Chapter.

3.2. Monitoring Scenarios

This topic presents a set of sensors for several scenarios selected according to the information in the second Chapter. After the description of the sets of sensors and the scenarios, cost estimation for each scenario is also presented due to its high relevance in economic decisions. These two approaches joined with the market trends analysis were presented to Biodevices S.A, leading to a decision of a specific prototype development.

3.2.1. Description

Gathering the research made in wearable health devices, wearable sensors, medical and personal ambulatory monitoring requirements and with market and trends analysis, it was possible to select the most important monitoring scenarios and define the setup of sensors for each one. These scenarios can be divided in four big monitoring groups: Sports&Activity Monitoring; Cardiovascular Monitoring; Sleep Monitoring; and Diabetes Monitoring. A fifth scenario was designed, named Multi-Parameter Monitoring (Figure 3.2.1). This last scenario is based on the most essential monitoring sensors in a clinical environment to evaluate human health, according to the research made and to the five most important vital signs referred in Chapter 2, section 3.



Figure 3.2.1 - Wearable health devices ambulatory monitoring scenarios, with the respective wearable sensors setup, according to each scenario needs.

3.2.2. Associated Costs

To better support Biodevices, S.A. decision an effective cost approach was made, analyzing and researching about the costs associated to each scenario, according to each set of sensors. To perform this cost estimation, first, it was made an individual approach in the sensors used to acquire each parameter, analyzing different ways to be implemented and sensors variations in the measure of same physiological sign using different technologies. Table II presents for each physiological/ambiance variable the maximum and the minimum possible public cost for one unit, regarding their acquisition, as also the several types of technologies and possibilities that were considered in this approach.

Table II- List off all the Physiological/ Ambiance Variables needed to be implemented to complete all the setups of sensor from each scenario. For each sensor it is made a public cost estimation based on the referred approaches made for each sensor, regarding its technology and way to wear or use.

Physiological/ Ambiance Variables	Cost Range estimation (€)	Approaches take in account for cost range estimation
Oxygen Saturation	≈ 15 - 125	-Analog and Digital Finger Sensors; -Analog Ear Sensors; -Analog Sensor for both Finger and Ear; -Digital Finger Sensors with Bluetooth.
Skin perspiration	≈ 15-280	-Digital and Analog Sensors.
Respiration Rate	≈ 7-68	-Digital and Analog Sensors based on chest belts or in wearable fabrics; -Analog Sensors based on the airflow in the mouth and nose; -Analog Sensor based on the flexibility.
Blood Pressure	≈ 12-240	-Digital Sensors based on an arm band to be used on the arm and on the wrist, with and without Bluetooth.
Blood Glucose	≈ 27-40	-Digital Sensors based on the reading of a small blood sample in a strip, with and without Bluetooth.
Capnography	≈ 350-1830	-Analog Sensors to measure the CO2 concentration in the airflow of user mouth or nose, with or without using an airway adapter (intubation).
Light sensor	≈ 4-5	-Digital sensors by their own to be implemented and already in pre-fabricated digital modules.
Sound Sensor	≈ 2-13	-Digital sensors by their own to be implemented and already in pre-fabricated digital modules.
Ambiance Temperature and Relative Humidity	≈ 7-10	-Digital sensors by their own to be implemented and already in pre-fabricated digital modules.

It is important to refer that the main influence of cost value variation is due to the fact of the most expensive analog or digital sensor being sold already with electrical components developed and some of them also with medical certifications. For this case of study both analog and digital sensors were considered, but the main interests for this Master Thesis were the analog sensors to allow a unique electronic implementation and adaptability to Biodevices, S.A. technology.

After this, cost estimation was made for each scenario, according to the sensors that make part of each scenario to obtain the defined set. Table III shows the public cost of each scenario according to the set of sensors chosen, representing the minimum and maximum costs based on the previous table. This table also refers the number of sensors needed to be added to complete the set of each scenario.

Table III- Public cost estimation for each setup of sensor of the presented scenarios. This estimation is based on the values presented in the individual sensor cost estimation.

Scenario	Minimum Cost (€)	Maximum Cost (€)	Number of sensors to be added
Sports&Activity Monitoring	≈ 45	≈ 1100	4
Cardiovascular Monitoring	≈ 40	≈ 650	3
Sleep Monitoring	≈ 380	≈ 2770	5
Diabetes Monitoring	≈ 55	≈ 325	2
Multi-Parameter Monitoring	≈ 34	≈ 1055	3

3.2.3. Biodevices, S.A. Development Decision

Although Biodevices, S.A. recognized these scenarios and their setup of sensors very relevant and with a high market impact, due to the restrict time of Master Thesis work and the complexity to implement a new sensor in their technology, none of these scenarios were chosen to be implemented. Instead of the implementation of a complete set of sensors from one scenario, a main sensor was chosen to be the main focus of this work. This sensor was the Oxygen Saturation Sensor to obtain an accurate value of the oxygen saturation percentage from user or patient blood. Ambiance Temperature and Relative Humidity variables where also chosen be acquired using a sensor, as also Gyroscope sensor to acquire actigraphy data.

The following topics of this chapter will be focus on the development of a prototype that extends Biodevices, S.A. to acquire Oxygen Saturation data, ambiance temperature and relative humidity, and also gyroscope data. It is important to refer that this prototype will extend the existing technology, so, beyond the new data that will be acquired, already implemented sensors will also be acquired, such as ECG, hear rate and Accelerometer. The prototype development topics will be divided in the hardware development, firmware development and calibration and validation of the new sensors implemented.

3.3. Hardware Development

To develop the prototype hardware new theoretical concepts were acquired and new areas were covered. Communication protocols master-slave were studied, namely Serial Port Interface (SPI) which was the protocol chosen to be used in this prototype; microelectronic fundamentals related to microcontrollers and analog to digital converters, also known as Analog Front-Ends (AFEs); and mainly related to the design of Printed Circuits Boards (PCB's) and all the process to make a PCB production. To design all the electronic schematics and PCB prototype development it was used a PCB design software.

After this study, a research was made to choose the best components to acquire the signals that were chosen by Biodevices, S.A., mainly the oxygen saturation which is the main focus of this prototype, as also the most complex. To read oxygen saturation it was chosen, joined with the company, an AFE named AFE4400. Developed by Texas Instrument, this fully-integrated AFE belongs to the first family of AFEs specially designed for pulse oximetry and presents a high reliability and configurability. This AFE controls the LEDs transmission and detection sections, converting analog readings into a digital output according to SPI protocol. The connection between the prototype and an Oxygen Saturation sensor was decided to be made through a DB9 connector because it is one of leading connectors in medical devices of this type. To get ambience temperature and relative humidity it was selected the HIH6130 digital sensor due to its ability to output a combination of these to variables in a digital format (SPI in this case). As a gyroscope sensor, it was chosen the LSM330DLC produced by STMicroelectronics, mainly due to its SPI communication possible configuration.

The main idea for the hardware structure was to produce a hardware board that could be able to connect to Biodevices S.A board (main board) through the same connector as the Vital Jacket® T-shirt connector, enabling the use of Biodevices S.A board microcontroller and extending their technology to evolve it into the VitalLogger device. To get this specification it was made an electronic prototype board where Vital Jacket® T-shirt connects in one side and, in the other side, a flat cable to connect with Biodevices, S.A. board. This design allows the prototype board to function as a bridge, where the acquired signals from the prototype are sent to the main board joined with the signals from Vital Jacket® T-shirt. Figure 3.3.1 shows a component diagram representing the interaction between VitalLogger prototype modules.

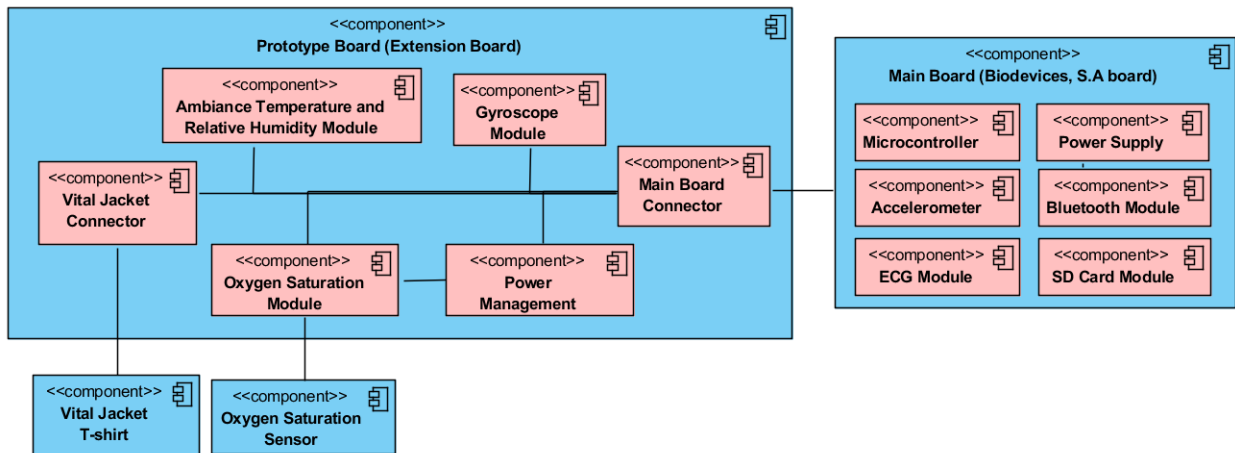


Figure 3.3.1-Component diagram of VitalLogger prototype.

The hardware development of this Master Thesis is based on the prototype board (extension board) development, extending the main board to acquire a higher number of physiological and ambiance variables.

The following topics will focus in the schematics of the electronic circuits made for each component of the extension board and in the PCB design this board.

3.3.1. Electronic Circuits Schematics

The schematics for the development of this prototype were divided in 6 main groups: Vital Jacket® connector, temperature and relative humidity sensor, AFE4400 module and DB9 connector, gyroscope sensor, power management module and the connector to the main Board of Biodevices, S.A., like it is presented in Figure 3.3.2.

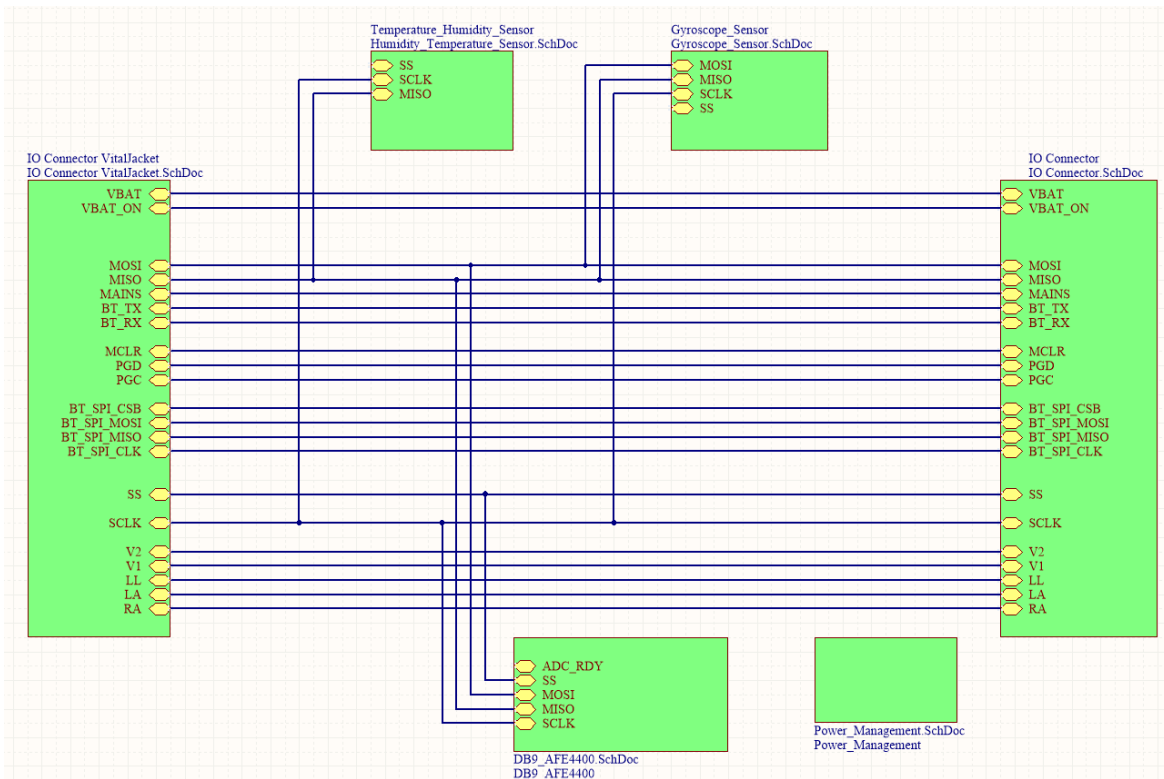


Figure 3.3.2- Schematic representation of the developed prototype hardware architecture, representing each developed module and their SPI communication interaction.

The image presented above is a schematic representation of the overall circuit that was developed, being the added modules connected to the existing channels in order to interact with the microcontroller from the main board.

To better understand the connections between the developed schematic modules it is important to explain SPI communication protocol fundamentals. SPI protocol is a communication protocol between one master and one or more slaves. A Slave Select (SS) channel allows to select which slave is going to communicate with the master and must be an individual channel for each slave. It is important to refer that a slave is active when it slave select

signal is low. In Figure 3.3.2 only the AFE4400 slave module has a slave select channel because the connector on the main board only has one. For the two remaining slaves modules it was made an external connection. Besides slave select channel, there are three more channels that are common to all slaves, communicating only with the slave that is active by the slave select channel. These three channels are the Serial Clock (SCLK) channel, the Master Output/Slave Input (MOSI) channel and the Master Input/Slave Output (MISO) channel. Serial clock is the communication pacemaker, when it goes high or low, depending of the microcontroller configuration, a bit is transferred to the slave. MISO and MOSI channels is where the information flows between master and slave, being the MOSI channel responsible for the information that goes from master to slave and in the MISO channel happens the opposite process, the information goes from slave to master.

In the following sub-topics each of these modules are going to be described and deeply discuss to explain all the details and decisions made. The SPI communications of each one will also be explained, but just in the firmware section of this Chapter.

3.3.1.1. Blood Oxygen Saturation Module

This module represents the schematic module of AFE4400 and DB9 connector, the main module of the developed prototype, being responsible to acquire pulse oximetry signal.

Analog front-end AFE4400 is developed by Texas Instruments, specifically design for pulse oximetry, having four main routes: clock route, Transmit Route (TX), Receive Route (RX) and SPI route communication. Both TX and RX have two routes, a cathode route and an anode route to connect to the oxygen oximeter sensor LED and photodiode respectively. To understand how all these sections work and inter-interacts, a study and analyses was made for a better comprehension of this AFE system. Here is going to be presented a small resume of how this system works to understand its complexity and functionality.

The main characteristic of this system are the timings when the each action occur. These timings are programmable in AFE initialization and can be changed, having all a common reference timing that is also programmable. This reference is directly correlated to an external clock of 8MHz in the clock route. The crystal oscillation when acquired by AFE4400 is converted in a 4MHz frequency and is used as AFE pacemaker.

The main idea how this system works relies on a cycle where the AFE turns on the LED in the external oximeter sensor using the TX route and then it turns off and samples the received intensity in the sensor photodiode using the RX route to convert this analog input into a digital signal using an analog-to-digital converter (ADC). This cycles is made two times because the oxygen saturation level determination requires the sample of two light wavelengths, a red and an infra-red, as it will be furthered discussed in Section 3.4.2. Two extra cycles are made to acquire ambient light and obtain a more accurate result. To better understand when these 4 cycles occur, it is possible to see in the Figure 3.3.3 the timings when each step of each cycle begins and ends.

It is important to refer that during one sampling process several measurements are made and the digital output of the ADC conversion is a mean of those values. The number of values

sampled is programmable and in the design of this prototype it will be used 3 samples. When a complete reading cycle is made and the digital data output is ready to be read, the ADC ready pin (ADC_RDY) gets high for a short instant and then turns low. One of the characteristics of this AFE is the capability to subtract the ambient sample to the correspondent LED value. This operation happens in the last ADC conversion, being also possible to be read in the SPI output.

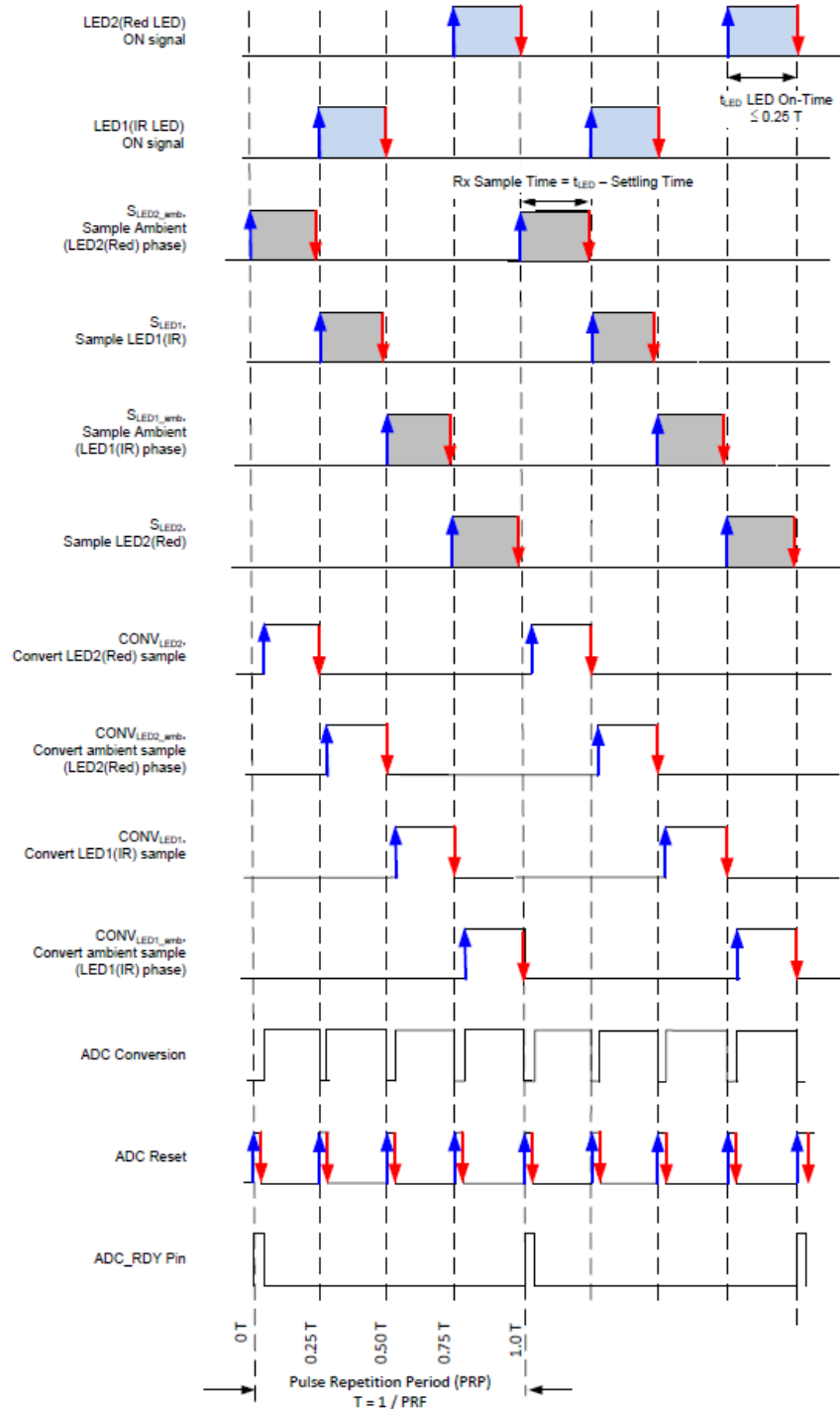


Figure 3.3.3- Sampling cycles of AFE4400. This images shows two complete cycles of acquisition and ADC conversion [86].

To design an initial working prototype, the electronic circuit was adapted from Texas Instruments recommended circuit for a typical application of this analog front-end. Some changes were made, such as: some unused resistors were removed; extra digital communication ports that were not going to be used in the SPI communication. In this case it is important to refer that ADC_RDY was initially used in the initial tests of the prototype, but then, due to its non-interaction and influence in the output data acquisition was disconnected. The following image (Figure 3.3.4) shows the final schematic with all the changes performed.

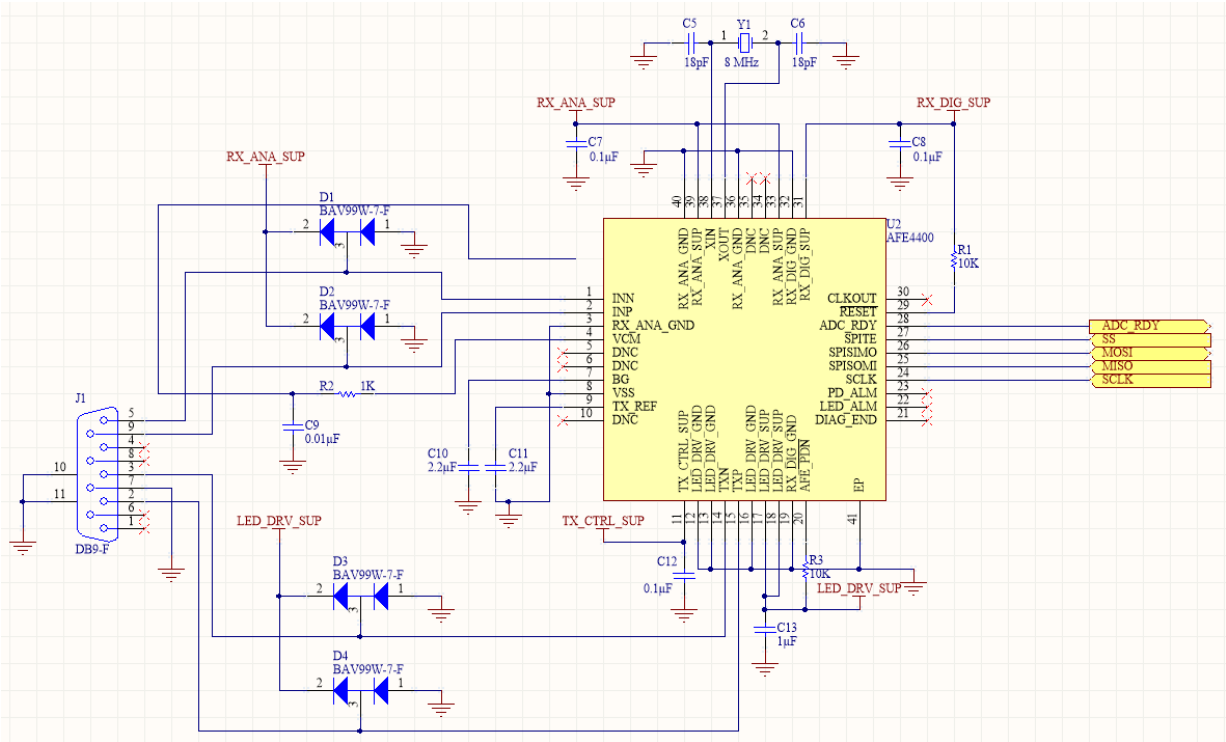


Figure 3.3.4- AFE4400 adapted schematic implemented in VitalLogger prototype [86].

Texas Instrument gives the advice to isolate the RX route, avoiding external electrical interferences. This fact can be observed in the wire of pin 4 (VCM), which was also designed in the hardware. Another important part of this electronic is its power supply which needs to be according to the AFE4400 power supply requirements.

3.3.1.2. Power Management Module

This module was specifically made to manage the power supply needed for AFE4400. Since power supply from main board was 3.3V and Texas Instrument already presents an electronic circuit to convert 3.3V in the voltage required for this AFE, the proposed circuit was adapted and designed to be implemented in VitalLogger prototype (Figure 3.3.5).

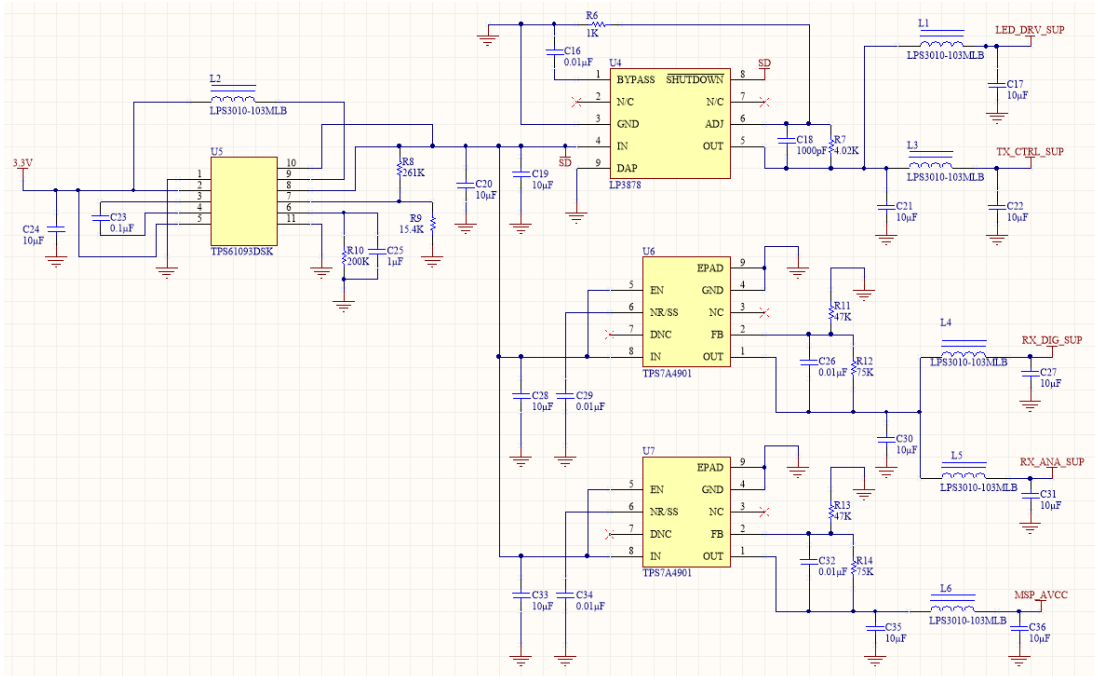


Figure 3.3.5- AFE4400 power management adapted schematic implemented in VitalLogger prototype [87].

AFE4400 has three main voltage requirements: one for RX route (2.0V – 3.6V), another for the TX route (3.0V – 5.25V) and a third one for the LEDs that can assume a maximum value of 5.25V and a minimum of 3.0V or a calculated value according to LEDs voltage. In this prototype the voltage used in LEDs is the same used in the TX route, simplifying the AFE4400 power supply to only two different voltages, RX and TX. This power management was the one advised by Texas Instruments and it was implemented to ensure AFE4400 normal behavior at an initial prototype phase. After prototype development and testing, it would be important to try to reduce the electronic of this power management, reducing significantly the board space required, obtaining, in the future, a smaller wearable system.

3.3.1.3. Ambiance Temperature and Relative Humidity Module

The acquisition of ambiance temperature and relative humidity were also proposed by Biodevices, S.A. to be implemented in this prototype. The sensor chosen to acquire both of these values was the HIH6130 with a SPI configuration. This digital sensor produced by Honeywell, outputs the ambiance temperature and relative humidity in a digital format which make it possible to be easily read by a microcontroller like the one in the main board. The electronic circuit designed was adapted from the recommended by the producer for an SPI configuration (Figure 3.3.6).

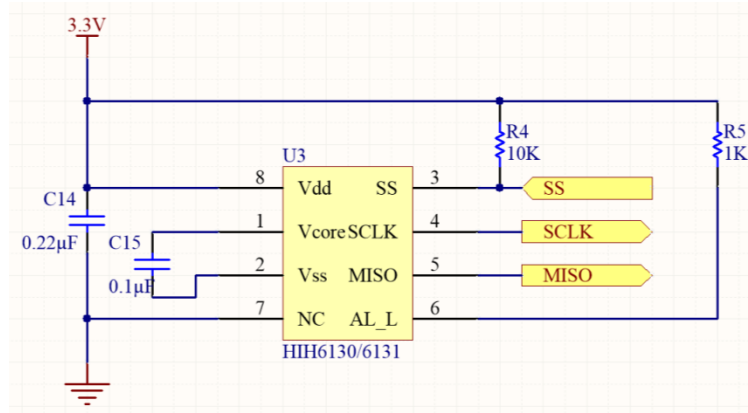


Figure 3.3.6- HIH6130 adapted schematic implemented in VitalLogger prototype [88].

This sensor has a maximum accuracy of the relative humidity in a range of 10% to 90% and for the temperature a range of 5°C to 50°C. It can measure higher and lower values inside its operating temperature range (-25°C to 85°C) but with lower accuracy. Regarding its resolution, it has a 14 bit of ADC resolution, which results in a relative humidity and temperature resolution of 0.04% and 0.025°C, respectively.

In the Figure 3.3.6, it is possible to observe that the sensor on the schematic has two possible models HIH6130 and HIH6131. These two sensors have the same configuration and both can be inserted in this schematic. The only difference is that HIH6131 is more expensive due to its extra characteristics that allow it to be used in condensing environments, which can be an important factor in future applications.

3.3.1.4. Gyroscope Module

To develop the gyroscope module it was used an inertial module produced by ST Microelectronics named LSM330DLC. This sensor has the ability to acquire three independent acceleration (3D accelerometer) channels and three angular rate channels (3D gyroscope). Its possibility to communication using SPI protocol and the fact of being possible to obtain accelerometer and gyroscope signals separately is a main advantage, allowing it to only extract gyroscope information. The electronic circuit represented in the schematic of Figure 3.3.7 was adapted from the recommended by the producer, including only the electronic and connections needed to acquire gyroscope values using SPI communication protocol.

Although this sensor was included in the hardware development and its firmware was prototyped, it was not implemented in this Master Thesis work due to time restrictions and main board PIC unavailable ports. Its SPI communication process will be briefly presented in the Firmware section of this Chapter, but it is important to retain that the firmware made was not tested.

The first version of VitalLogger extension board prototype is presented in the following figure. In Figure 3.3.8 both layers are shown, where the top is represented in the left image and the bottom layer in the right image.

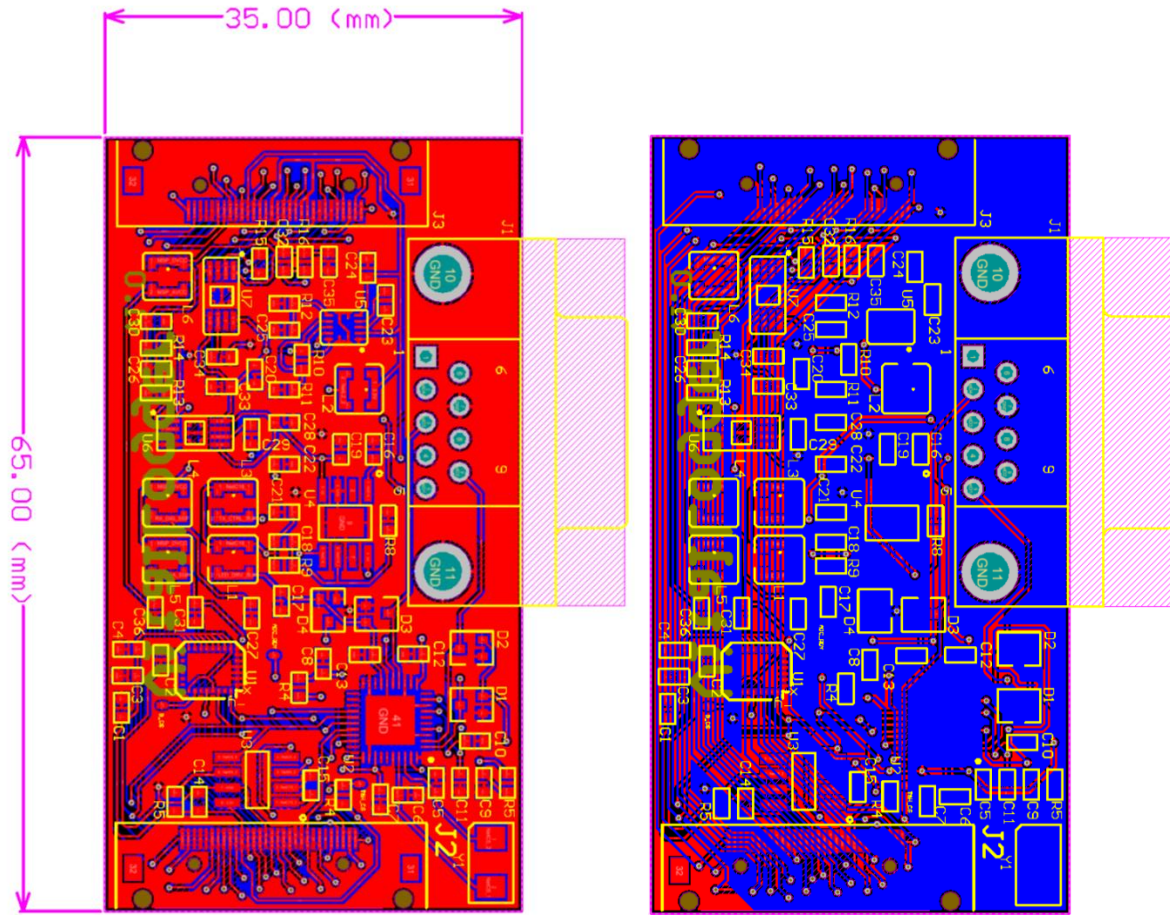


Figure 3.3.8- PCB design of VitalLogger extension board first prototype. The left image shows the top layer and the right image the bottom layer.

In each designed layer it was created a ground plan with two main objectives. First, is to reduce any external interference with the main components, functioning almost as an electrical magnetic protector. The second purpose is to easily connect all the ground pads of the components, reducing the number of printed routes needed. These ground plans are represented as red (on top layer) and blue (on bottom layer) large areas that are not connected directly to the designed printed routes.

The next image (Figure 3.3.9) shows the 3D model of the first version of VitalLogger extension board prototype, where each component is represented in three dimensions.

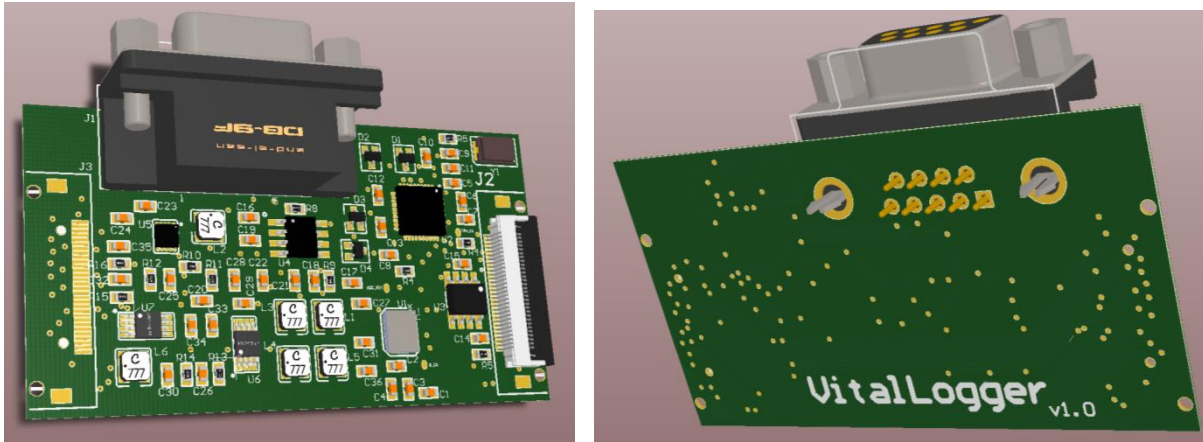


Figure 3.3.9- 3D model of the VitalLogger extension board first prototype. The left image shows the top view of the prototype and the right image the bottom view.

As it can be seen in the previous images, half of the board space is almost only occupied by the DB9 connector and the by electronic bellow that is related to the power management module. One of the main specifications of wearable health devices is their small size, characteristic that was not very well accomplished in this case, knowing that it is missing the main board and the battery. To resolve the power management oversize problem, some tests must be done after prototype finalization, as it has been already referred regarding the power management schematic section, analyzing the possibility to remove it. If these test lead to a positive result the next step will be to make a smaller board to connect to the main board or even do a small module to be mounted directly in the main board. This last solution is related to the size of the BD9 connection, which would have to evolve into a smaller connector. This conversion is possible because oxygen saturation sensor only uses five of the nine channels, and adapting the sensor cable into a smaller connector with only five channels would reduce an amount of space, obtaining a higher portability and wearability.

3.3.3. Board Assembly

The process how to produce a PCB was also learned. This process has two main phases: a phase where the files to fabricate the PCB are generated; and the phase where the PCB is ordered. The first one consists in the generation of two main files: a Gerber file with all the layers design, used for the fabrication; and another Gerber file with all the drills needed to make in the PCB fabrication. The next phase is to order the PCB in a PCB's producer. To obtain the exactly PCB as it was designed, it is essential to verify the Gerber design generated by the producer, to see if the top and bottom layers are according the design made. This process can take some time depending on the producer Gerber generator and normally some changes must be done to get a good result. During this process some errors have occurred in the producer Gerber generator such as some undesirable unions between two "vias" or between a "via" and a route. Another problem was in the ground plans, where some of them were not designed by the producer Gerber generator. These problems were resolved by trial and error and some of them were not possible to solve, making a route of ground to connect directly to ground pads avowing ground plans errors. The plans that were not accepted by the producer can be seen in Figure 3.3.11 represented by a larger area in a darker green color on the board.

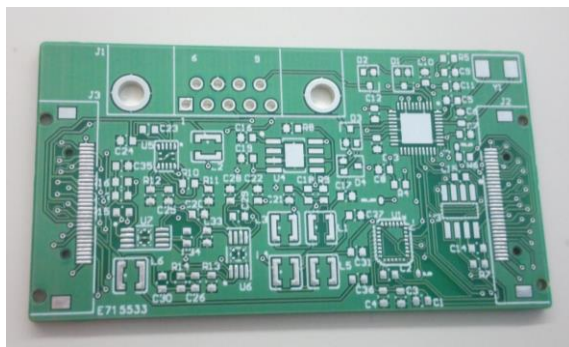


Figure 3.3.10- Produced PCB of the first VitalLogger prototype.

After ordered the production of the prototype PCB, all the components needed were also ordered from two distributors due to the unavailability of some components in both distributors.

When all the components and the PCB were received, the assembly was made. This process was learned and improved with some techniques acquired with Biodevices, S.A. personnel. Figure 3.3.12 demonstrates one of the three assembled boards, with the designation of each module and also with some electronic changes due to schematic design errors that were discovered during the firmware development phase.

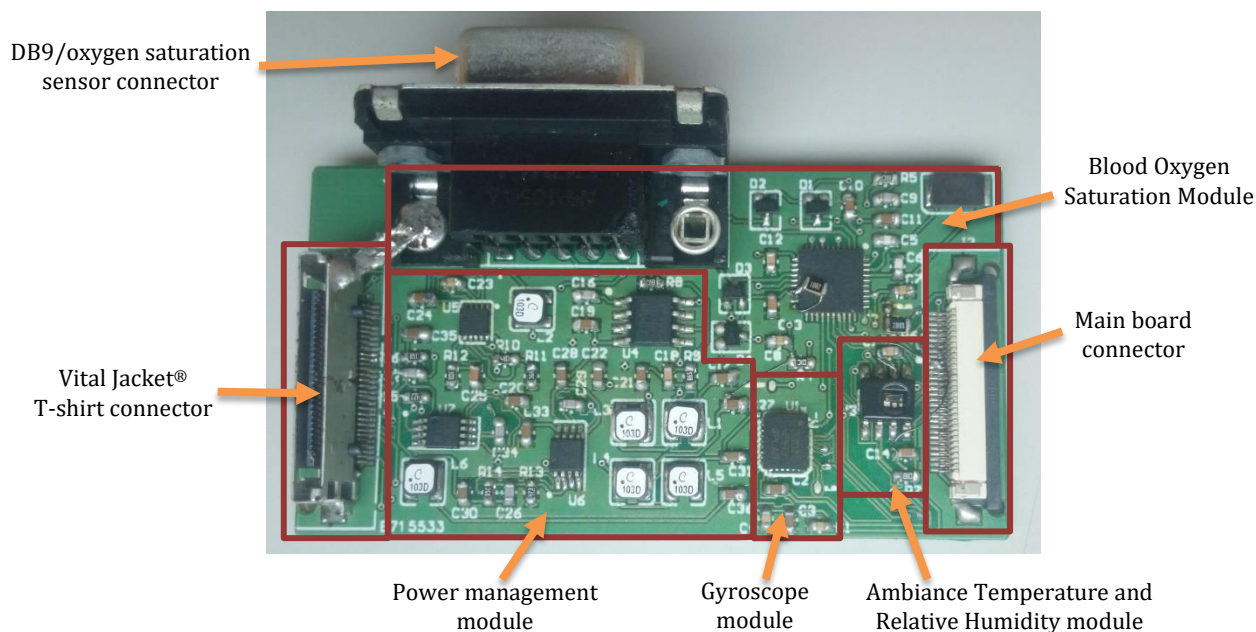


Figure 3.3.11- The first version of VitalLogger prototype assembled with each module and connector label.

To evaluate AFE4400 power supply, the values of the TX root and RX root supply were verified, obtaining values of 5.03V and 3.07V respectively. These are the expected values of the power management circuit developed and are inside the considered range for each of these roots. Then, the connection with the main board was made, as it can be seen in the Figure 3.3.13. In this image it is possible to see that the Vital Jacket® T-shirt connector is in a vertical position, fact that was due to an error in the first schematics design of this first prototype. In the same

image it is possible to visualize, above the flat connection, a wire made connection for the slave selection channel of the HIH6130 sensor.

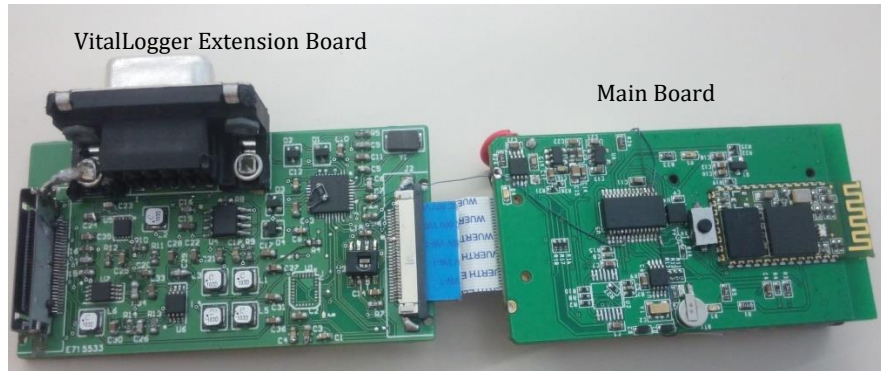


Figure 3.3.12-VitalLogger first prototype connected to a main board through a flat connection.

In order to correct some of the errors made in the schematics design, a second version of this prototype was designed, but not produced. This second prototype with all the modifications is presented in the Appendix A, regarding its schematics and PCB design.

After the connection of these two boards, a more secure process was used to keep these boards together using a rubber band. Figure 3.3.14 shows this more compact module with the oxygen saturation sensor plugged.



Figure 3.3.13- VitalLogger first prototype connected to the main board and with the Oxygen Saturation sensor plugged in.

Regarding the oxygen saturation sensor, three sensors were acquired from two different places. One was borrowed by *Covidian Portugal* to be used exclusively for scientific purpose and the other two were bought to a distributor in China. The model was the Nellcor™ DS100A Adult SpO₂ Sensor and its LEDs operate at 660nm (Red) and 905nm (Infra-red) wavelengths.

After the hardware explanation of the development of this prototype, it will be presented in the next section how the firmware was developed. In this section will be discuss the firmware architecture for each of the developed sensors modules.

3.4. Firmware Development

The firmware development was made using *Microchip IDE* software, namely *MPLAB IDE X* to implement, using C programming language, the firmware for a specific Microchip microcontroller, like the one in the main board. This software as a configuration tool that was used to automatically generate the code to the initialization and control of the microcontroller pins. The remaining code was made from scratch and divided in four files, three of them related to each sensor (AFE4400, HIH6130 and LSM330DLC) and a fourth one to calculate oxygen saturation using the acquired values from AFE4400. Beside these four files an SPI control file was also done to control and configure SPI communication, allowing sending and receiving bits from a selected slave. The microcontroller used in this work has an 8-bit architecture allowing to send and/or receive SPI data with 8-bit. The Main file of this firmware was also designed, containing all the initializations needed when the system is powered and then a while cycle containing all the sampling procedures to obtain a final result from each sensor. Figure 3.4.1 shows a workflow diagram of the Main file to initialize and read samples from sensors. This workflow does not include the gyroscope module because it was not implemented, but its firmware will be presented in Gyroscope Module Firmware section.

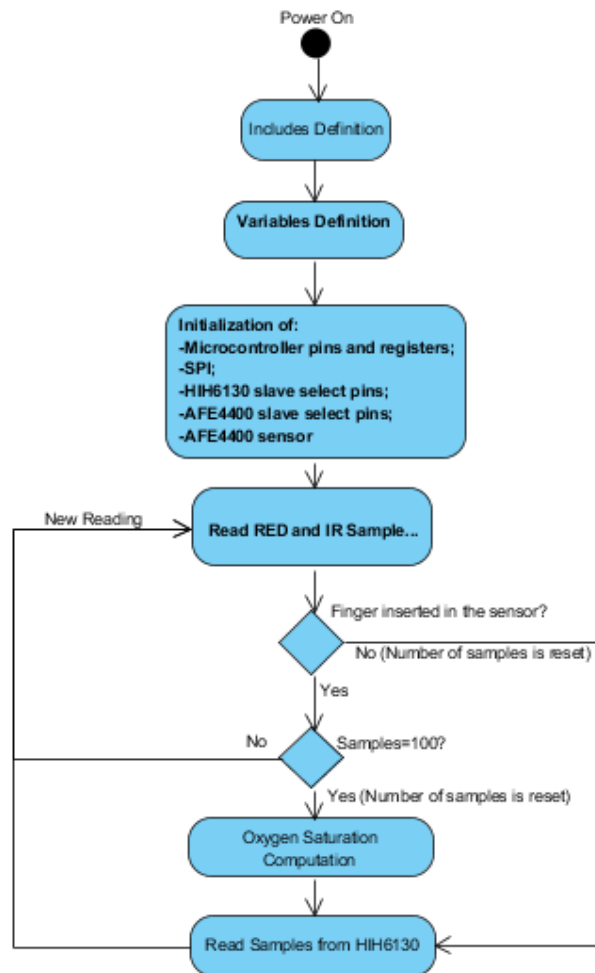


Figure 3.4.1- Workflow diagram representing the main file of the developed firmware.

After the initialization process, a reading from the sensor is performed to get the Red and Infra-Red wavelength samples. These values are used to verify if the finger is inserted or not in the sensor, avoiding invalid measurements. In the finger presence, more acquisitions are made until obtain 100 samples. During this process, after each acquisition a verification of the finger is made, so, if the finger is removed after obtain 100 samples, the oxygen saturation level is not calculated. When the finger is removed or after the oxygen saturation calculation an ambience variables acquisition is performed.

The oxygen saturation acquisitions needed to calculate its level are one hundred with a 20Hz frequency due to two main causes: the first one is due to the microcontroller that is used to acquire samples that has some priority tasks which cannot be stopped, being necessary to get readings between those tasks which restrict the sampling frequency; the second cause takes in account the physiological heart rate. To calculation oxygen saturation it is needed to get a typical oxygen saturation curve and with 20Hz of sampling frequency it is possible to obtain the main characteristic of this wave, maximum and minimum values, from 30BPM to 240BPM, fact experimentally proven.

Concerning SPI communication in the developed firmware, it is important to explain that the communication between the master and slave is in groups of 8-bit due to the microcontroller architecture. These groups are named as register and normally they contain some bits or even a byte (8 bits) to identify what is the address of the register and then, the remaining bits or bytes contains the information related to that specific register. For example, to define some setting in a slave it is necessary, first, to send the address of the register that contains the settings wanted and then the remaining register with the high or low bits according to the specification needed. Components datasheets has a list of specific registers and their description concerning the address and the settings that each bit defines. This concept is going to be used along this section.

The initialization represented in the workflow diagram is shown in the following image (Figure 3.4.2), but now acquired during SPI communication between the microcontroller and both slaves, the AFE4400 and the HIH6130. The overall SPI communication process of the workflow is presented in Figure 3.4.3.

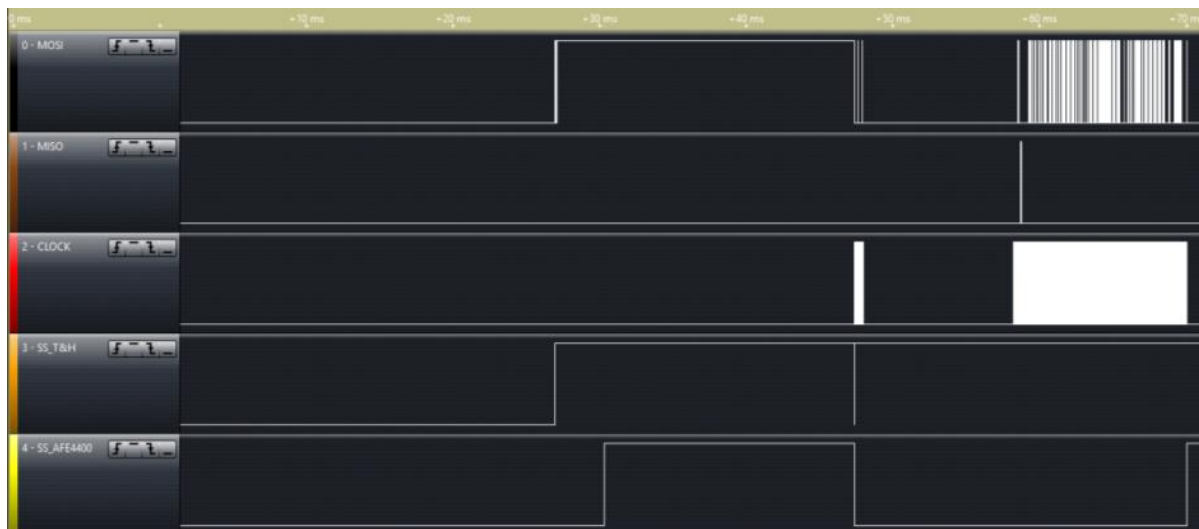


Figure 3.4.2- SPI digital acquisition of the initialization process. First the pins are initialized such as the SPI microcontroller module. The HIH6130 initialization occurs when its slave select (“SS_T&H”) goes

down, which is a very quick process. Just after that the AFE4400 slave select (“SS_AFE4400”) goes active to start AFE4400 initialization process that will be discuss in the following topic.



Figure 3.4.3- SPI digital acquisition of the first cycle including the initialization. First it is visible a higher density of SPI communication which represents the initialization referred above. Then a reading until 100 samples it’s made. The following space without communication corresponds to the time where the oxygen saturation value is computed and then an ambience temperature and relative humidity reading is performed. It is still possible to view the start of a new reading, without the initialization process.

The following topics will explain each file of the developed firmware related to the sensors and oxygen saturation calculation, explaining its architecture and how each sensor works, including their SPI communication process.

3.4.1. Blood Oxygen Saturation Module

This module is related to the AFE4400 firmware. This AFE needs four main different developed functions to work and acquired data from the sensor and sent it to the microcontroller. First, its slave select pins need to be initialized in the microcontroller as already presented in the main workflow diagram as “Initialization of AFE4400 slave select pins”.

The second function has the objective to initialize the AFE4400 itself. This step is made according to four phases like the workflow in Figure 3.4.4 shows. The first step is *reset all* the registers, cleaning all the programming that was made in the last time that the system was powered up. Then it is made a check to know if AFE has any fault or not, returning a certain amount of bits to inform its status. These bits information was only used in initial tests. Then the microcontroller sends twenty seven timing control registers to set when each operation starts and ends, like is was explained in the Hardware section of this module. The last step before end the initialization process is to send five register related to the AFE400 operational mode defining some essential configurations. These registers can be changed to obtain different configurations, such as, for example, change the LEDs current or to activate/deactivate AFE4400 SPI reading module.

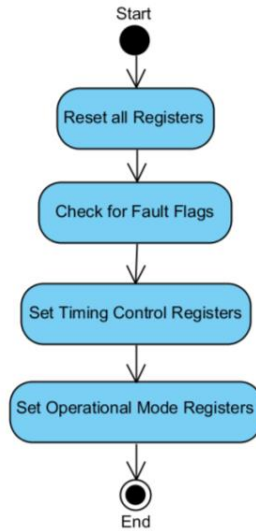


Figure 3.4.4- Workflow diagram representing the AFE4400 initialization process.

After the reset and initialization, two main functions are still missing, the reading and writing functions, also used in the initialization process, being responsible for the communication between the microcontroller and the AFE4400. To explain these functions it is important to understand how AFE4400 registers are designed by the manufacture: each register contains 32 bits (4 bytes) where the first 8 bits (first byte) indicate the address of the register that is being sent and the remaining 24 bits (3 bytes) represent the information about that register. If it is a timing control register it contains the instant, inside a range, when the action defined by the register address must occur. Another example is when it is an operational register: in this case it will contain a first byte with the register address and then the information with the wanted configuration, being this chosen according to the datasheet, where all the possible configurations are described.

The writing process in AFE4400 is made sending 32 bits from the microcontroller, divided in four groups of 8 bits due to the microcontroller architecture.

The reading process is more complex. First, the AFE4400 must be set in the reading mode, sending a specific register which has a bit to configures the reading mode as active. When this register is sent, the reading mode turns on and only can be switch off when the same register is send with the opposite value of the same bit, inactivating the reading mode and activating the writing mode. With the reading mode active, to get a register from AFE4400 it is firstly needed to send the 8 bits that has the register address that is going to be read. After receive the register address, the AFE writes the information of the requested register in the next 24 clock cycles. These are read by the microcontroller and saved. The following image (Figure 3.4.5) is a captured SPI signal from the developed prototype, where a reading from AFE4400 is made. It is possible to see the slave select, named "ENABLE", being activated (when it goes down) and the register request in the first 8 bits in the MOSI channel. After this, the remaining 24 bits are sent by the AFE4400 in the MISO channel, representing the information of the requested register. The initialization process use both writing and reading functions, being this last one only used to read the register that sends the faults flags checking.

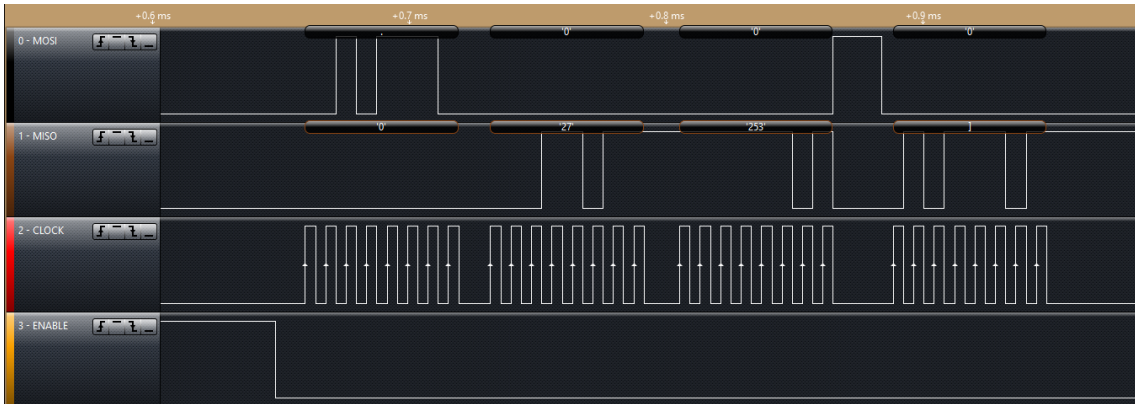


Figure 3.4.5- - SPI digital acquisition showing the process to get a reading from AFE4400. First, AFE4400 slave select (“ENABLE”) is activated (value zero) and then the first 8 bits send the register address that the microcontroller wants to get the information. The next 24 bits are received by the microcontroller and represent the value of the requested register.

To read the oxygen saturation sensor values it is only needed the reading function. The requested values were the LEDs samples without the ambient light contribution, being made two readings, one to get the Red led value and the other to get the Infrared value, both without the ambience light contribution. Figure 3.4.6 shows the complete reading process with the writing of both registers addresses and respective sampled digital information. The separation between both registers is due to the sending process of the acquired value through Bluetooth that was activated to make some tests with the prototype sampled values. To decrease power consumption, the LEDs are only turned for the readings process. In Figure 3.4.6 is possible to see the ADC_RDY being activated when new values are ready to be read. Due to its independence with the reading process, fact proved experimentally, its connection was removed not being acquired by the microcontroller. It is important to mention that the samples acquired from the AFE4400 are converted into millivolts, according to the manufacture conversion.

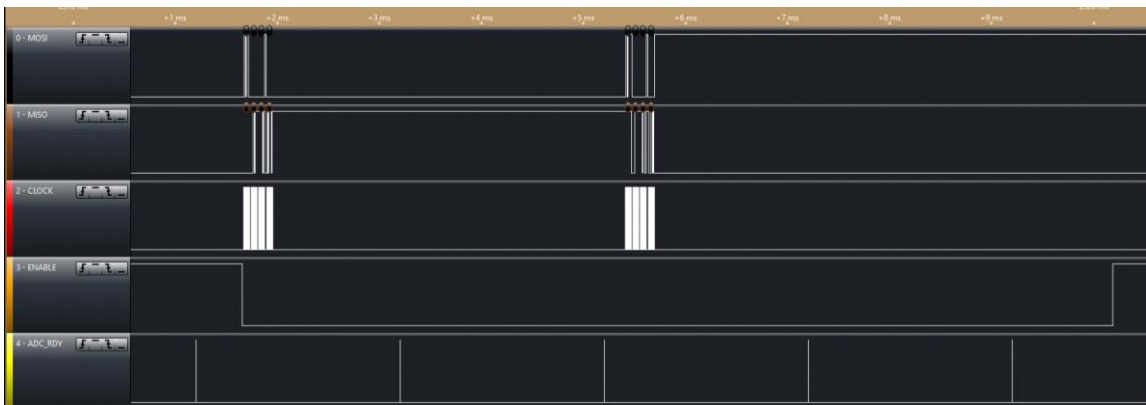


Figure 3.4.6- SPI digital acquisition of the process to acquire both needed readings to obtain oxygen saturation signal from the Red and the Infrared LEDs. The readings have some space after them due to a debug process that is not implemented in the final firmware version. The ADC_RDY is represented in the last channel and is constantly being actualized. After some tests, it was possible to verify its independence with the reading process, being disconnected from the microcontroller.

After this firmware implementation, the signal obtained from the oxygen saturation sensor was acquired using a laptop, through a Bluetooth connection. Figure 3.4.7 shows the acquisition procedure to acquire the oxygen saturation curves, containing the VitalLogger prototype with

the oxygen saturation sensor connected and the laptop external Bluetooth device. The *PComm Terminal Emulator* software was used to acquire and record the values sent by the VitalLogger.



Figure 3.4.7- Sampling acquisition procedure to acquire the oxygen saturation curve.

The following figure (Figure 3.4.8) shows an example of 100 samples acquired from the finger using the VitalLogger prototype. This left image of this pictures shows the direct signal obtained from the oxygen saturation sensor. As explained in the oxygen saturation section (Figure 2.3.3), the PPG waveform is due to blood attenuation, decreasing it value when the blood flow increase. The most common and conventionally used PPG waveform is an inversion of this attenuation. The right image of Figure 3.4.8 shows the inverted waveform of the acquired signal. In the following representations of this signal it will be used the inverted representation.

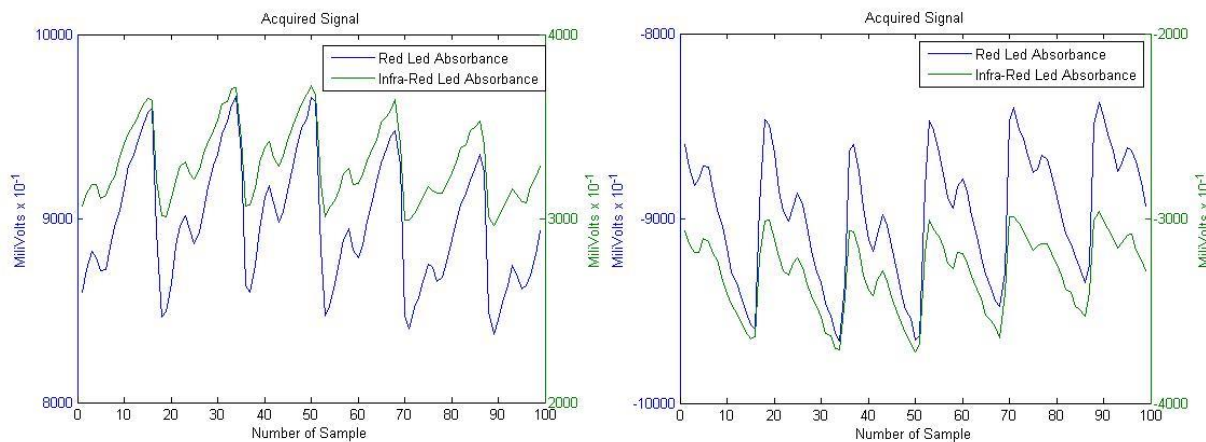


Figure 3.4.8- Oxygen saturation sensor acquisition with the VitalLogger prototype, showing the PPG waveform. The left image represents the acquired signal and the right image represents an inversion of this signal.

The next step is to use the 100 samples of this process to calculate the oxygen saturation value. Before this step, some theoretical fundamentals will be present to understand how oxygen saturation is calculate nowadays, and then the method used will be discuss as also the steps made until get to the final oxygen saturation value.

3.4.2. Theoretical fundamentals for SpO2 Calculation

As it was presented in Chapter 2 (Figure 2.3.3), pulse oximetry is based on a light source that is attenuated by a DC component related to tissues, venous-blood and a continuous component of arterial blood that is non-pulsatile, and is also attenuated by an AC component that has a pulsatile behavior due to variations on arterial blood flow caused by heart beats that injects oxygenated blood in the circulatory systemic system originated from the circulatory pulmonary system. In oximetry, one of the causes that lead to the variation of this component value is the presence of hemoglobin and its derived molecules [90].

In our blood exists several molecules derived of hemoglobin depending of which ligand is bind to the hemoglobin molecule. Two of these derived molecules are the one with a molecule of oxygen bound which is the most present in arterial blood, named Oxyhemoglobin (HbO_2), and hemoglobin without any ligand, mainly present in the venous blood, named Deoxyhemoglobin (Hb). These two main derived of hemoglobin have different absorption spectra's, like it is showed in the following image (Figure 3.4.9). [90, 91]

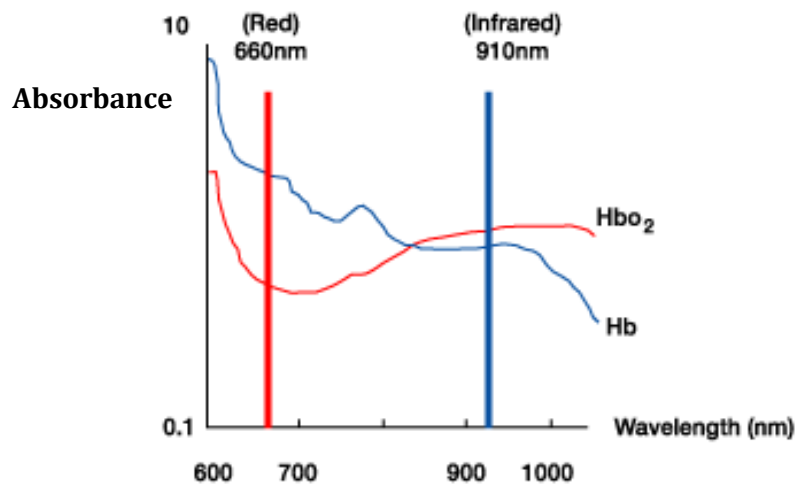


Figure 3.4.9- Absorbance spectrum of oxyhemoglobin (HbO_2) and deoxyhemoglobin (Hb) from 600nm to approximately 1000nm. The wavelengths used in pulse oximetry are represented in a red stripe for the Red source (660nm) and in a blue stripe the Infrared source (910nm). Adapted from [92].

As it can be seen, at approximately 660nm (Red), the absorbance of HbO_2 is lower than Hb and at approximately 910nm (infrared) the opposite is verified. This fact is the main theoretical fundament that will allow obtain oxygen saturation. Pulse oximetry uses these two wavelengths to obtain the total intensity of each one of them. For the Red wavelength example, if the HbO_2 concentration is higher than the Hb concentration the total intensity absorbed will be lower, indicating a higher oxygen concentration. In the other hand, if the HbO_2 decrease the Hb will increase and the total intensity absorbed will be higher, indicating a lower oxygen concentration. In the Infrared case, the opposite is verified because the HbO_2 has a higher absorbance, so, if its concentration increases, the total intensity will also increase indicating a higher oxygen concentration. In this case, the intensity increasing is going to be lower than in the Red LED. [90, 91]

Pulse oximeters sensors have LEDs with these two wavelengths and photodiodes to receive both of these wavelengths. As it was shown in the cycle of AFE4400, pulse oximeters emit these

two wavelengths separately and acquire each signal to obtain the total intensity of each wavelength. The oxygen saturation percentage is based on these intensities using its ratio to obtain a correlation between the concentration of HbO₂ and Hb. This ratio is described by the literature as the “R value”, and is a simplified equation that allows to correlate its value with the oxygen saturation percentage. Equation 1 shows the R value calculation for the wavelengths of the sensor used in this work. [91]

$$R = \frac{\left(\frac{AC}{DC}\right)_{\approx 660nm}}{\left(\frac{AC}{DC}\right)_{\approx 905nm}} \quad (\text{Eq.1})$$

The R value correlation with the oxygen saturation is then obtained through a pulse oximeter calibration curve. Figure 3.4.10 shows an example of a calibration curve, and its correlation is normally made with a second degree equation, like it is made in this work.

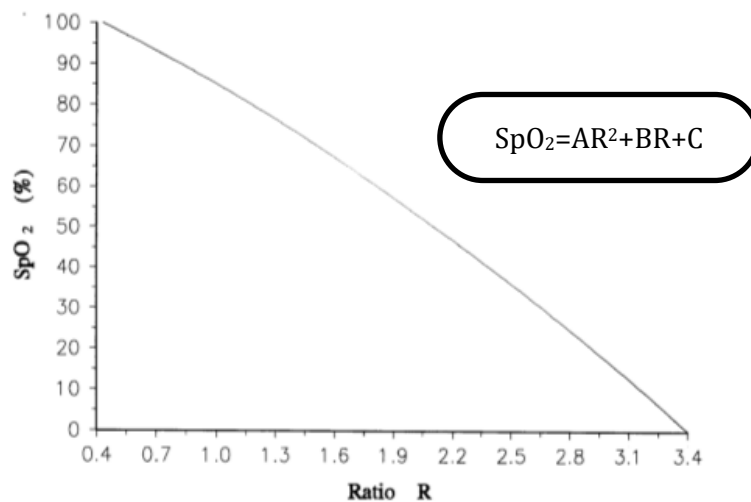


Figure 3.4.10- Example of an oxygen saturation curve that correlates the R value with the oxygen saturation level with a polynomial second degree equation. Adapted from [91]

The R value calculation can be made using three different mathematical operations using the PPG signal obtained from the pulse oximeter sensor. The first one is to use the AC amplitude in both wavelengths in the R equation. Knowing that the amplitude is given by the maximum and minimum value of AC component, where the minimum value corresponds to the DC value. Another method is based on the same logic, but applied to parts of the PPG signal instead of its application in a complete PPG wave like in the previous method. This method allows to compute the R value along its acquisition and with less motion artifacts, which is a better approach in real time monitoring application. Both of these methods were tested in this work and one was chosen one of them to be implemented like it will be discussed in the next topic. A third method to get the R value uses the Fast-Fourier Transform (FFT) computation, correlating the intensity of specific frequencies. This method was put aside from the beginning due to the high computation cost of the FFT calculation for the main board microcontroller, not being analyzed in this project. [91]

To better evaluate which of the first two mentioned methods were the best to get the R value, it was made a *MATLAB* script to make this evaluation automatically. This evaluation will be discussed in the following topic, explaining all steps made and results obtained.

3.4.3. Evaluation of the Best Method to Calculate the R Value

In this section two methods for the R value calculation are evaluated, one based on the maximum and minimum value (MaxMin Method) and the other that gets a certain number of samples of the PPG signal and calculates the R value (By Parts Method). To better evaluate these methods, this analysis was made already with acquired values from the prototype sensor develop in this project. After values acquisition it was made a MATLAB script to first make a signal analysis and processing using basic operations, to then transform it in C language and implement in the microcontroller the best processing method and the best R value calculation method.

To obtain a more robust decision of which is the best method to calculate the R value it was acquired SpO₂ signals at different heart rates (Beats Per Minute - BPM) and at different oxygen saturation levels. These experimental values were obtained using a SpO₂ simulator, which will be deeply discussed in the Sensor Calibration section. It is important to refer that the simulator used has defined values for BPM and SpO₂ values (Table IV). For each SpO₂ value it was acquired a PPG simulated signal at all the BPMs values possible to be simulated, being described both variables range on the following table.

Table IV- Values of Oxygen Saturation levels and heart rate (BPM) levels simulated by the simulator device. For each value of these two variables the other variable can assume all the referred values. For example, for a 70% of oxygen saturation, it is possible to simulate this level in all the heart rate levels presented in the table.

SpO ₂ values (%)	Heart rate values (BPM)
70	30
75	60
80	65
85	80
90	100
95	120
97	150
98	180
99	240
100	

Before the R value calculation some signal process was made according to the signals obtained in the SpO₂ simulator, as also using samples acquired from a finger. Figure 3.4.9 shows the workflow of the signal processing made.

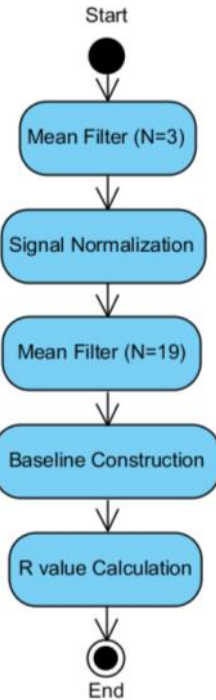


Figure 3.4.11- Workflow diagram representing the signal processing made until the R value calculation.

The designed workflow was developed to allow the use of this signal processing in all the BPMs acquired in the simulator, choosing a fixed number of samples in average filters according to its analysis and to human signals. The first operation (“Mean Filter”) objective is to smooth the acquired value, removing some high frequency noise. Then, a normalization process is made to obtain a more similar DC value between both LEDs signals, equalizing the reference value and obtaining a more consistent value in the R value calculation. After this a mean filter with a high number of samples (N=19) is applied to get a mean line of the signal. The last step is to subtract this line to the original signal, obtaining a signal with a constant baseline and removing some signal oscillations (low frequencies). Figure 3.4.12 shows an acquisition from a finger in movement to illustrate this process implementation in *MATLAB*. This signal processing allows removing signal originated by the finger movement, leading to a more feasible R value determination.

The next and last step was to calculate the R value. Both methods were already explained, only is missing the number of samples used in the “By Parts Method”. Several tests were made to achieve the best number of samples and in the end it was considered 5 samples. This value was achieved testing several sampling numbers at the several BPMs values and a sampling of 5 values showed the best results regarding the variation of the oxygen saturation levels. Even though this was the sampling window with best results, one value at 30 BPM was very different from the expected value. Table V shows the mean results obtained in the R value calculation for each oxygen saturation level, considering all the simulator possible BPM. To obtain these results, the outside value at 30 BPM was replaced by a medium value between the next and the previous oxygen saturation R value obtained.

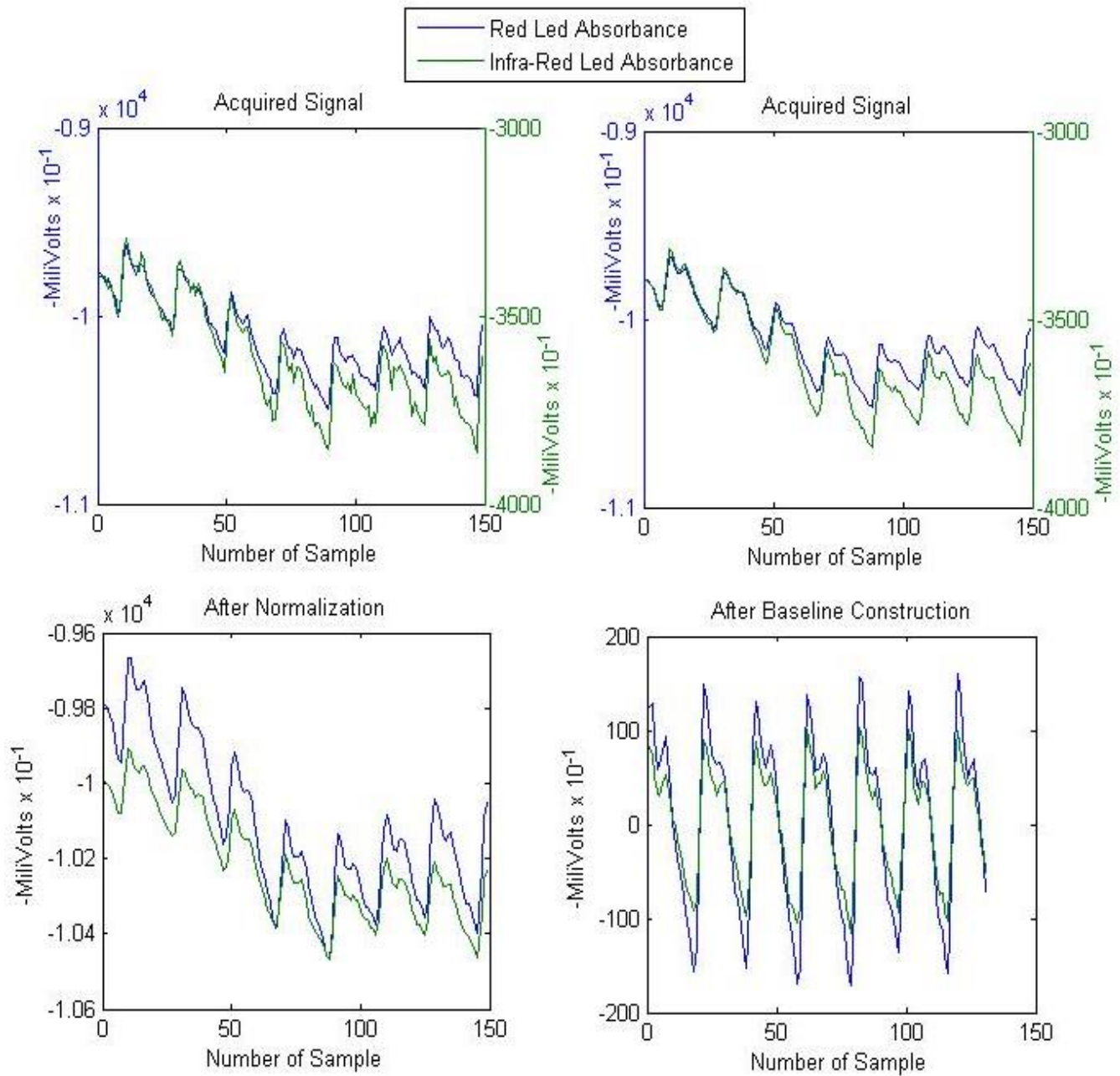


Figure 3.4.12- Example of the signal processing steps made before R value calculation using a signal acquired on a human finger with the developed prototype. To obtain this signal the number of samples restriction was increased to 150 and the finger was moved during the acquisition. The first image (top left) represents the signal acquired by the prototype. The second image (top right) shows the signal after the first mean filter (N=3). The third image (bottom left) shows the normalization result of both waves. The last image (bottom right) represents the final signal after the baseline construction.

Table V- This table shows the mean values and respective standards deviation of the R value result for each oxygen saturation level when the heart rate frequency goes from 30 to 240 BPMs according to the simulator scale. The R value is calculated using two methods, “MaxMin” and “By Parts” in order to analyze the best method to calculate the R value.

Oxygen Saturation	MaxMin Method		By Parts Method (n=5)	
	Mean	Standard Deviation	Mean	Standard Deviation
70	10.55	3.05	10.78	3.91
75	10.01	2.94	12.74	5.50
80	9.23	2.74	8.94	2.94
85	8.41	2.64	7.56	2.28
90	7.18	2.20	6.19	2.41
95	5.77	1.78	7.41	4.72
97	5.26	1.57	4.45	3.07
98	5.09	1.60	5.98	4.48
99	4.70	1.43	4.27	1.21
100	4.34	1.30	3.66	1.21

Analyzing the previous table (Table V) it is possible to conclude that the “MaxMin Method” has better results due to its increasing consistence and lower standard deviation along the BPM variation. “By Parts Method” also shows good results, but not as good as the “MaxMin”. To get a more consistent conclusion, and after an analysis of the oxygen saturation in each BPM, it was made the same comparison between these two methods without the R values from 30 and 240 BPMs as it is showed in the following table (Table VI).

Table VI- This table shows the mean values and respective standards deviation of the R value result for each oxygen saturation level when the heart rate frequency goes only from 60 to 180 BPMs according to the simulator scale. The R value is calculated using two methods, “MaxMin” and “By Parts” in order to analyze the best method to calculate the R value.

Oxygen Saturation	MaxMin Method		By Parts Method (n=5)	
	Mean	Standard Deviation	Mean	Standard Deviation
70	11.50	0.40	11.10	2.42
75	11.01	0.44	15.28	2.98
80	10.03	0.36	10.34	0.82
85	8.99	0.37	8.27	0.83
90	7.69	0.30	7.20	1.60
95	6.17	0.24	8.10	4.37
97	5.78	0.21	5.72	2.31
98	5.40	0.17	7.02	4.70
99	5.14	0.38	4.69	0.90
100	4.72	0.17	4.18	0.64

The obtained values in Table VI confirm that the first method has better results in the R value calculation due to its low standard deviation when the BPM range was changed. These results led to choose the “MaxMin Method” to be implemented in the microcontroller to calculate the R value, joined with all the previous presented signal processing.

After its implementation, samples from the microcontroller calculated R value where acquire to compare its values with the obtained using the *MATLAB* script and the results were very positive, obtaining a very small error percentage. The following figure (Figure 3.4.13) shows the

results of an acquisition at different oxygen levels at 80 BPMs. The table presented (Table VII) compares, for the same acquisition, the R values calculated using the *MATLAB* script with the ones acquired directly from the prototype in a laptop through a Bluetooth connection.

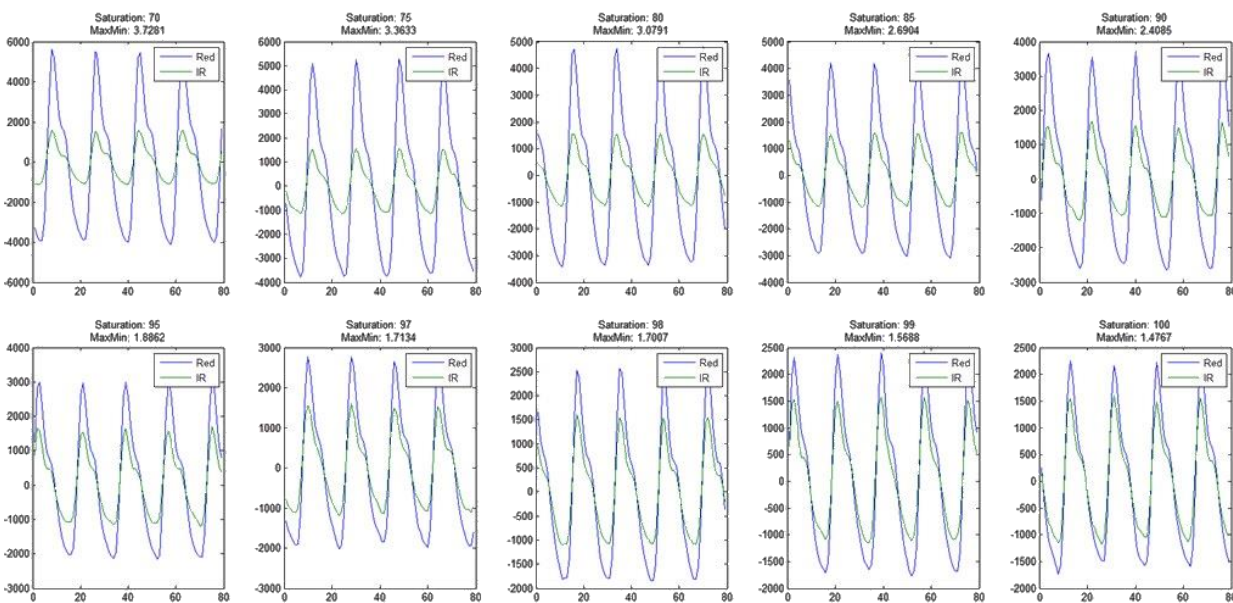


Figure 3.4.13- Photoplethysmograph signal obtained using the developed prototype and acquired from the oxygen saturation simulator at 80 BPMs. In this case, the signal processing and R value calculation (“MaxMin Method”) were both made using the developed *MATLAB* script. The abscissa values correspond to the number of the sample and the ordinate values to integer values acquired from the sensor, but these do not represent the acquired voltage.

Table VII- This table shows the R values obtained for each oxygen saturation level at 80 BPMs in the oxygen saturation simulator. The R values presented in the “*MATLAB*” column are the ones calculated using the *MATLAB* script and the values obtained directly from the microcontroller on the developed prototype are represented in the “Prototype” column. The last column shows the error percentage of Prototype obtained values in relation to the values obtained using the *MATLAB* script.

Saturation	R value		Error (%)
	<i>MATLAB</i>	Prototype	
70	3.728	3.728	0.00461
75	3.363	3.364	0.0249
80	3.079	3.080	0.0259
85	2.690	2.690	0.00119
90	2.409	2.409	0.0131
95	1.886	1.886	0.00297
97	1.713	1.739	1.48
98	1.701	1.701	0.0153
99	1.569	1.569	0.0204
100	1.477	1.477	0.0133

3.4.4. Ambiance Temperature and Relative Humidity Module

The HIH6130 sensor firmware is less complex than AFE4400 due to its acquisition autonomy. This sensor does not need to receive any register from the microcontroller to configure its operating mode and does not even need MOSI SPI channel, being totally autonomous in its configuration due to the lower complexity to sample the ambience variables. The firmware of this sensor is mainly divided in two files: one to initialize the microcontroller slave select pins of HIH6130 and the second one to acquire a sample from the sensor.

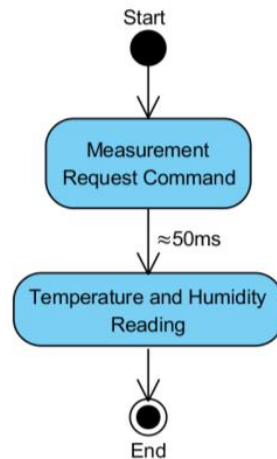


Figure 3.4.14- Workflow diagram representing the HIH6130 reading cycle.

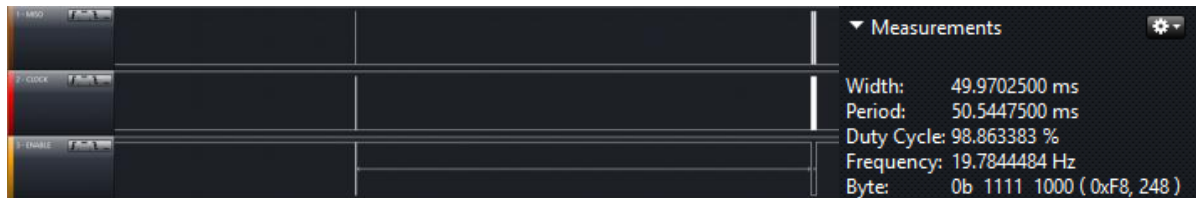


Figure 3.4.15- SPI digital acquisition of the HIH6130 reading cycle, where the slave select channel is represented by the “ENABLE” channel. The time distance between the measurement request command and the reading is approximately 50ms as it can be seen in the “width” measurement represented in the right corner of the figure.

Figure 3.4.14 and Figure 3.4.15 show the HIH6130 acquisition process. It consists in two phases: the first phase is a simple 8-bit clock signal (Figure 3.4.16) to wake-up the sensor; and request a temperature and relative humidity reading. During this process the MISO SPI channel data is ignored due to its insignificant data in this phase.

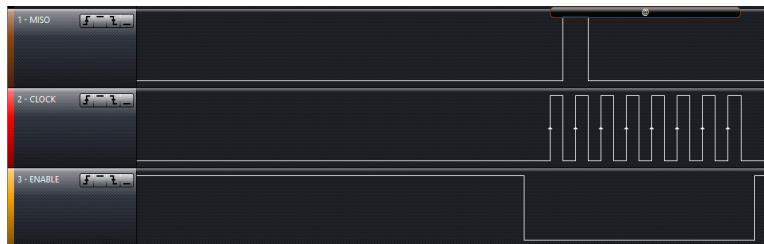


Figure 3.4.16- SPI digital acquisition of the HIH6130 data request made by the microcontroller.

After request a measurement it is needed to wait approximately 50ms to let the sensor make a complete environment reading and convert it in digital signal. Passed more or less 50ms a reading in the SPI MISO channel can be done (Figure 3.4.15). This reading consists in a 64 bits reading. The first 32 bits are to acquire temperature values and the 32 remaining bits are to acquire the relative humidity values. In these two segments of 32-bit only a few bits really represents the wanted variable. In the 32-bit of temperature only the bits from bit 15 to bit 2 contains the temperature value and in the 32-bit segment of relative humidity, its value is contained from bit 13 to bit 0. The following figure (Figure 3.4.17) shows the SPI communication during this process.



Figure 3.4.17- SPI digital acquisition of the HIH6130 reading process. First 32-bit represents the temperature reading and the remaining 32-bit represents the relative humidity reading.

After the isolation of the both 14-bit segments, temperature and relative humidity, its conversion to real values, according to the manufacture, is performed using equations 2 and 3 respectively [88].

$$Temperature (^{\circ}C) = \left(\frac{14_bit\ Temperature\ segment}{2^{14}-2} * 165 \right) - 40 \quad (Eq.2)$$

$$Relative\ Humidity\ (%RH) = \frac{14_bit\ Relative\ Humidity\ segment}{2^{14}-2} * 100 \quad (Eq.3)$$

Although this sensor description says that the obtained values are already calibrated, a validation will be done to confirm the values acquired. This will be presented in the Sensors Calibration and Validation section.

3.4.5. Gyroscope Module

Although this sensor was not implemented as already mentioned, its functionalization was study and analyzed, creating a prototype of its firmware implementation. LSM330DLC working workflow is similar to the AFE440 but with a simple initialization process and each register with only 16 bits (Figure 3.4.18).

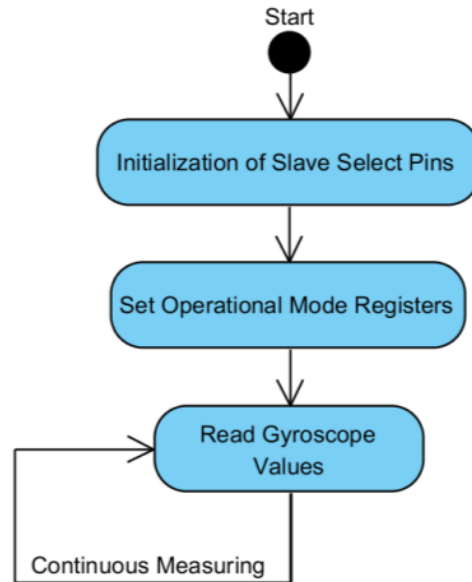


Figure 3.4.18- Workflow diagram representing the working cycle of LSM330DLC gyroscope sensor. First it is represented the initialization process and then the reading process.

The initialization is divided in the initialization of slave select pins in the microcontroller and then the operating mode registers are sent, each one, in two groups of 8-bit, one with the address and the other with the register information. These operating mode registers are eight, and only control the gyroscope module of LSM330DLC, since it would be the only variable acquired from this sensor. If the accelerometer was also needed it were going to be sent more control registers to set the operating mode of the accelerometer module of this sensor. After the initialization, that only needs to be done when the circuit powers on, the acquisition can be made continuously. To read gyroscope samples it is sent the register address related to the required variable and then 8 bits are returned and read with the requested variable value. In this acquisition are requested five values of the gyroscope sensor: the X, Y and Z axis, as also the sensor temperature and the sensor status to see if the read is new or the same as the last reading, informing if the sampled data is valid and different from the previous acquired. It is important to refer that each X, Y and Z variable has 16 bits, and so, to get a complete sample, two different registers are needed to be sent to acquire a sample from each axis.

As this sensor was not implemented in this prototype, it will not be presented in the next section of sensors calibration and validation.

3.5. Sensors Calibration and Validation

The calibration and validation of the implemented sensors is very important, mainly in the SpO₂ sensor because it needs to have a calibration curve to be accurate to and allow a possible future use as a medical device.

To make the calibration and validation of both sensors it was needed to search for similar commercial sensors to compare obtained values and in the SpO₂ also an oxygen saturation simulator to obtain the calibration curve. The validation procedure is going to be supported by the Bland Altman plot [93], a method used to quantify the agreement between two quantitative measurements. This statistical analysis was made using *MedCalc* software.

All these topics and all the methods and tests performed are going to be discussed in the following topics, first for the SpO₂ sensor and then for the ambiance temperature and relative humidity sensor.

3.5.1. Blood Oxygen Saturation

Blood Oxygen Saturation is a medical measurement that needs to be highly accurate to provide correct physiological information. The calibration process consists in the construction of a correlation between the calculated R value and the percentage of oxygen in blood. To do such correlation, an oxygen simulator is needed to simulate several specific oxygen levels and correlate the R value obtained with the simulated levels. To simulate oxygen saturation levels a *ProSim SPOT Light* from *FLUKE* [94] was used. The characteristics of this device will be referred in the following topic where the sensor calibration is discussed. After prototype sensor calibration the next step was to validate its oxygen saturation measurements in a human finger and comparing its results with a commercial oxygen saturation device used in medical environment. For this measurement validation it was used the model *M3046A* from *Philips* [95], a compact portable patient monitor used to monitor patients physiological signs in the hospital.

It is important to refer that all these tests, calibrations and validation procedures were made in *Hospital de São João*, in their Metrology Laboratory, the Hospital section responsible by the calibration of all the hospital medical devices.

3.5.1.1. Sensor Calibration

As mentioned above, a *FLUKE ProSim SPOT Light* was used to simulate oxygen saturation levels. The oxygen saturation sensor probe is attached to a small probe in the simulator to acquire simulated values. One side of this probe has light sensors (photodiodes) to read oxygen saturation LEDs intensity and periodicity of each LED. The other side has LEDs with an pulsatile intensity that depends of the oxygen saturation sensor LEDs intensity minus the simulation of the absorbed intensity according to the oxygen saturation level selected in the simulator. Resuming, it is an inversion of an oxygen saturation sensor with an emission of simulated values. This specific simulator device, beside different oxygen saturation levels, can also simulate different heart rates (Table IV), perfusions levels, finger sizes and can also simulate artifacts like

50Hz or 60Hz noise. Figure 3.5.1 shows an image of the *FLUKE* simulator with the prototype. This image shows the prototype and the *FLUKE* simulator device during the calibration process.



Figure 3.5.1- This image shows the *FLUKE* simulator device and the prototype during the calibration process. The prototype was connected with a laptop through a Bluetooth connection, sending the calculated R values.

For this calibration procedure only oxygen saturation and heart rate were changed from the simulator initial configuration to create the calibration curve which correlates the calculated R value with the Oxygen Saturation level. For each heart rate frequency the oxygen saturation levels were changed according to the values that were possible to simulate. For each different combination of heart rate and oxygen saturation level the R value was acquired in a laptop directly from the developed prototype through a Bluetooth connection. The following figure (Figure 3.5.2) shows the calibration curve obtained with the oxygen saturation values simulated by *FLUKE* device, with the respective standard deviation according to the variation of heart rate between 60BPM and 180BPM.

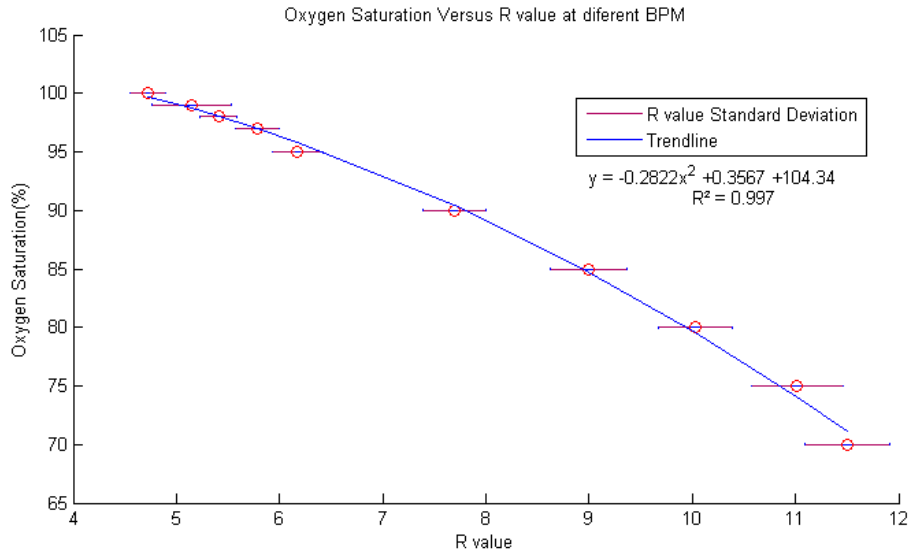


Figure 3.5.2- Graphical representation of the correlation between the R value obtained from 60 to 180 BPM (differences represented by the standard deviation) and the oxygen saturation level. The respective trendline and square error from the acquired samples are below the graphic legend.

The calibration curve obtained has a high correlation value ($R^2=0.9968$) when the saturation value is between 70% and 100% and the heart beat between 60 and 180BPM, with a small standard deviation between those BPM.

After the implementation of this calibration curve in the microcontroller firmware it was time to make the test with a real finger. When these tests were made a problem was detected: the R value was not a constant value between acquisitions; and when the sensor position was changed, even with small movements, the R value changed its greatness, indicating, in both cases, a wrong oxygen saturation value. To try to understand this problem the prototype was extensively tested in the oxygen simulator to observe the R value behavior. In these tests the R value showed consistence in its values, but when the position on the simulator was changed, the values showed also consistence when the saturation level was increased but in a higher or lower range. For example, in a certain position the R value range was from 5 to 15 (Figure 3.5.3 – left image) and when that position was changed the R value range was only from 1.5 to 3.7 approximately (Figure 3.5.3 – right image).

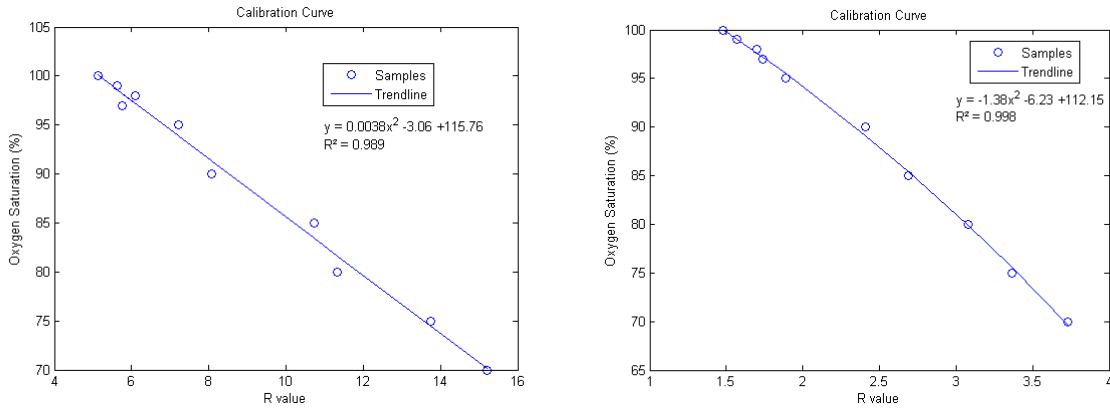


Figure 3.5.3- Two different calibration curves obtained due to a different position in the simulator probe. For these tests it was used only the oxygen saturation levels at 80 BPMs.

To try to understand this problem it was investigated the difference in the simulator between the developed prototype and a conventional oxygen saturation device used in a medical environment, being this last one connected to the simulator. When this test was done a difference was spotted: the light intensity indicated by the simulator was much higher compared to the developed prototype sensor intensity. This fact was considered plausible to be the cause of why different positions in the simulator were changing the R value, leading to different calibration curves. This intensity problem also explains why small position deviations presented wrong oxygen saturation levels.

To overtake this problem, some registers of AFE4400 were change to increase LEDs intensity. At the first tests the LEDs were with a current supply of 3.9mA, and it was increased to 35mA, of a maximum value of 50mA, equalizing the visual light intensity of the conventional oxygen saturation device used. When this was done another problem was spotted: the main board Bluetooth, after more or less a minute with the LEDs at 35mA, crashes and re-initialize, interrupting data transmission. After some tests and LEDs current variations, it was concluded that the main board did not provide the amount of current needed when the LEDs had more than 20mA of current supply. Since the main board power management was design to limit the current supply to 200mA, it was necessary to change the power management. To do this change it was acquired and mounted a different voltage regulator, with a higher current supply limit of 400mA. While this process was in progress, the device with the original power management was used to analyze the R value obtained with LEDs current with about 15mA. Although, with this current supply, the LEDs had a lower light intensity compared with a conventional oxygen saturation device, the R value obtained was much less discrepant and when the sensor position was changed in the finger only small variations were observed. While the new power management was being implemented, to improve the R value regarding the sensor position in the finger, it was made an automatic LEDs intensity adjustment allowing maintaining a pre-defined range in the receiving sensor. This automatic adjustment was included in the main firmware workflow after the verification of the finger in the sensor.

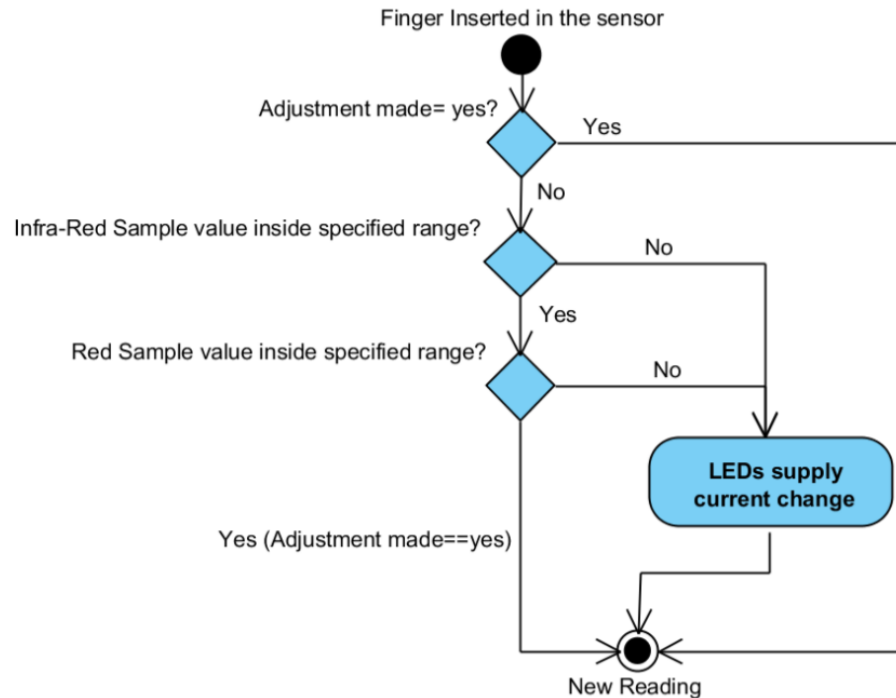


Figure 3.5.4- Workflow diagram of the automatic adjustment of the sensor LEDs supply current. This is performed after verifying that the finger is inserted in the sensor. After the acquisition of HIH6130 the “Adjustment made” is equalled to “no”. The samples acquired in this procedure are not use in the oxygen saturation calculation, for which 100 samples are needed.

As figure 3.4.5 shows, only if the acquired values are out of the required sampling range, it is firstly made an adjustment to LEDs supply current based on the Infra-Red value acquired, and then an adjustment is made using the Red value acquired. LEDs current variation can be a high or low adjustment, according to the difference between the acquired samples and the wanted sampling range. It is important to refer that the LEDs power supply changing is always the same for both LEDs, obtaining no difference in the light emission intensity between these two wavelengths. After the implementation of the LEDs adaptive light intensity function it was possible to obtain the R value inside the same range, without variations regarding the sensor position. This light intensity adaptation also increase the viability of this sensor for different finger sizes, adapting LED’s intensity to acquire always samples inside the same range.

When the new voltage regulator was assembled, it was possible to increase LEDs intensity and also increase the pre-defined intensity range in the receiving sensor to regarding the automatic LEDs intensity adjustment. After this, it was performed a new calibration curve as shown in Figure 3.5.5. With this higher intensity it was verified a much lower standard deviation and it was possible get a calibration curve with a BPM range from 30BPM to 240BPM, increasing the viability of the developed sensor.

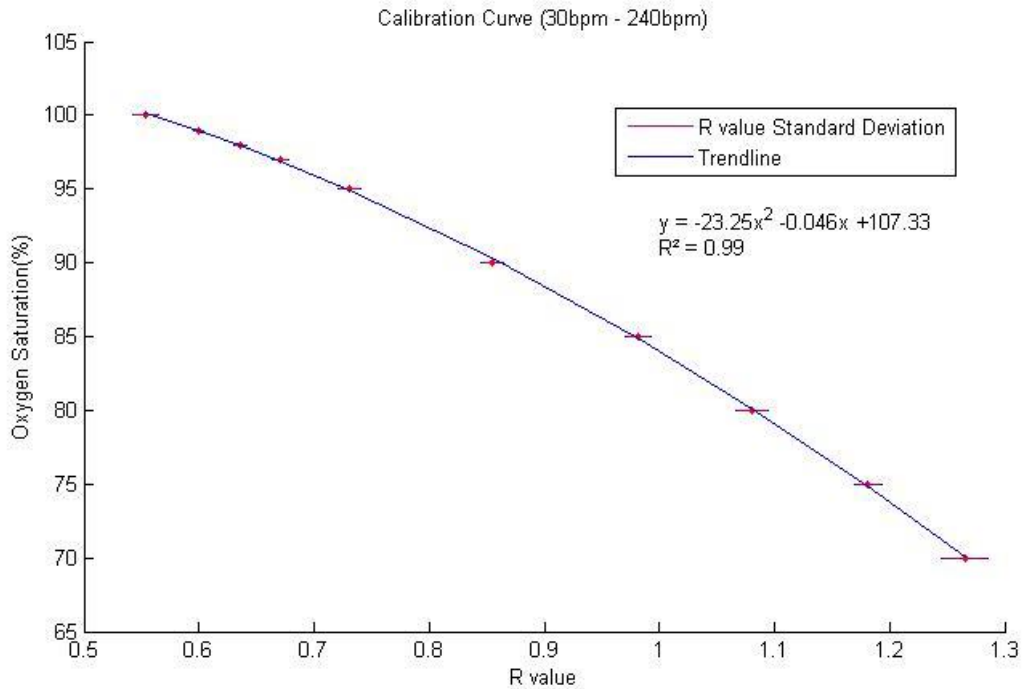


Figure 3.5.5- Calibration curve obtained with the new calibration made using the new voltage regulator. The respective trendline and square error from the acquired samples are below the graphic legend.

After this calibration procedure, the validation of the prototype oxygen saturation sensor was performed, comparing it with a commercial device used in medical environment as it will be discussed in the following topic.

3.5.1.2. Sensor Validation

Sensor validation is very important to confirm that the oxygen saturation levels obtained with VitalLogger prototype device are the same as a medical device used in a medical environment. To validate the prototype it was used a medical device from *Philips*, model *M3046A*, performing two tests. For both tests the procedure was to insert the left index finger in the *Philips* SpO₂ sensor and the right one in the VitalLogger SpO₂ prototype sensor. When a reading was made by the prototype, more or less 6 seconds, the oxygen saturation values from both devices were annotated. The following image (Figure 3.5.6) shows the apparatus used in the validation procedure, where both devices are presented, with the respective SpO₂ sensors.

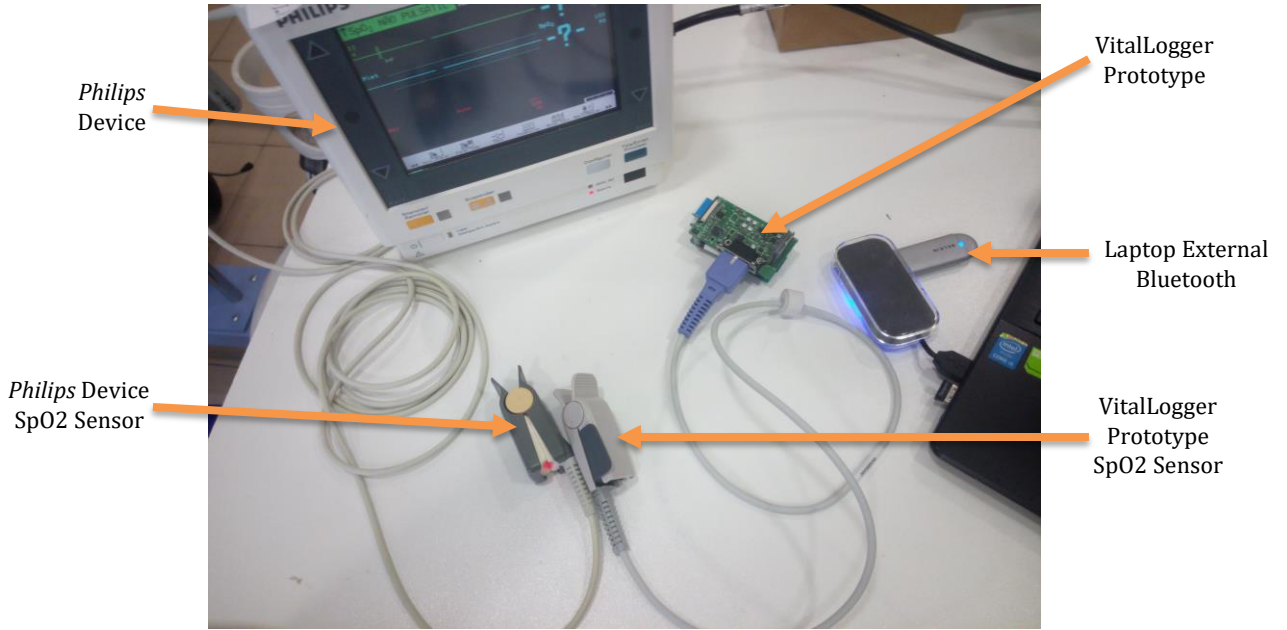


Figure 3.5.6- Apparatus used in the validation procedure of the oxygen saturation values. In this image it is possible to see the *Philips* device with its SpO₂ sensor and the VitalLogger Prototype also with its SpO₂ sensor. The external laptop Bluetooth is also present to acquire VitalLogger transmitted data.

For the first test, one hundred samples were saved from the same person, obtaining the result presented in Figure 3.5.7. To try to simulate different oxygen saturation values the breath was not constant. The results obtained in this test were very similar between both devices, with an average error percentage of approximately 0.5%. Although, almost 50% of the prototype saturation percentage acquired values were different from the medical device values, this difference is only 1%, which can be considered a very small difference.

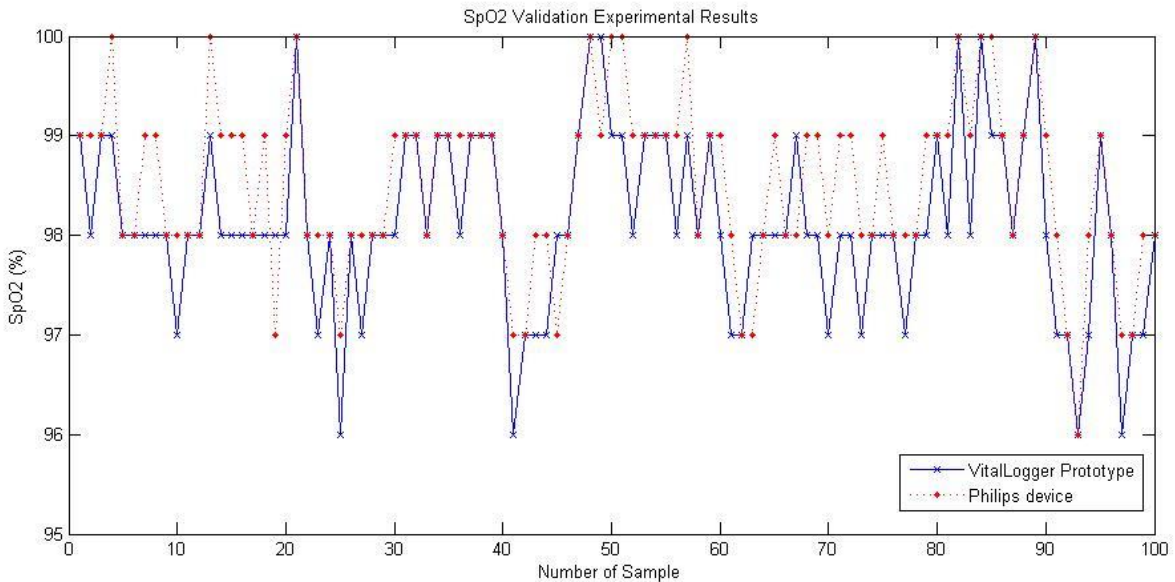


Figure 3.5.7- First test experimental results obtained during the acquisition of oxygen saturation percentage values to validate the prototype values. This image presents the values from VitalLogger prototype and *Philips* device during the acquisition of one hundred samples.

To better analyze these data, it was performed a Bland Altman analysis which consists in a plot analysis where the difference between both measurements (Philips device and VitalLogger) is correlated with the mean of the same measurements. Bland Altman plot shows an agreement interval between ± 1.96 of the standard deviation (SD) of the differences, where 95% of the differences should be between them (with a confidence interval (CI) of 95%) when considered that the difference is normally distributed. The normal distribution is evaluated using the D'Agostino-Pearson test (if $P < 0.05$ the normality is rejected) [93]. The following figure 3.5.8 shows the Bland Altman plot (left side) and the distribution plot of differences between both measurements (right side).

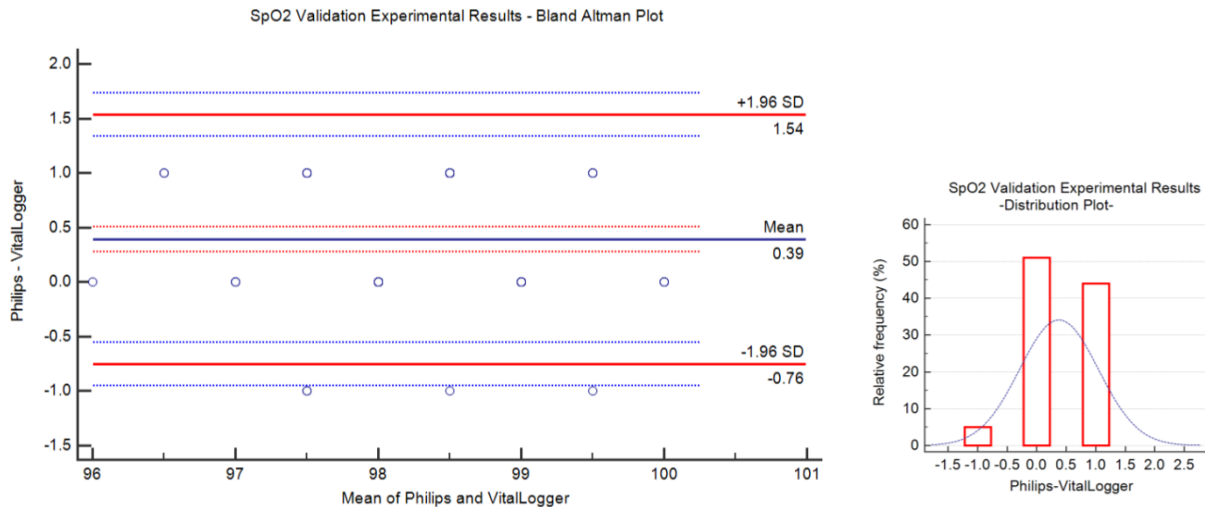


Figure 3.5.8- On the right side is represented the Bland Altman plot (blue line-mean difference; red lines- limits of agreement; red dotted line- mean difference CI; blue dotted line- limits of agreement CI). On the left side a distribution plot of the differences is presented. Although normality is not accepted according to D'Agostino-Pearson test ($P=0.0465$), due to its very small difference from normality acceptance the Bland Altman plot was done considering that the differences are normally distributed.

By observing both plots in Figure 3.5.8 it is possible to see that 95% of the acquired measurements are inside the agreement limits, and the remaining 5% are almost inside the CI of the lower agreement limit. These samples have a similar difference behavior along the increase of the several values of measurement, and due to a mean higher than zero, it is possible to assume that VitalLogger prototype values have a higher probability to acquire one value below the *Philips* device values than above it. This could be improved by making another calibration curve or a small adjustment according to these data.

A second test was made to simulate a small acquisition from a patient. This consisted in the acquisition of only twenty samples from another person to verify the adaptation of the VitalLogger prototype to different fingers (Figure 3.5.9). The results from the developed sensor are also very similar to the medical device used, obtaining a smaller average error than in the previous test, of 0.41%. In this case, 40% of the prototype saturation percentage acquired values were different from the medical device values, the difference only deviate in 1%, a very small difference.

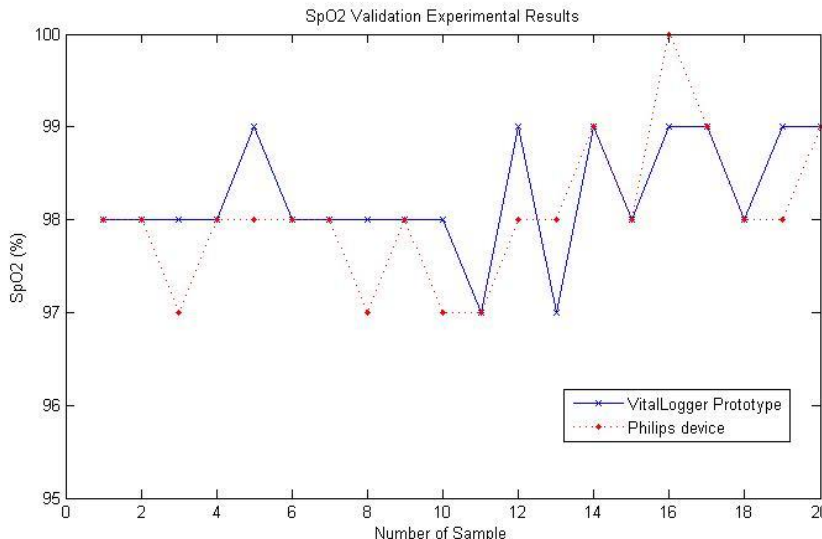


Figure 3.5.9- Experimental results obtained during the second test made in the validation procedure. This image presents the values from VitalLogger prototype and *Philips* device during the acquisition of twenty samples.

Regarding the Bland Altman plot, Figure 3.5.10 shows the obtained results, joined with the distribution plot of differences between both measurements (right side).

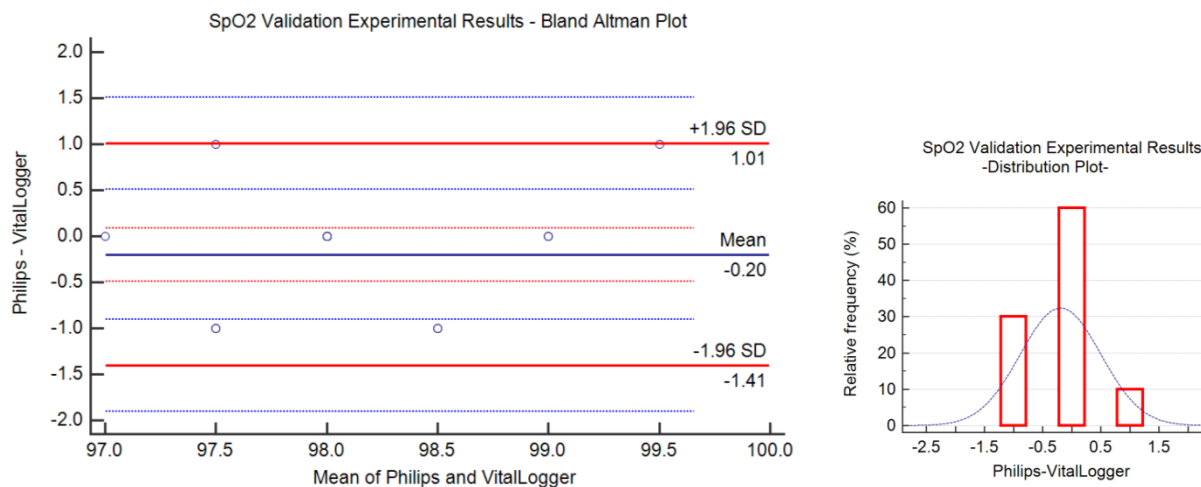


Figure 3.5.10- On the right side is represented the Bland Altman plot (blue line-mean difference; red lines- limits of agreement; red dotted line- mean difference CI; blue dotted line- limits of agreement CI). On the left side a distribution plot of the differences is presented. Normality of the differences is accepted according to D’Agostino-Pearson test (P=0.9693).

In this case, Figure 3.5.10 shows that all the acquired values are inside the agreement limits , showing also a consist of the differences along the increase of the acquired values. Although this acquisition has lower number of samples, the mean of the differences is lower than zero, the opposite behavior than in the previous acquisition. To better understand the real behavior between these two devices, if VitalLogger prototype as the tendency to get a lower or higher value than *Philips* device, a larger number of samples should be acquired to different subjects.

With both of these tests it is possible to affirm that the developed oxygen saturation sensor is capable to acquire SpO₂ values almost as good as a conventional medical device normally used in

the hospitals, varying only one percent above or below. It would be of great interest to validate this prototype on patients with lower oxygen saturation levels than the normal ones, evaluating the prototype behavior.

3.5.2. Ambiance Temperature and Relative Humidity Validation

The calibration and validation of this sensor values was easier than the SpO₂ due to the simplicity to get the wanted final values, reading already the values of the ambience temperature and relative humidity directly from the sensor. According to the sensor manufacture the values obtained are already the right ones and don't need a calibration process. Even though, to analyze this sensor accuracy a validation procedure was performed. As it will be discussed, after this test it was concluded that a small calibration on the outputted values from the sensor was needed.

To compare the obtained values from the prototype, it was used a commercial device *DVM8010* produced by *Velleman* [96], which provide temperature and relative humidity measurements. To simulate a small atmosphere where relative humidity and temperature could be changed, it was used a small transparent sealed reactor (Figure 3.5.11) from chemical engineering laboratories on the Chemical Engineering Department from the Faculty of Engineering of the University of Porto. Temperature limitation of this container and also its construction material did not allow to change the temperature using a hot source. Due to this, the procedure to change the temperature, and mainly the relative humidity was expiring air from the lungs into the container using its unique opening located in the plastic tube on the bottom of the reactor as Figure 3.5.11 shows.

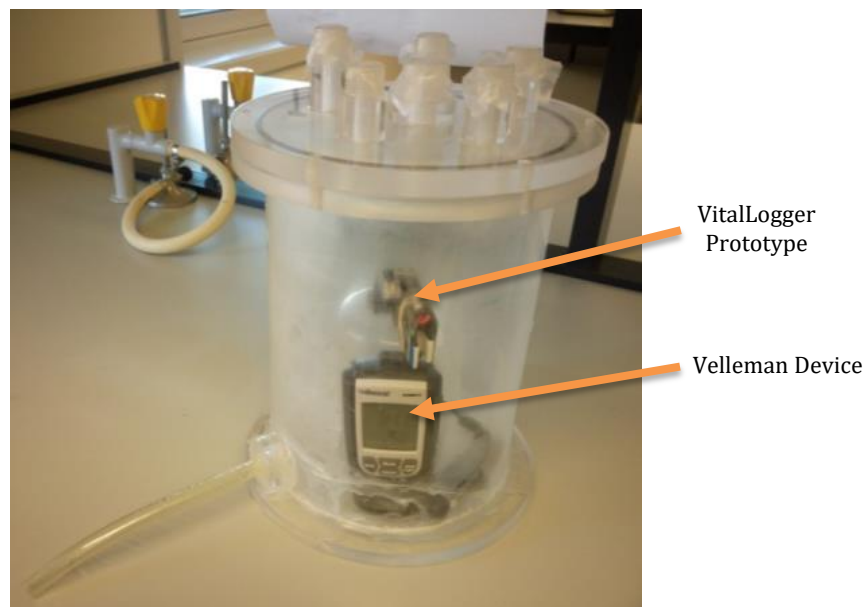


Figure 3.5.11- In this image it is possible to observe the *Velleman* device and the developed prototype inside the container to simulate a different atmosphere from the one in the outside.

The procedure was based on the expiration of some air into the container through the plastic tube to increase the humidity and temperature value. When an increase was verified some

seconds were waited until the stabilization of the *Velleman* device. When this stabilization was verified, a temperature and relative humidity reading was made from this device and from the prototype. Along the increase of relative humidity more expired air was needed to raise even more this value. After reaching a value where some breaths did not change significantly the acquired values, both sensors were removed from the container and samples were taken along time. When a stabilization was observed the values were sampled and a small air flow was induced in both sensor at the same time, in order to mixed the air inside the sensors with the ambience air. This procedure was repeated while a decreasing of ambience relative humidity was verified, always waiting some seconds until *Velleman* device stabilization. It is important to refer that the air flow to mix the air inside the container was also perform with strong expirations.

Both sensors were kept together as Figure 3.5.12 shows for the case when the sensors were inside the container. Sensors proximity allows to remove any measurement difference due to different air properties.

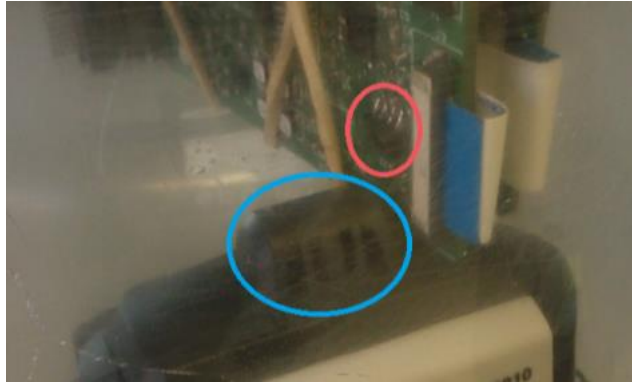


Figure 3.5.12- This image shows both devices sensors, visualizing their high proximity. In the red circle is the prototype HIH6130 sensor and in the blue circle is the *Velleman* device air entry.

Regarding the samples obtained, the described procedure was made two times and the results are presented on the following image (Figure 3.5.13).

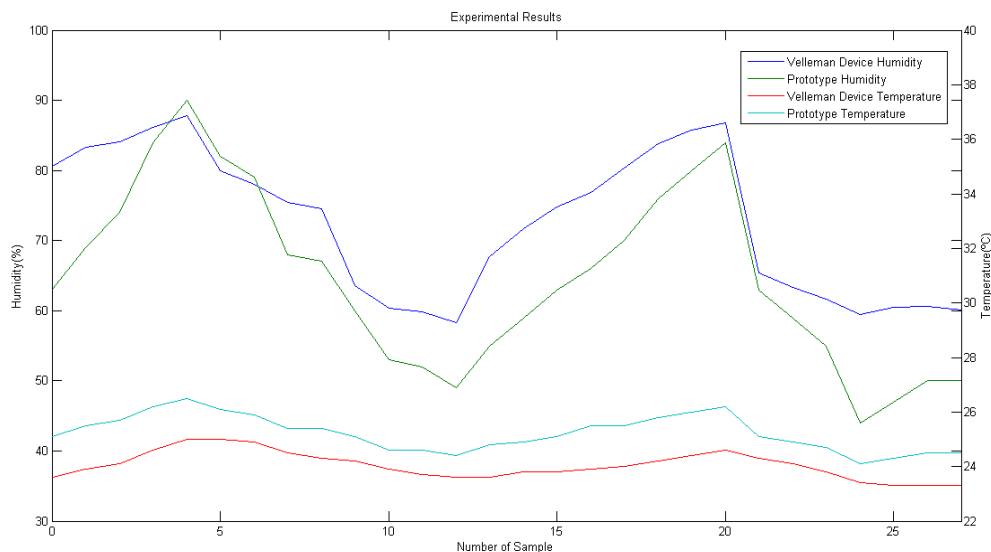


Figure 3.5.13- Graphical representation of the samples acquired from the *Velleman* device and the developed prototype during the procedure above described.

Analyzing the data acquired in Figure 3.5.13 it is possible to conclude that both sensors have a similar behavior, but the prototype present different values from the obtained with the *Velleman* device. To get better values a calibration was made to the developed prototype with the aim to obtain a smaller difference in the values acquired. Two correlation curves were made to perform a calibration, one for the temperature and another for the relative humidity (Figure 3.5.14)

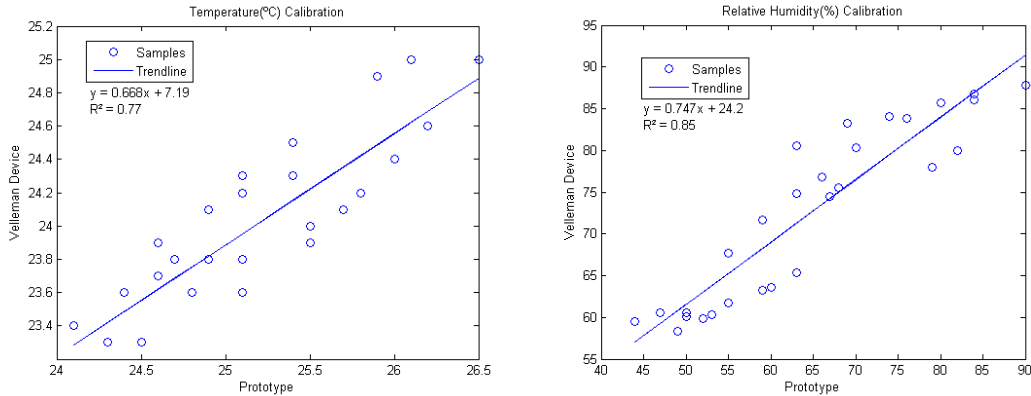


Figure 3.5.14- Calibration curves obtained from the experimental results presented in Figure 3.5.5. The left image represent a graphical representation of the samples from *Velleman* device versus the developed prototype and the respective regression line. The right image shows the same relation but for the relative humidity samples.

In the relative humidity calibration curve the first five samples were not considered due to a high deviation from the value measured with the *Velleman* device, obtaining a calibration curve with a better correlation. Also the values acquired with the prototype in those samples are not according to the obtained after at the same relative humidity measured with the *Velleman* device. The following figure (Figure 3.5.15) shows the same samples acquired, but with the correlation curve implemented, observing a much higher similarity between both sensors.

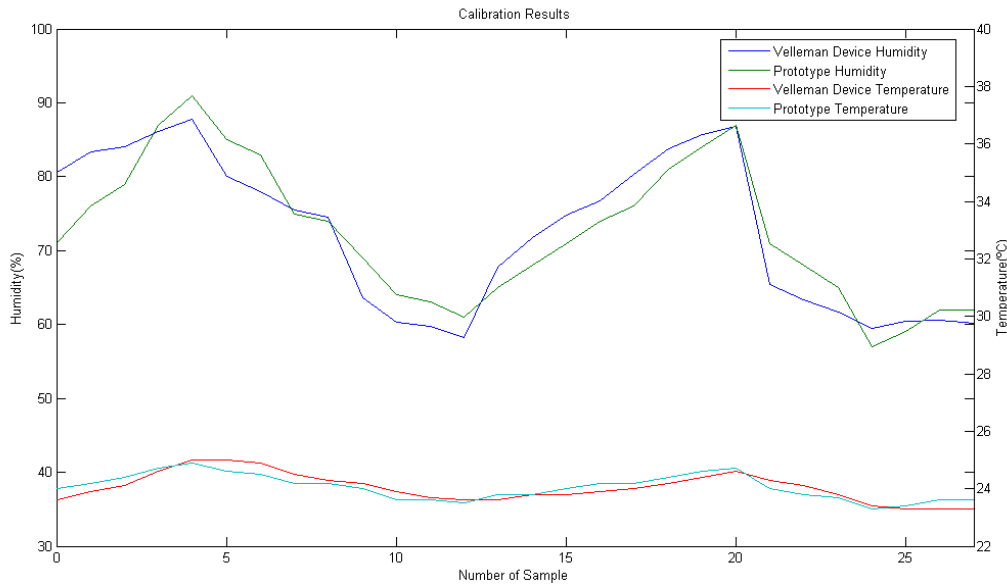


Figure 3.5.15- Graphical representation of the obtained values after the adaptation of the regression lines. The calculation was made in the computer applying the regression lines to the already obtained samples values.

After this test, a Bland Altman analysis was made with these new better correlated between both devices acquired data. As already present in the oxygen saturation sensor validation, the following figures (X and Y) shows the shows the Bland Altman plot in the left side and the distribution plot of differences between both measurements in the right side. This analysis is firstly made for the temperature and then for the relative humidity.

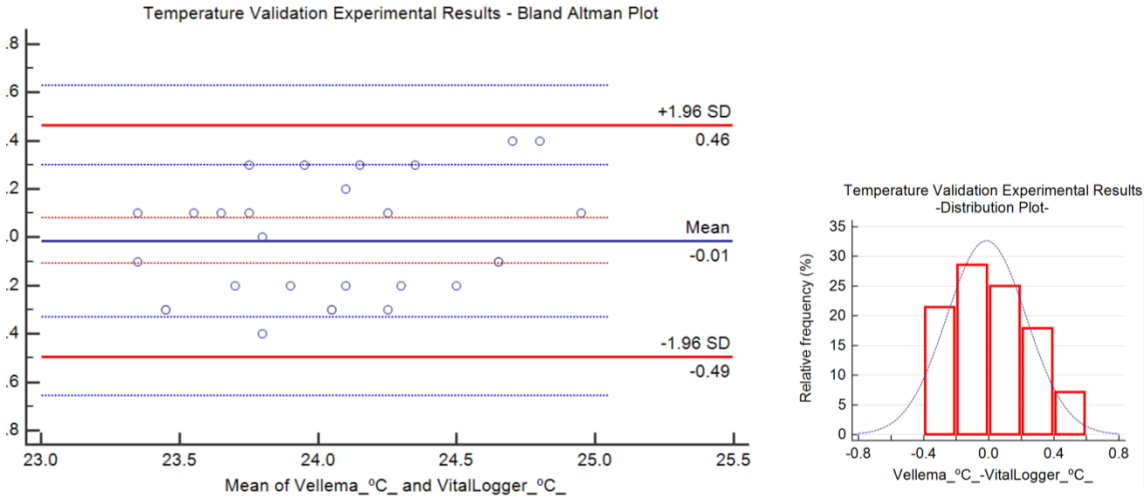


Figure 3.5.16- On the right side is represented the Bland Altman plot (blue line-mean difference; red lines- limits of agreement; red dotted line- mean difference CI; blue dotted line- limits of agreement CI). On the left side a distribution plot is presented. Although normality of the differences is not accepted according to D’Agostino-Pearson test ($P=0.0473$), due to its very small difference from normality acceptance and shape, the Bland Altman plot was done considering that the differences are normally distributed.

Plots presented in Figure 3.5.16 shows a high agreement between both devices, obtaining all the differences of the acquired samples from both devices inside the agreement limits, with a mean of almost zero. These good results can be due to a low range of ambience temperature values, being necessary to perform future tests with a higher range of temperature values.

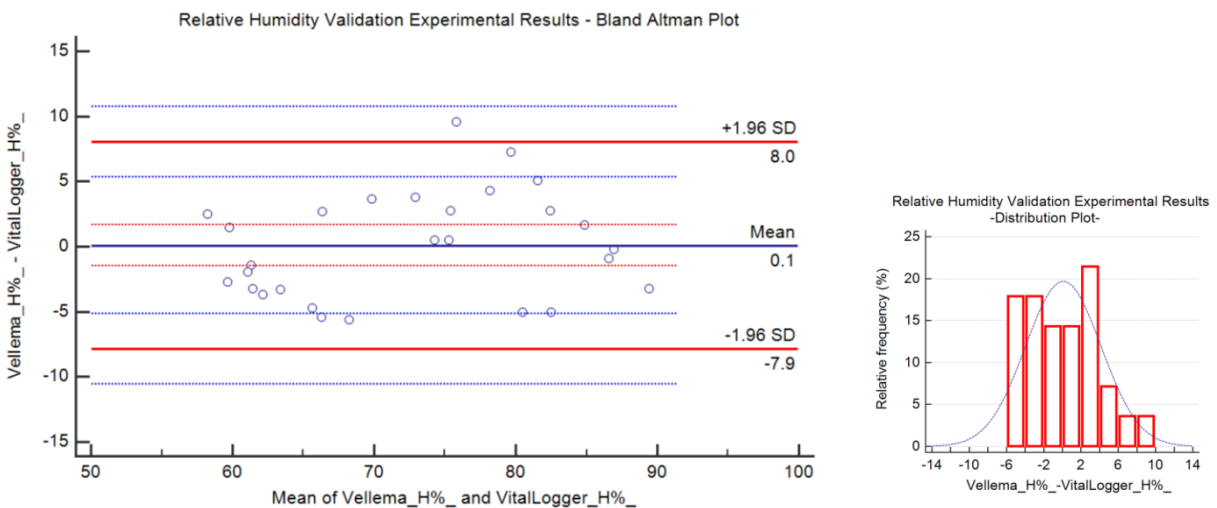


Figure 3.5.17- On the right side is represented the Bland Altman plot (blue line-mean difference; red lines- limits of agreement; red dotted line- mean difference CI; blue dotted line- limits of agreement CI). On the left side a distribution plot of the differences is presented. Normality of the differences is accepted according to D’Agostino-Pearson test ($P=0.5561$).

The Bland Altman plot in Figure 3.5.17 shows that all the differences, except one, of the acquired values from both devices, are inside the agreement limits. Also it is possible to visualize a mean of differences very close to zero, showing a high similarity between values acquired from the *Velleman* device and the VitalLogger prototype.

After this analysis, the temperature and relative humidity calibration curves were implemented in the sensor firmware. To better calibrate this sensor and obtain ambient temperature and relative humidity values with a higher accuracy, a precise test should be performed with a higher range of these two variables to validate, and if needed, to calibrate the sensor in a larger scale for both temperature and relative humidity variables.

3.6. Prototype Specifications Analysis

To better understand the possible future viability of the developed prototype, this topic is going to present its characteristics as also it associated costs. In this analysis it will be considerate the second version of the VitalLogger extension board presented in Appendix.

The associated costs can be divided in three main components: Oxygen Saturation sensor; Printed Circuit Board (PCB); and the electronic components. Oxygen saturation sensor has a high cost variation depending where it is both. If it is both in China or another Asiatic Country where the sensor is produced the costs range is approximately from 10€ to 30€, depending on the company where the acquisition is made and also of the requested quantity of sensors. On the other hand, if the acquisition is made in a Portuguese distributor the costs increase until 150€ approximately. The costs associated to the PCB's and the electronic components also change according to the number of units requested. The following table (Table VIII) resumes the associated cost for the electronic components needed and PCBs according to the produced units of VitalLogger second version prototype.

Table VIII- This table shows the associated costs of the VitalLogger second version prototype regarding the electrical components and PCB costs per each unit produced according to the number of units produced. In the last column of the table a total cost per unit is presented.

Produced Units	Electrical Components Cost per unit	PCB Cost per unit	Prototype Cost per unit
10	34.54 €	8.27 €	42.81 €
50	30.51 €	3.36 €	33.87 €
100	26.90 €	2.32 €	29.22 €

As the table below shows, a production of only 10 prototypes is expensive compared to the production of one hundred, mainly due to the electrical components. This could be resolved with the reduction of the electronic components as it was already referred for the power management case. If this circuit module was removed the components cost would decrease obtaining a cheaper prototype price. This aspect will be discussed in the following topic, where a new prototype is proposed, with a much lower cost.

Regarding electrical characteristics, mainly the consumption requirements it can be divided in two main contributions: electronic components consumption; and sensor LED consumption. The first one related to the electronics consumption, making a battery life-time estimation regarding the consumption properties of each component used, obtaining approximately 4.2mA. Knowing that the main board from Biodevices, S.A. has a current consumption of about 30 mA, already with the Bluetooth and SD memory card both on, and using a 1000mAh battery, it would be possible to use this prototype during, approximately, 29 hours in continuous acquisition, storing and transmission. The second contribution is from the oxygen sensor by its LEDs. These can suffer small variations from user to user according to the light intensity needed and also because the LEDs are only on when the reading is being done, which difficult the consumption time estimation. To obtain a practical and correct battery life-time estimation, VitalLogger prototype was be submitted to a battery life test. For this test the battery was totally charged and then turned on. To simulate a finger inserted in the sensor it was inserted a paper in the oxygen saturation sensor. The Bluetooth was turned on but was not connected to any device,

obtaining 15 hours of continuous measurement from all the VitalLogger prototype variables. More battery life-time tests should be done to know how long can the prototype continuously acquired samples and send it via Bluetooth.

The final VitalLogger prototype is presented in Figure 3.6.1. In order to add the developed prototype firmware to the already existing from Biodevices, S.A. technology, the developed firmware was adapted and improved to decrease the power computation need. This incorporation resulted in a final device that is able to acquire, save in the SD memory card and send via Bluetooth the ECG signal, heart rate, tri-axis accelerometer values, oxygen saturation percentage and ambience temperature and relative humidity.



Figure 3.6.1- Final developed VitalLogger prototype system with the following sensors: electrocardiogram (ECG) and heart rate and tri-axis accelerometer from the main board and oxygen saturation percentage and ambience temperature and relative humidity from the developed extension board.

Besides the already implement variables from Biodevices, S.A. technology, VitalLogger is also able to transmit, via Bluetooth, the oxygen saturation percentage each second and both of the ambience variables (temperature and relative humidity) with a frequency of 5 seconds. Figure 3.6.2 shows a Windows SDK application from Biodevices, S.A. with all the variables acquired by VitalLogger prototype. When the finger was not inserted in the oxygen saturation sensor, VitalLogger sends this information to advice the user, as it is possible to observe in Figure 3.6.3.

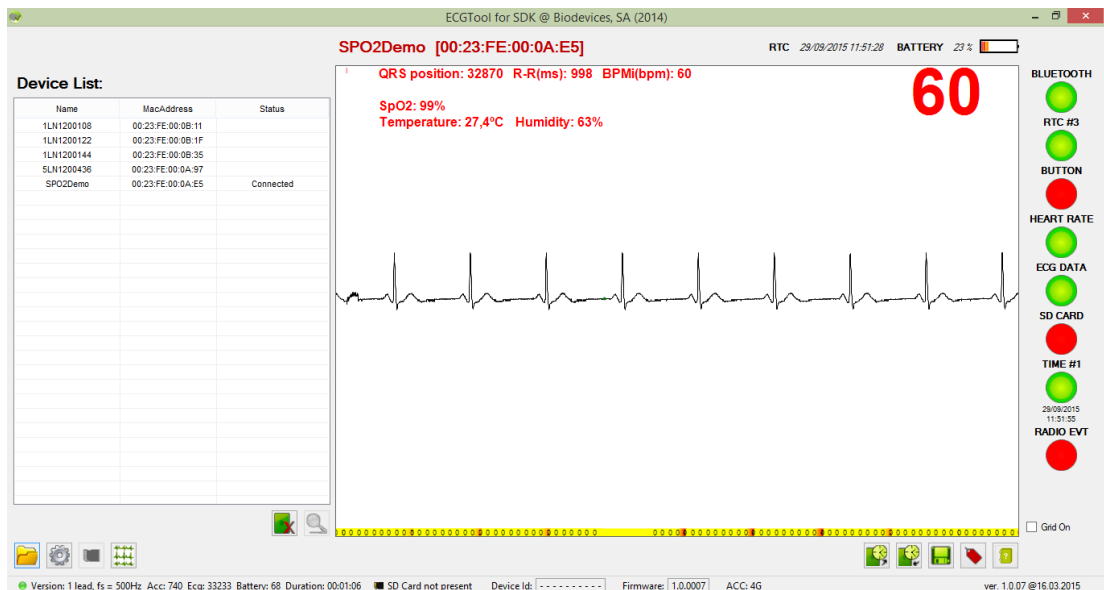


Figure 3.6.2- Windows SDK application from Biodevices, S.A. during a normal acquisition from VitalLogger prototype. It is possible to see the new variables above the ECG waveform.

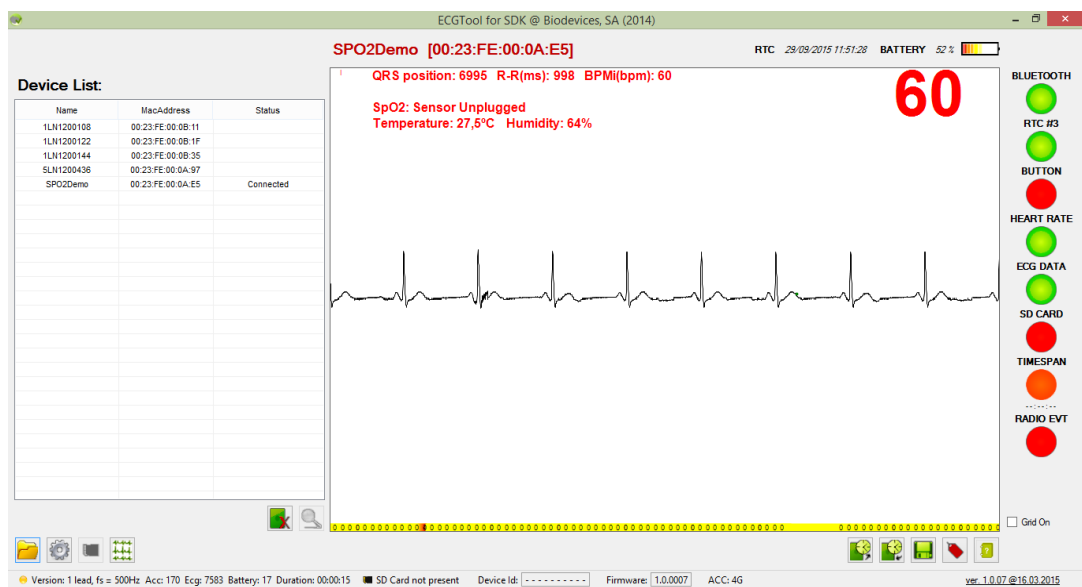


Figure 3.6.3- Windows SDK application from Biodevices, S.A. during a normal acquisition from VitalLogger prototype, but without a finger inserted in the oxygen saturation sensor.

The developed prototype, due to its size, cannot be introduced in Vital Jacket® portable case which is a disadvantage, mainly for a possible future product implementation. To resolve this problem it will be presented in the next topic a new prototype idea, with a much more wearable solution to transform VitalLogger prototype in a possible product.

3.7. Prototype Improvements

In the last topic the final prototype was showed and, as it was possible to see, it is big and cannot be putted inside Vital Jacket® case. The extension prototype size could be reduced if the power management was removed and if oxygen saturation sensor connector (DB9 connector) evolves to a different and smaller connector. To solve these problems and try to evolve this extension prototype into a possible product, it was made an improvement suggestion for a future implementation of the developed extension prototype directly on the Biodevices, S.A. board.

To resolve the power management space needed, the extension prototype board was tested with a direct supply off 3.3V and 5V in the AFE4400 RX and TX routes respectively. As shown in Appendix B, the test was successfully done, obtaining the same electrical characteristics signals as the first developed extension board. After the validation of the results obtained with these new power supply (Appendix B), a size reduction was made as also some modifications that are going to be discussed in the following lines.

The main idea of the prototype improvement was to make a module for the main board with a won microcontroller to acquire the signal, performing all the signal processing needed and calculating the SpO2 percentage value. This improvement will allow acquire values at a higher frequency, obtaining a more detailed SpO2 curve, mainly at high heart rates. The SpO2 value and the ambience and relative humidity would be then read by the main microcontroller in the main board, requiring a much lower computation effort from it comparing to the developed prototype. To make this communication the new microcontroller would work as a master to acquire samples from the sensors and then as a slave to send the final values to the main microcontroller, alternating its SPI initialization between master and slave.

The microcontroller chosen was the PIC18F26K20 from *Microchip*, due to its similarity to the one in the main board, decreasing the effort in the firmware adaptation. Another problem concerning the implementation of a microcontroller is its programming operation. This problem was solved using a specific group of pads in the proposed module hardware, using spring connectors (Figure 3.7.1) to import the firmware directly to the module microcontroller. With this technology it is possible to change/update this microcontroller firmware without interfering with the main board microcontroller, having an independent module. It was also included an ADC_RDY digital pin in the module, named D_RDY, allowing the microcontroller from the module to inform the main board microcontroller when new data is ready to be read.



Figure 3.7.1- Programming connector used to program the microcontroller in the module. This connector has six connections with spring connector and three metal guides to help in the connector positioning in the board. It is developed by Tag-Connect and the other side of the cable is an internet connector (RJ12 connector) that plugs directly to ICD-3, which is the programmer used in this work. [97]

The components architecture concerning the implementation of this prototype in the main board is represented in Figure 3.7.2. In this figure the communication between components is only represented when related to the new prototype module.

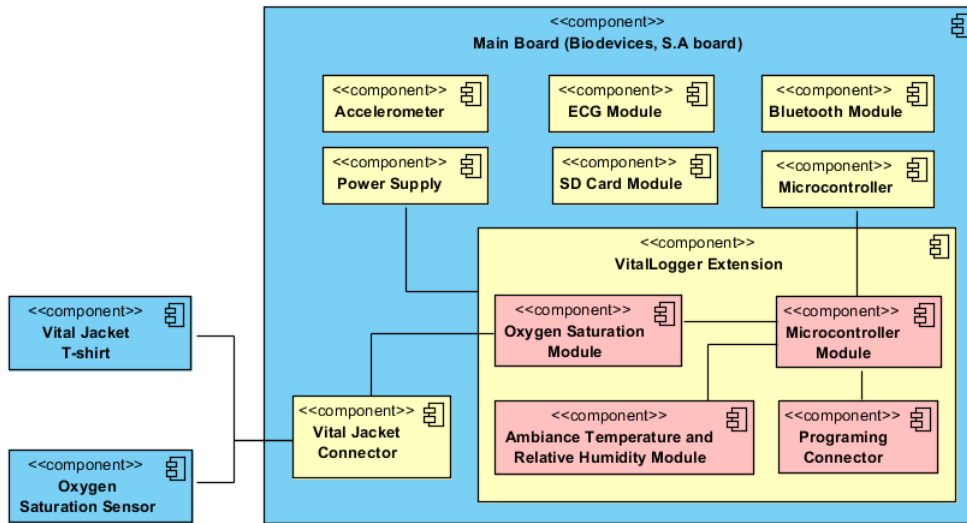


Figure 3.7.2- New VitalLogger components architecture with the new suggested module implemented in the main board.

The following image (Figure 3.7.3) shows the microcontroller schematic of this VitalLogger module version prototype, as also the programming module (TC1) and a pull-up power supply protector for the 3.3V.

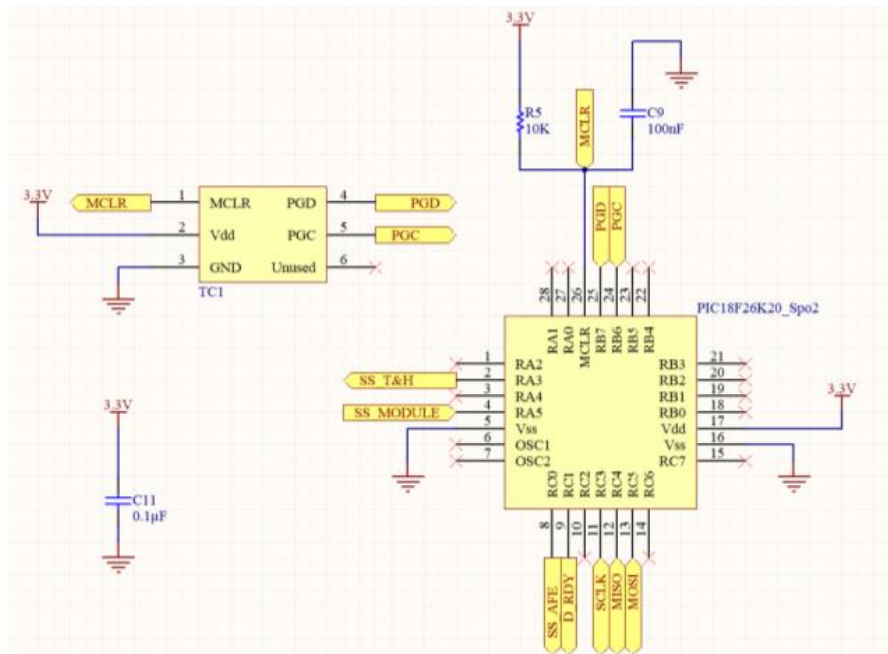


Figure 3.7.3- Microcontroller schematic (PIC18F26K20_Spo2) designed for this module application. In the left bottom of the image is represented the schematic of the programming connector (TC1) and below is the pull-up resistor used in the 3.3V supply voltage. [97, 98]

The AFE4400 schematic (Figure 3.7.4) was also changed to reduce its size and introduce the new direct power supply of 3.3V and 5V. The previous DB9 connector was also removed and it

approximately 2.2 cm per 3cm, which is less than half the size of the developed prototype and has already a microcontroller included. All the electronic components were putted in the top layer to allow the module to be mounted on the top of the main board without any component between both boards. The following images (Figures 3.7.6 and 3.7.7) show the designed PCB, also with two layers, and the respective 3D board model with all the needed components.

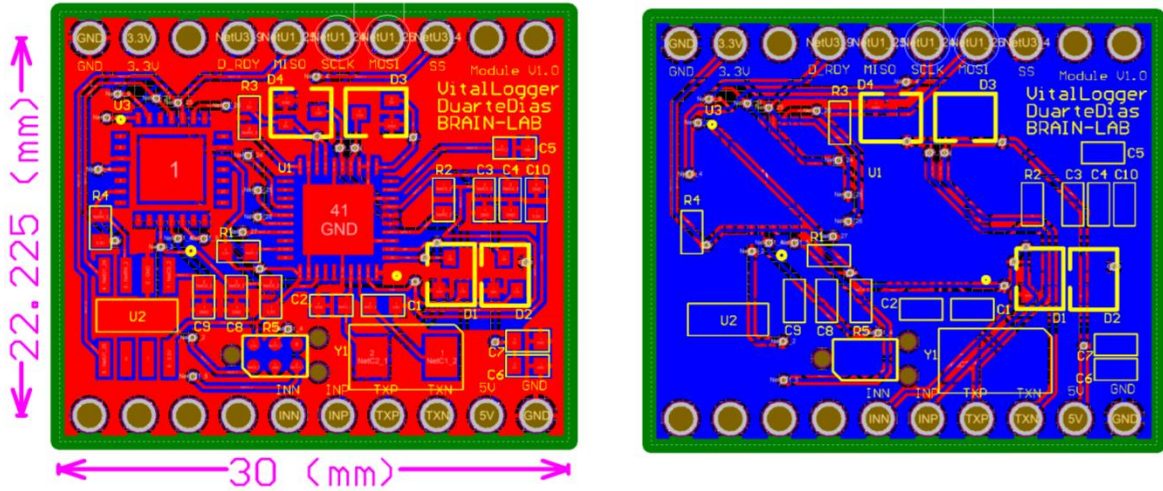


Figure 3.7.6- Printed circuit board layers of the new module unit (top layer-left image; bottom layer-right image).

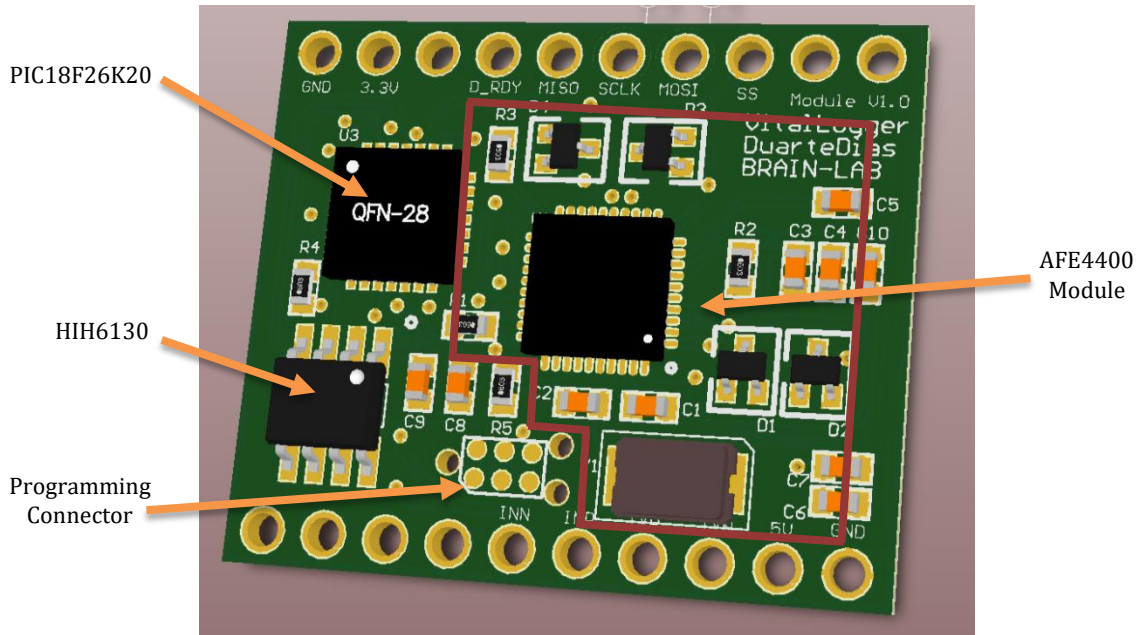


Figure 3.7.7- 3D model of the new developed module unit. The label in the figure indicates the main components and the AFE4400 module.

Regarding the electrical consumption characteristics, this module is very similar to the developed prototype, with a theoretical current consumption of 5mA, a bit more due to the microcontroller implementation. This will provide almost the same continuous monitoring time as the developed prototype, of about 28.5 hours.

The associated costs (Table IX) is one of the most improved characteristic of this module, decreasing more than 10€ independently of the number of produced units. This decrease is due to a smaller PCB and a small amount of electronic components used.

Table IX- This table shows the associated costs of the designed module regarding the electrical components and PCB costs per each unit produced according to the number of units produced In the last column of the table a total cost per unit is presented.

Produced Units	Electrical Components Cost per unit	PCB Cost per unit	Prototype Cost per unit
10	20.77 €	6.44 €	27.21 €
50	18.76 €	1.88 €	20.64 €
100	17.28 €	1.30 €	18.58 €

In relation to the costs and electrical consumption of the new sensor idea previously referred, it is expected to have a lower production cost comparing with the commercial ones, due to its structure simplicity and smaller size, but a similar consume if implemented in the finger.

Chapter 4

Conclusions and Future Work

Wearable health devices interest is growing and this Master Thesis showed that the technology in this area still has much to evolve and increase during the following years. In this work an effort was made to contribute in this emerging area by creating a prototype for a possible market expansion of a commercial wearable health device. The prototype was successfully developed and implemented, creating the first VitalLogger prototype capable to acquire three more variables (physiological oxygen saturation level and ambiance temperature and relative humidity) beyond the already acquired by Vital Jacket®. As expected, more work must be done to take this prototype closer from a possible commercialization. The following lines will refer some aspects that must be improved as also some problems to overcome, both to increase this prototype feasibility for medical and personal use.

The proposed module version of the developed board prototype needs to be produced, assembled, tested and validated. It is also necessary to develop the code implementation to change the microcontroller SPI module from master to slave and vice versa, as also its communication with the microcontroller from the main board. Since a microcontroller will be used only for the developed prototype new variables acquisition, a higher sampling rate should be implemented, obtaining a better PPG waveform, even at high heart rates. An FFT oxygen saturation level calculation could also be implemented and tested to evaluate its performance in this system. To test this module it is fundamental to improve the existing VitalJacket® connector to be able to incorporate an oxygen saturation sensor. Regarding this sensor itself, it would be of great value to create a personalized sensor and, if possible, with a possible implementation for the human ear. This solution was already discussed, but is important to retain that, in my opinion, an ear oxygen saturation sensor would be better to use in wearable system, not needing to have wires along the arm, until the finger, just a short cable from the T-shirt collar to the ear. This sensor should be small and easy to attach to the ear. Due to a smaller tissue volume

compared to the finger, an ear sensor could reduce the electrical consumption from the LEDs sensor, increasing wearable system battery lifetime.

Regarding the oxygen saturation module, it would be very important to get access to the medical certification characteristics document for this type of sensor (ISO 80601-2-61:2011). With this document, it would be possible to adapt the properties and acquisition procedure of the pulse oximeter module, obtaining a sensor capable to be medically certified and used for medical purpose as an oxygen saturation sensor.

With these improvements it would be possible extend Biodevices, S.A. technology, with an already certified pulse oximetry sensor, a higher benefit that would allow a direct use of it in the medical environment. After this improvement it would be interesting to study the possibility to estimate blood pressure from ECG and PPG signals as mentioned in the researched literature.

All the small technology advances are important in its evolution and this Master Thesis had the aim to contribute in the expansion of a WHD, contributing with one more step in this area.

References

1. Yussuff, V. and R. Sanderson, *The World Market for Wireless Charging in Wearable Technology*, in *Wireless Power Intelligence Service*, Edition, Editor. December 2014, IHS.
2. Yilmaz, T., R. Foster, and Y. Hao, *Detecting vital signs with wearable wireless sensors*. *Sensors (Basel)*, 2010. **10**(12): p. 10837-62.
3. Lymberis A, G.L. *Wearable health systems: from smart technologies to real applications*. in *Annual International Conference of the IEEE Engineering in Medicine and Biology Society. IEEE Engineering in Medicine and Biology Society. Annual Conference*. 2006.
4. Chan, M., et al., *Smart wearable systems: current status and future challenges*. *Artif Intell Med*, 2012. **56**(3): p. 137-56.
5. Marco Di Rienzo, G.P., Gabriella Brambilla, Maurizio Ferratini and Paolo Castiglioni, *MagIC System: a New Textile-Based Wearable Device for Biological Signal Monitoring. Applicability in Daily Life and Clinical Setting*. *Proceedings of the 2005 IEEE, Engineering in Medicine and Biology 27th Annual Conference*, 2005: p. 7167-7169.
6. Rita Paradiso, G.L., and Nicola Taccini, *A Wearable Health Care System Based on Knitted Integrated Sensors*. *IEEE Transaction on information technology in Biomedicine*, 2005. **9**(3): p. 337-344.
7. Seoane, F., et al., *Wearable biomedical measurement systems for assessment of mental stress of combatants in real time*. *Sensors (Basel)*, 2014. **14**(4): p. 7120-41.
8. Custodio, V., et al., *A review on architectures and communications technologies for wearable health-monitoring systems*. *Sensors (Basel)*, 2012. **12**(10): p. 13907-46.
9. Khan, Z.A., et al., *ZEQoS: A New Energy and QoS-Aware Routing Protocol for Communication of Sensor Devices in Healthcare System*. *International Journal of Distributed Sensor Networks*, 2014. **2014**: p. 1-18.
10. Cunha, J.P.S., et al. *Vital-Jacket®: A wearable wireless vital signs monitor for patients' mobility in cardiology and sports*. in *Pervasive Computing Technologies for Healthcare (PervasiveHealth), 2010 4th International Conference on Pervasive Computing Technologies for Healthcare*. 2010.
11. Pantelopoulos, A. and N.G. Bourbakis, *A Survey on Wearable Sensor-Based Systems for Health Monitoring and Prognosis*. *Systems, Man, and Cybernetics, Part C: Applications and Reviews*, *IEEE Transactions on*, 2010. **40**(1): p. 1-12.
12. Appelboom, G., et al., *Smart wearable body sensors for patient self-assessment and monitoring*. *Arch Public Health*, 2014. **72**(1): p. 28.
13. Bandodkar, A.J. and J. Wang, *Non-invasive wearable electrochemical sensors: a review*. *Trends Biotechnol*, 2014. **32**(7): p. 363-71.
14. Garbarino, M., et al. *Empatica E3 — A wearable wireless multi-sensor device for real-time computerized biofeedback and data acquisition*. in *Wireless Mobile Communication and Healthcare (Mobihealth), 2014 EAI 4th International Conference on*. 2014.
15. Sharma, H., K.K. Sharma, and O.L. Bhagat, *Respiratory rate extraction from single-lead ECG using homomorphic filtering*. *Computers in Biology and Medicine*, 2015. **59**(0): p. 80-86.
16. Banaee, H., M.U. Ahmed, and A. Loutfi, *Data mining for wearable sensors in health monitoring systems: a review of recent trends and challenges*. *Sensors*, 2013. **13**(12): p. 17472-500.

17. Rifat Shahriyar, M.F.B., Gourab Kundu, Sheikh Iqbal Ahamed, Md. Mostofa Akbar, *Intelligent Mobile Health Monitoring System (IMHMS)* International Journal of Control and Automation, 2009. **2**(3): p. 13-28.
18. Lukowicz, P., *et al.* AMON: a wearable medical computer for high risk patients. in *Wearable Computers, 2002. (ISWC 2002). Proceedings. Sixth International Symposium on.* 2002.
19. Bieber, G., M. Haescher, and M. Vahl, *Sensor requirements for activity recognition on smart watches.* 2013: p. 1-6.
20. Withings - Inspire Health. *Pulse O_x - Track. Improve.* [cited February 2015; Available from: <http://www.withings.com/eu/withings-pulse.html>].
21. BASIS. *PEAK - The Ultimate Fitness and Sleep Tracker.* [cited February 2015; Available from: <https://www.mybasis.com/>].
22. Zephyr Technology Corp. January 2015]; Available from: <http://zephyranywhere.com/>.
23. Xiao-Fei, T., *et al.*, *Wearable Medical Systems for p-Health.* Biomedical Engineering, IEEE Reviews in, 2008. **1**: p. 62-74.
24. Mouradian, V., A. Poghosyan, and L. Hovhannisyan. *Continuous wearable health monitoring using novel PPG optical sensor and device.* in *Wireless and Mobile Computing, Networking and Communications (WiMob), 2014 IEEE 10th International Conference on.* 2014.
25. Biodevices, S.A. *VitalJacket®.* January 2015]; Available from: <http://www.vitaljacket.com/>.
26. Biodevices, S.A. *VitalJacket® informative document.* 2013 January 2015]; Available from: <http://www.vitaljacket.com/>.
27. nuubo - Wearable Medical Technologies. January 2015]; Available from: <http://www.nuubo.com/>.
28. Vivonoetics. January 2015]; Available from: <http://vivonoetics.com/>.
29. HealthWatch Technologies Ltd. January 2015]; Available from: <http://www.personal-healthwatch.com/>.
30. Hexoskin. January 2015]; Available from: <http://www.hexoskin.com/>.
31. AiQ Smart Clothing Ltd. January 2015]; Available from: <http://www.aiqsmartclothing.com/>.
32. OMSignal Inc. January 2015]; Available from: <http://www.omsignal.com/>.
33. Zhang, Z.-B., *Journal of Medical and Biological Engineering*, 2011. **31**(3): p. 207.
34. Sardini, E., M. Serpelloni, and M. Ometto. *Multi-parameters wireless shirt for physiological monitoring.* in *Medical Measurements and Applications Proceedings (MeMeA), 2011 IEEE International Workshop on.* 2013.
35. Farjadian, A.B., M.L. Sivak, and C. Mavroidis. *SQUID: Sensorized shirt with smartphone interface for exercise monitoring and home rehabilitation.* in *Rehabilitation Robotics (ICORR), 2013 IEEE International Conference on.* 2013.
36. Cafagna, C., A. Diterlizzi, and F. Voorhorst. *MyWear: Customized green, safe, healthy and smart work- and sports-wear.* in *Engineering, Technology and Innovation (ICE), 2014 International ICE Conference on.* 2014.
37. Ahrens, T., *The most important vital signs are not being measured.* Aust Crit Care, 2008. **21**(1): p. 3-5.
38. Elliott M, C.A., *Critical care: the eight vital signs of patient monitoring.* Br J Nurs, 2012. **21**(10): p. 621-625.
39. Xu, P.J., H. Zhang, and X.M. Tao, *Textile-structured electrodes for electrocardiogram.* Textile Progress, 2008. **40**(4): p. 183-213.
40. Saritha, C., V. Sukanya, and Y.N. Murthy, *ECG Signal Analysis Using Wavelet Transforms.* Bulg. J. Phys. , 2008. **35**: p. 68-77.

41. Luo, N., et al., *Mobile Health: Design of Flexible and Stretchable Electrophysiological Sensors for Wearable Healthcare Systems*. 2014: p. 87-91.
42. Tamura, T., et al., *Wearable Photoplethysmographic Sensors—Past and Present*. Electronics, 2014. **3**(2): p. 282-302.
43. Turner, J.R., A.J. Viera, and D. Shimbo, *Ambulatory Blood Pressure Monitoring in Clinical Practice: A Review*. Am J Med, 2015. **128**(1): p. 14-20.
44. Puke, S., et al. *Blood pressure estimation from pulse wave velocity measured on the chest*. in *Engineering in Medicine and Biology Society (EMBC), 2013 35th Annual International Conference of the IEEE*. 2013.
45. Yu-Pin, H. and D.J. Young, *Skin-Coupled Personal Wearable Ambulatory Pulse Wave Velocity Monitoring System Using Microelectromechanical Sensors*. Sensors Journal, IEEE, 2014. **14**(10): p. 3490-3497.
46. Woo, S.H., et al., *Tissue-informative mechanism for wearable non-invasive continuous blood pressure monitoring*. Sci Rep, 2014. **4**: p. 6618.
47. Zhang, Z., et al., *Development of a respiratory inductive plethysmography module supporting multiple sensors for wearable systems*. Sensors (Basel), 2012. **12**(10): p. 13167-84.
48. Guo, L., et al., *Design of a garment-based sensing system for breathing monitoring*. Textile Research Journal, 2012. **83**(5): p. 499-509.
49. Gandis G. Mazeika, M. and R. Rick Swanson, CRTT. *Respiratory Inductance Plethysmography An Introduction*. 2007 January 2015]; Available from: <http://www.protech.com/>.
50. Atalay, O., W.R. Kennon, and E. Demirok, *Weft-Knitted Strain Sensor for Monitoring Respiratory Rate and Its Electro-Mechanical Modeling*. Sensors Journal, IEEE, 2015. **15**(1): p. 110-122.
51. Anmin, J., et al. *Performance evaluation of a tri-axial accelerometry-based respiration monitoring for ambient assisted living*. in *Engineering in Medicine and Biology Society, 2009. EMBC 2009. Annual International Conference of the IEEE*. 2009.
52. Chiu, Y.-Y., et al., *Development of a piezoelectric polyvinylidene fluoride (PVDF) polymer-based sensor patch for simultaneous heartbeat and respiration monitoring*. Sensors and Actuators A: Physical, 2013. **189**: p. 328-334.
53. Krehel, M., et al., *An optical fibre-based sensor for respiratory monitoring*. Sensors (Basel), 2014. **14**(7): p. 13088-101.
54. S Tognarelli, L.D., F Cecchi, R Scaramuzzo, A Cuttano, C Laschi, A Menciassi, P Dario. *Analysis of a dielectric EAP as smart component for a neonatal respiratory simulator*. in *Conf Proc IEEE Eng Med Biol Soc*. 2013.
55. al., J.S.e. *SpO2 Sensor Embedded in a Finger Ring: desing and implementation*. in *Proc. 28th Annual IEEE EBMS conf*. 2006.
56. Mendelson, Y., D.K. Dao, and K.H. Chon. *Multi-channel pulse oximetry for wearable physiological monitoring*. in *Body Sensor Networks (BSN), 2013 IEEE International Conference on*. 2013.
57. Chen, C.-M., et al., *Wearable Tissue Oxygenation Monitoring Sensor and a Forearm Vascular Phantom Design for Data Validation*. 2014: p. 64-68.
58. Christoph Zysset, e.a., *Textile integrated sensors and actuators for near-infrared spectroscopy*. Virtual Journal for Biomedical Optics, 2013. **8**(3).
59. Krehel, M., et al., *Development of a luminous textile for reflective pulse oximetry measurements*. Biomed Opt Express, 2014. **5**(8): p. 2537-47.
60. Takahashi, M., et al. *Portable continuous glucose monitoring systems with implantable fluorescent hydrogel microfibers*. in *Micro Electro Mechanical Systems (MEMS), 2013 IEEE 26th International Conference on*. 2013.

61. Tierney, M.J., *et al.*, *Clinical evaluation of the GlucoWatch® biographer: a continual, non-invasive glucose monitor for patients with diabetes*. *Biosensors and Bioelectronics*, 2001. **16**(9-12): p. 621-629.
62. So, C.F., *et al.*, *Recent advances in noninvasive glucose monitoring*. *Med Devices (Auckl)*, 2012. **5**: p. 45-52.
63. Sobel, S.I., *et al.*, *Accuracy of a Novel Noninvasive Multisensor Technology to Estimate Glucose in Diabetic Subjects During Dynamic Conditions*. *J Diabetes Sci Technol*, 2014. **8**(1): p. 54-63.
64. MedCityNews. *FDA Approval for First Glucose Monitoring App*. 2015 [January 2015]; Available from: <http://healthmanagement.org/>.
65. Jeehoon, K., *et al.* *Highly wearable galvanic skin response sensor using flexible and conductive polymer foam*. in *Engineering in Medicine and Biology Society (EMBC), 2014 36th Annual International Conference of the IEEE*. 2014.
66. Nikolic-Popovic, J. and R. Goubran. *Measuring heart rate, breathing rate and skin conductance during exercise*. in *Medical Measurements and Applications Proceedings (MeMeA), 2011 IEEE International Workshop on*. 2011.
67. Gengchen, L., K. Smith, and T. Kaya. *Implementation of a microfluidic conductivity sensor — A potential sweat electrolyte sensing system for dehydration detection*. in *Engineering in Medicine and Biology Society (EMBC), 2014 36th Annual International Conference of the IEEE*. 2014.
68. BS., K., *Capnography outside the operating rooms*. *Anesthesiology*, 2013. **118**(1): p. 192-201.
69. Wac, K. and C. Tsiourti, *Ambulatory Assessment of Affect: Survey of Sensor Systems for Monitoring of Autonomic Nervous Systems Activation in Emotion*. *Affective Computing, IEEE Transactions on*, 2014. **5**(3): p. 251-272.
70. Dziewas R, e.a., *Capnography screening for sleep apnea in patients with acute stroke*. *Neurol Res*, 2005. **27**(1): p. 83-87.
71. Ontario, O.B.R.-T.o.j.f.b.i. *Braebon taps into the growing sleep apnea market*. 2012 [January 2015]; Available from: <http://www.mri.gov.on.ca/obr/2012/07/braebon-taps-into-the-growing-sleep-apnea-market/>.
72. Schlader, Z.J., *et al.*, *Skin temperature as a thermal controller of exercise intensity*. *European Journal of Applied Physiology*, 2011. **111**(8): p. 1631-1639.
73. Saurabh, K., *et al.* , *CONTINUOUS CORE BODY TEMPERATURE ESTIMATION VIA SURFACE TEMPERATURE MEASUREMENTS USING WEARABLE SENSORS: IS IT FEASIBLE?* Indian Institute Of Science.
74. A, L., *Remote, wireless, ambulatory monitoring of implantable pacemakers, cardioverter defibrillators, and cardiac resynchronization therapy systems: analysis of a worldwide database*. *Pacing Clin Electrophysiol*, 2007. **30**(11): p. S2-S12.
75. Jin, M.Z., Han; Weekly, Kevin; Jia, Ruoxi; Bayen, Alexandre M.; Spanos, Costas J., *Environmental Sensing by Wearable Device for Indoor Activity and Location Estimation*. . 2014.
76. Bartell, S.M., *et al.*, *Particulate air pollution, ambulatory heart rate variability, and cardiac arrhythmia in retirement community residents with coronary artery disease*. *Environ Health Perspect*, 2013. **121**(10): p. 1135-1141.
77. Ambulatory Monitoring Inc. *Application Areas*. [cited January 2015; Available from: <http://www.ambulatory-monitoring.com/environmental.html>].
78. Business Insider and © Statista, *Wearable device market value from 2010 to 2018 (in million U.S. dollars)*. 2015.
79. Worldwide ABI Research and © Statista, *Shipments of wearable computing devices worldwide by category from 2013 to 2015 (in millions)*. 2015.

80. MobileHealthNews and © Statista, *Shipments of smart clothing/fabrics worldwide from 2013 to 2015 (in millions)*. 2014.
81. SensiAn Research, *mHealth Wellness Wearable Devices: Activity Trackers, Sports Watches, Heart Rate Monitors, Smart Sports Clothing, Connected Weighing Scales and Other Consumer Wellness Devices*. 2014.
82. Berg Insight, *Connected home medical monitoring devices, million units (World 2011–2017)*. 2014.
83. © Statista, *Growth rate of Chinas wearable mobile medical equipment market from 2012 to 2017*. 2015.
84. IHS Technology, *Top Healthcare Technology Trend Predictions for 2014 - IHS Medical Devices & Healthcare IT*. 2014.
85. Lauren Soelberg Treasure. *MHEALTH IN THE FUTURE – KEY TRENDS (INFOGRAPHIC)*. 2012 [cited January 2015; Available from: <http://healthdecide.orcahealth.com>].
86. Incorporated, T.I., *AFE4400 Integrated Analog Front-End for Heart Rate Monitors and Low-Cost Pulse Oximeters*. 2014.
87. Incorporated, T.I., *AFE4400 and AFE4490 Development Guide*. 2014.
88. Control, H.S.a., *Honeywell HumidIcon™ Digital Humidity/Temperature Sensors: HIH6130/6131 and HIH6120/6121 Series*. 2012.
89. Microelectronics, S., *iNEMO inertial module: 3D accelerometer and 3D gyroscope*. 2012.
90. Lopez, S., *Pulse Oximeter Fundamentals and Design*. 2011, Freescale Semiconductor, Inc.
91. Damianou, D., *The Wavelength Dependence of the Photoplethysmogram and its Implication to Pulse Oximetry*. 1995, University of Nottingham.
92. AnaesthesiaUK. *Principles of pulse oximetry*. 2004 [cited August 2015; Available from: <http://www.frca.co.uk/>].
93. Giavarina, D., *Understanding Bland Altman analysis*. *Biochemia Medica*, 2015. **25**(2): p. 141-51.
94. Fluke Biomedical. *ProSim SPOT Light SpO2 Tester pulse oximeter analyzer*. Available from: <http://www.flukebiomedical.com/biomedical/usen/home/>.
95. Philips. *Patient Monitoring Documents and Downloads - M3046A - M2/M3/M4 Compact Monitor Display*. September 2015]; Available from: <http://incenter.medical.philips.com/>.
96. Velleman®. *TEMPERATURE / HUMIDITY / DEW POINT METER*. Available from: <http://www.velleman.eu/home/>.
97. Tag-Connect, L. *TC2030-MCP-NL 6-Pin No-Legs Cable with RJ12 Modular Plug (for Microchip ICD)*. 2015 [cited August 2015; Available from: <http://www.tag-connect.com/>].
98. Inc., M.T., *PIC18F23K20/24K20/25K20/26K20/43K20/44K20/45K20/46K20 Data Sheet*. 2010.

Appendix

Appendix A – Second Version of VitalLogger Extension Board

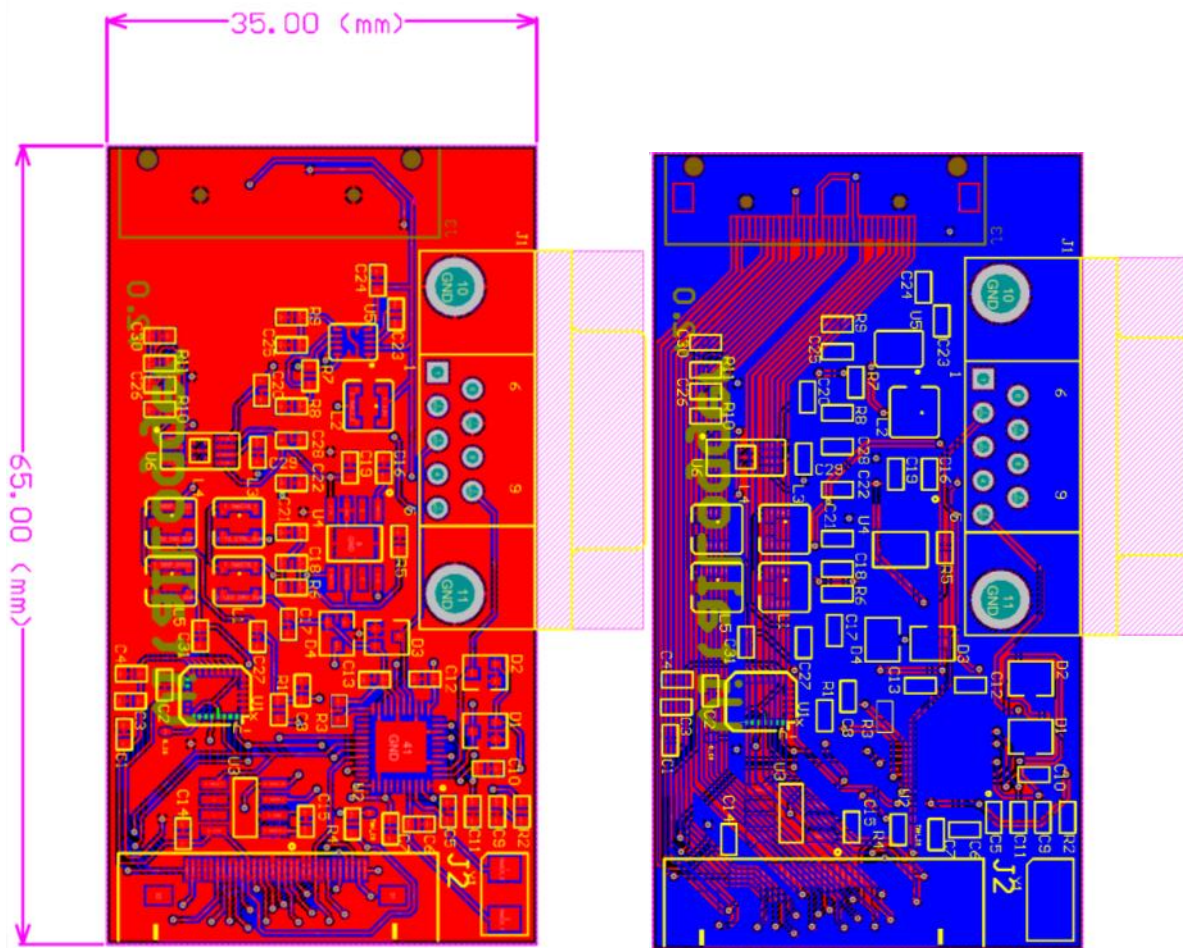


Figure A. 1- PCB design of VitalLogger extension board second prototype that was not produced. The left image shows the top layer and the right image the bottom layer.

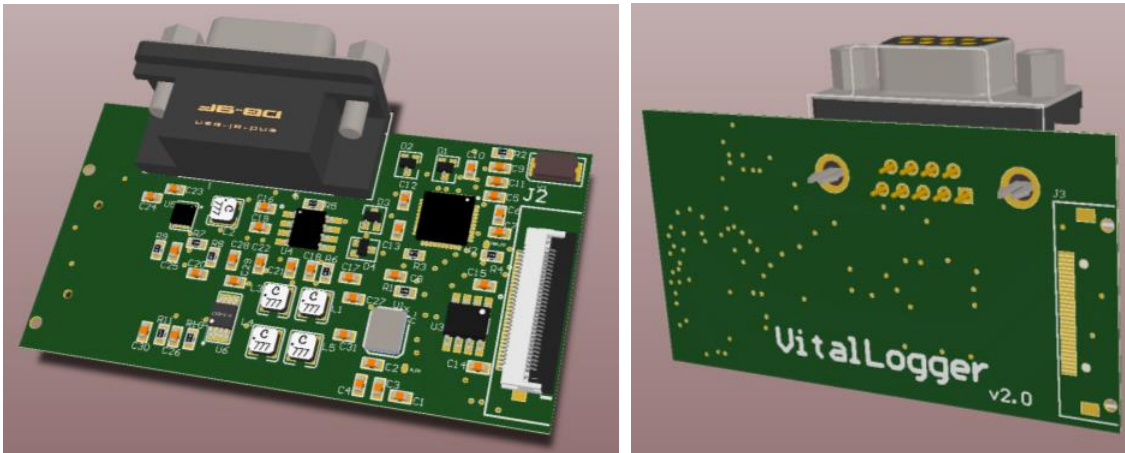


Figure A. 2- 3D model of the VitalLogger extension board second prototype that was not produced. The left image shows the top view of the prototype and the right image the bottom view.

Appendix B - VitalLogger Modular Extension Power Supply Verification

To verify the possibility to supply the AFE4400 with a direct supply of 3.3V and 5V, the components not related to this module were removed from one of the three boards assembled (Figure A.3). This evaluation was based on the TXP and TXN comparison between this board with a new configuration and the developed prototype extension, concluding that the results are very similar (Figure A.4-5). This evaluation is made based on the Texas Instrument AFE4400 evaluation module datasheet [87].

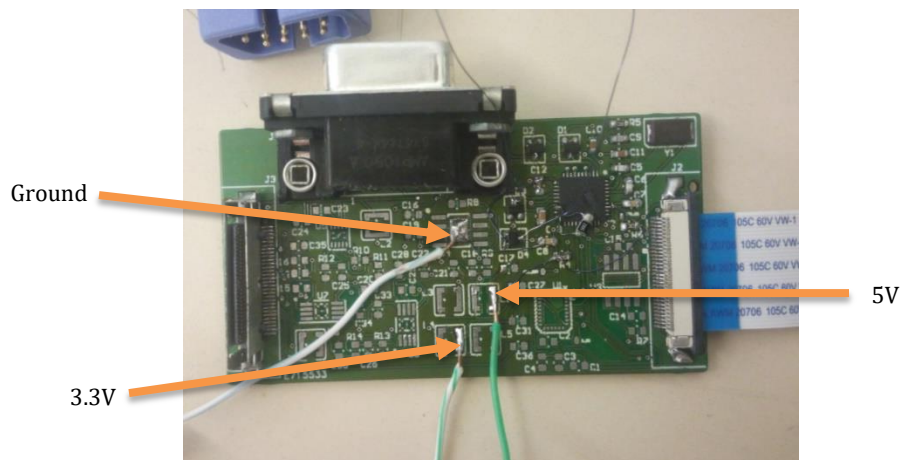


Figure A. 3- Prototype extension board adaptation to test the direct power supply of 3.3V and 5V.

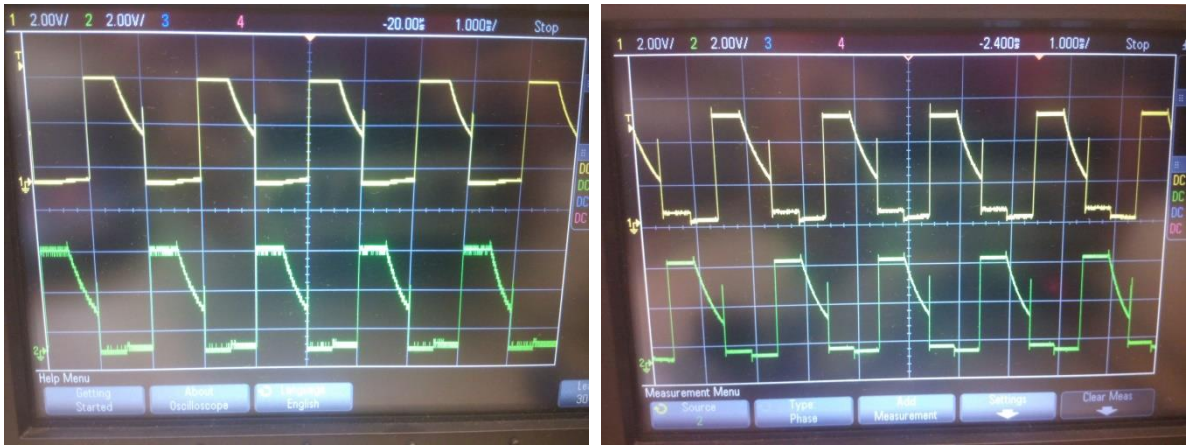


Figure A. 4- TXP (yellow signal) and TXN (green signal) signals obtained, when the sensor is disconnected, from the developed prototype extension (left image) and from the board with a new configuration (right image).



Figure A. 5- TXP (yellow signal) and TXN (green signal) signals obtained, when the sensor is connected, from the developed prototype extension (left image) and from the board with a new configuration (right image).

